

ENCLOSURE 3

**Arizona Public Service Company
PWR Reactor Physics Methodology Using
CASMO-4/SIMULATE-3, September 1999**

Redacted Version

ARIZONA PUBLIC SERVICE COMPANY
PWR REACTOR PHYSICS METHODOLOGY
USING
CASMO-4/SIMULATE-3

September 1999



Revision 0

Redacted Version

ARIZONA PUBLIC SERVICE COMPANY
PWR REACTOR PHYSICS METHODOLOGY

USING

CASMO-4/SIMULATE-3

SEPTEMBER 1999

Prepared By: Sandra G. Zimmerman 9/9/99
S. G. Zimmerman, Senior Engineer (Date)
Nuclear Analysis

Prepared By: James C. Brittingham 9/9/99
J. C. Brittingham, Senior Consulting Engineer (Date)
Nuclear Analysis

Prepared By: Michael S. Reed 9/9/99
M. L. Reed, Consulting Engineer (Date)
Nuclear Analysis

Approved By: TPBander 9/9/99
R. P. Bandera, Section Leader (Date)
Nuclear Analysis

Approved By: Paul F. Crawley 9/9/99
P. F. Crawley, Director (Date)
Nuclear Fuel Management

PALO VERDE NUCLEAR GENERATING STATION
5801 SOUTH WINTERSBURG ROAD
TONOPA, AZ 85354-7529

DISCLAIMER

This document was prepared by Arizona Public Service Company for its own use. The use of information contained in this document by anyone other than Arizona Public Service Company is not authorized, and in regard to unauthorized use, neither Arizona Public Service Company nor any of its officers, directors, agents, or employees assumes any obligation, responsibility or liability, or makes any warranty or representation, with respect to the contents of this document, or its accuracy or completeness.

ABSTRACT

In Arizona Public Service's continuing effort to improve its reload design methods, the CASMO-4/SIMULATE-3 reactor physics method has been developed. This report documents the validation and level of accuracy of the reactor core physics method used by Arizona Public Service Company to perform analyses for Pressurized Water Reactors (PWR). The method is based on the CASMO-4/SIMULATE-3 computer program package used by many in the nuclear industry. The APS method has been validated by an in-house benchmark effort of CASMO-4/SIMULATE-3 predictions with measured data using a variety of fuel designs and operating conditions in power reactors and critical experiments. Arizona Public Service Company intends to use this method to perform PWR calculations, including:

- reload design
- physics input to safety analysis
- physics input to fuel and clad performance
- physics input to mechanical design
- physics input to thermal-hydraulic analysis
- input to LOCA/Non-LOCA transient analysis
- CECOR coefficients
- startup test predictions
- core physics data books
- Shutdown Margin
- inputs to reactor protection system and monitoring system (COLSS/CPC) functions and set-point and uncertainty updates
- other safety related physics parameters in support of refueling, safety analysis, and operation

Based on the results from this benchmark effort, a set of biases and uncertainties and a method for maintaining and updating these biases and uncertainties has been established. The biases and uncertainties will be updated if proved necessary as new data is collected for each new cycle. Arizona Public Service intends to replace the DIT/ROCS/MC method with CASMO-4/SIMULATE-3 while retaining the ability to use the DIT/ROCS/MC method.

TABLE OF CONTENTS

	<u>Page</u>
DISCLAIMER	3
ABSTRACT	4
1.0 INTRODUCTION, OVERVIEW, AND SUMMARY	13
1.1 INTRODUCTION	13
1.2 OVERVIEW	13
1.3 SUMMARY	15
2.0 DESCRIPTION OF METHOD	19
2.1 INTRODUCTION	19
2.2 COMPUTER PROGRAM DESCRIPTIONS	19
2.2.1 CASMO-4	19
2.2.2 CASLIB	20
2.2.3 TABLES-3/CMS-LINK	20
2.2.4 SIMULATE-3	20
2.2.5 CECORLIB	21
2.2.6 CECOR	21
2.3 MODEL DESCRIPTIONS	21
2.3.1 CASMO-4 FUEL ASSEMBLY AND REFLECTOR MODELS	21
2.3.2 TABLES-3/CMS-LINK MODEL	22
2.3.3 SIMULATE-3 MODEL	22
3.0 DESCRIPTION OF REACTORS USED IN THE BENCHMARK	25
4.0 BENCHMARK COMPARISONS	28
4.1 INTRODUCTION	28
4.2 REACTIVITY BIASES AND UNCERTAINTY	29
4.2.1 BOC HOT-ZERO-POWER REACTIVITY	29
4.2.2 HOT-FULL-POWER REACTIVITY COMPARISONS	35
4.3 ITC BIAS AND UNCERTAINTY	49
4.4 CONTROL ROD WORTH BIAS AND UNCERTAINTY	55
4.5 INVERSE BORON WORTH BIAS AND UNCERTAINTY	71
4.6 DOPPLER POWER COEFFICIENT	75
4.7 FUEL TEMPERATURE COEFFICIENT	79

4.8	DROPPED ROD	80
4.9	EJECTED ROD	93
5.0	POWER PEAKING FACTOR UNCERTAINTY	105
5.1	INTRODUCTION	105
5.2	PIN PEAKING CALCULATION UNCERTAINTY	106
5.2.1	CASMO-4/DOT UNCERTAINTY FROM RPI CRITICALS	106
5.2.2	CASMO-4 UNCERTAINTY FROM RPI AND B&W CRITICALS	108
5.2.3	SIMULATE-3 UNCERTAINTY FROM B&W CRITICALS	110
5.2.4	CASMO-4/SIMULATE-3 UNCERTAINTY FROM RPI AND B&W CRITICALS	111
5.3	INSTRUMENTED BOX POWER UNCERTAINTY FOR F_q , F_r , and F_{xy}	124
5.3.1	INTRODUCTION	124
5.3.2	DESCRIPTION OF MEASURED DATA	124
5.3.3	OPERATING HISTORIES	124
5.3.4	DESCRIPTION OF CALCULATIONS	128
5.3.5	STATISTICAL MODEL FOR CALCULATION OF INSTRUMENTED ASSEMBLY POWER DISTRIBUTION UNCERTAINTIES	128
5.3.6	EVALUATION OF INSTRUMENTED BOX POWER PEAKING FACTOR CALCULATION UNCERTAINTY	141
5.3.7	EVALUATION OF INSTRUMENTED BOX POWER PEAKING FACTOR MEASUREMENT UNCERTAINTY WITH 61 DETECTOR STRINGS	154
5.3.8	EVALUATION OF INSTRUMENTED BOX POWER PEAKING FACTOR MEASUREMENT UNCERTAINTY WITH 50 DETECTOR STRINGS	165
5.4	POWER PEAKING FACTOR SYNTHESIS UNCERTAINTY	176
5.4.1	ABB POWER PEAKING FACTOR SYNTHESIS UNCERTAINTY	176
5.4.2	APS POWER PEAKING FACTOR SYNTHESIS UNCERTAINTY	176
5.5	PIN POWER PEAKING FACTOR UNCERTAINTY	178
5.5.1	EVALUATION OF PIN POWER CALCULATION UNCERTAINTY	178
5.5.2	EVALUATION OF PIN POWER MEASUREMENT UNCERTAINTY WITH 61 DETECTOR STRINGS	182
5.5.3	EVALUATION OF PIN POWER MEASUREMENT UNCERTAINTY WITH 50 DETECTOR STRINGS	187
6.0	COLD MODEL AND NET (N - 1) ROD WORTH	190
7.0	CONCLUSIONS	197
8.0	REFERENCES	198

LIST OF TABLES

<u>Number</u>	<u>Title</u>	<u>Page</u>
Table 1-1	List of Key PWR Physics Parameters	16
Table 1-2	List of 95/95 Tolerance Limits (Bias \pm Uncertainty)	17
Table 4-1	HZP BOC Reactivity Differences	33
Table 4-2	HZP BOC Reactivity Multiple Linear Regression Model Statistics	34
Table 4-3	HZP BOC Reactivity Multiple Linear Regression Model 95/95 Uncertainty	34
Table 4-4	Significant Downpowers for Cycles with at Least 2 Batches of Erbium	36
Table 4-5	HFP Critical Boron/Reactivity Comparisons	37
Table 4-6	Full Power Reactivity Difference Statistics	48
Table 4-7	HZP ITC Comparisons	51
Table 4-8	At-Power ITC Comparisons	52
Table 4-9	ITC Difference Statistics	54
Table 4-10	Unit 1 Rod Worth Comparisons	59
Table 4-11	Unit 2 Rod Worth Comparisons	62
Table 4-12	Unit 3 Rod Worth Comparisons	65
Table 4-13	Rod Worth Percent Difference Statistics	68
Table 4-14	Palo Verde Measured Worths -- Dilution	69
Table 4-15	Palo Verde Measured Worths -- Rod Exchange	69
Table 4-16	Summary of Statistics for Rod Worth for PVNGS Units 1, 2, and 3	70
Table 4-17	Units 1, 2, and 3 IBW Comparisons	73
Table 4-18	IBW Difference Statistics	74
Table 4-19	Doppler Power Coefficient Comparisons	77
Table 4-20	Doppler Power Coefficient Statistics for Relative Differences	78
Table 4-21	Functionalization for the DOPC Relative Differences	78
Table 4-22	U1C1 Dropped Rod Worths from ROCS, SIMULATE-3, and Measurement	83
Table 4-23	U1C8 Dropped Rod Worths from ROCS	84
Table 4-24	U2C8 Dropped Rod Worths from ROCS	85
Table 4-25	U3C8 Dropped Rod Worths from ROCS	86

Table 4-26	U1C8 Dropped Rod Worths from SIMULATE-3	87
Table 4-27	U2C8 Dropped Rod Worths from SIMULATE-3	88
Table 4-28	U3C8 Dropped Rod Worths from SIMULATE-3	89
Table 4-29	Differences Between U1C1 Measured Dropped Rod Worths and the SIMULATE-3 and ROCS Calculations	90
Table 4-30	Differences Between SIMULATE-3 and ROCS Dropped Rod Worths for Cycle 8 for Units 1, 2, and 3	91
Table 4-31	U1C1 Ejected Rod Worths from ROCS, SIMULATE-3, and Measurement	96
Table 4-32	U1C8 Ejected Rod Worths from ROCS	97
Table 4-33	U2C8 Ejected Rod Worths from ROCS	98
Table 4-34	U3C8 Ejected Rod Worths from ROCS	99
Table 4-35	U1C8 Ejected Rod Worths from SIMULATE-3	100
Table 4-36	U2C8 Ejected Rod Worths from SIMULATE-3	101
Table 4-37	U3C8 Ejected Rod Worths from SIMULATE-3	102
Table 4-38	Differences Between U1C1 Measured Ejected Rod Worths and the SIMULATE-3 and ROCS Calculations	103
Table 4-39	Differences Between SIMULATE-3 and ROCS Ejected Rod Worths for Cycle 8 for Units 1, 2, and 3	104
Table 5-1	RPI Criticals - W Test for Normality of CASMO-4/DOT Pin Peaking Data	112
Table 5-2	RPI Criticals - CASMO-4/DOT Uncertainty	113
Table 5-3	RPI Criticals - DIT/DOT, CASMO-3/DORT, and CASMO-4/DOT Uncertainty	114
Table 5-4	RPI Criticals - CASMO-4 Uncertainty	115
Table 5-5	B&W Criticals - CASMO-4 and CASMO-4/SIMULATE-3 Uncertainty	116
Table 5-6	RPI and B&W Criticals - CASMO-4 Uncertainty	117
Table 5-7	B&W Criticals - SIMULATE-3 Uncertainty	118
Table 5-8	RPI and B&W Criticals - CASMO-4/SIMULATE-3 Uncertainty	119
Table 5-9	Summary of Uncertainties for the Calculation of Peak Assembly Power	143
Table 5-10	Chi-Square Test Results for Instrumented Box Fq Calculation	144
Table 5-11	Chi-Square Test Results for Instrumented Box Fr Calculation	145
Table 5-12	Chi-Square Test Results for Instrumented Box Fxy Calculation	146
Table 5-13	Normal Uncertainties for Instrumented Box Fq Calculation	148

Table 5-14	Normal Uncertainties for Instrumented Box Fr Calculation	149
Table 5-15	Normal Uncertainties for Instrumented Box Fxy Calculation	150
Table 5-16	Non-Normal Uncertainties for Instrumented Box Fq Calculation	151
Table 5-17	Non-Normal Uncertainties for Instrumented Box Fr Calculation	152
Table 5-18	Non-Normal Uncertainties for Instrumented Box Fxy Calculation	153
Table 5-19	Summary of Uncertainties for the Measurement of Peak Assembly Power with 61 Detector Strings	155
Table 5-20	Chi-Square Test Results for Instrumented Box Fq Measurement with 61 Detector Strings	156
Table 5-21	Chi-Square Test Results for Instrumented Box Fr Measurement with 61 Detector Strings	157
Table 5-22	Chi-Square Test Results for Instrumented Box Fxy Measurement with 61 Detector Strings	158
Table 5-23	Normal Uncertainties for Instrumented Box Fq Measurement with 61 Detector Strings	159
Table 5-24	Normal Uncertainties for Instrumented Box Fr Measurement with 61 Detector Strings	160
Table 5-25	Normal Uncertainties for Instrumented Box Fxy Measurement with 61 Detector Strings	161
Table 5-26	Non-Normal Uncertainties for Instrumented Box Fq Measurement with 61 Detector Strings	162
Table 5-27	Non-Normal Uncertainties for Instrumented Box Fr Measurement with 61 Detector Strings	163
Table 5-28	Non-Normal Uncertainties for Instrumented Box Fxy Measurement with 61 Detector Strings	164
Table 5-29	Summary of Uncertainties for the Measurement of Peak Assembly Power with 50 Detector Strings	166
Table 5-30	Chi-Square Test Results for Instrumented Box Fq Measurement with 50 Detector Strings	167
Table 5-31	Chi-Square Test Results for Instrumented Box Fr Measurement with 50 Detector Strings	168
Table 5-32	Chi-Square Test Results for Instrumented Box Fxy Measurement with 50 Detector Strings	169
Table 5-33	Normal Uncertainties for Instrumented Box Fq Measurement with 50 Detector Strings	170
Table 5-34	Normal Uncertainties for Instrumented Box Fr Measurement with 50 Detector Strings	171

Table 5-35	Normal Uncertainties for Instrumented Box Fxy Measurement with 50 Detector Strings	172
Table 5-36	Non-Normal Uncertainties for Instrumented Box Fq Measurement with 50 Detector Strings	173
Table 5-37	Non-Normal Uncertainties for Instrumented Box Fr Measurement with 50 Detector Strings	174
Table 5-38	Non-Normal Uncertainties for Instrumented Box Fxy Measurement with 50 Detector Strings	175
Table 5-39	ABB and APS Uncertainties of the Synthesis Components of the Peak Pin Power Measurements	177
Table 5-40	Uncertainties of the Components of the Peak Pin Power Calculations	180
Table 5-41	Summary of Uncertainties of the Peak Pin Power Calculations	181
Table 5-42	Uncertainties of the Components of the Peak Pin Power Measurements with 61 Detector Strings	185
Table 5-43	Summary of Uncertainties of the Peak Pin Power Measurements with 61 Detector Strings	186
Table 5-44	Uncertainties of the Components of the Peak Pin Power Measurements with 50 Detector Strings	188
Table 5-45	Summary of Uncertainties of the Peak Pin Power Measurements with 50 Detector Strings	189
Table 6-1	U1C1 Cold Model Comparisons at 320×F	193
Table 6-2	U1C1 Cold Model Comparisons at 565×F	194
Table 6-3	U2C8 Cold Model Comparisons at 565×F	195
Table 6-4	U3C7 Cold Model Comparisons at 565×F	196

LIST OF FIGURES

<u>Number</u>	<u>Title</u>	<u>Page</u>
Figure 2-1	Program Sequence Flow Chart	24
Figure 3-1	Reactor Core and Control Rod Layout	27
Figure 5-1	Central 1/4 Assembly of RPI Critical 0 Erbium Pin Core	120
Figure 5-2	Central 1/4 Assembly of RPI Critical 20 Erbium Pin Core	121
Figure 5-3	Central 1/4 Assembly of RPI Critical 44 Erbium Pin Core	122
Figure 5-4	Central 1/4 Assembly of RPI Critical 56 Erbium Pin Core	123

ACKNOWLEDGEMENTS

The authors wish to acknowledge the individuals who assisted in the development of the CASMO-4/SIMULATE-3 PWR method. Many people within Arizona Public Service assisted. In particular, we would like to acknowledge Nuclear Fuel Management Department engineers Tom Cahill, Shawn Gill, Joe Napier, Craig Hasson, and Chuck Karlson. We would also like to acknowledge PVNGS Reactor Engineering for conducting the startup testing and core surveillance programs which provided much of the physics data used in this benchmark.

1.0 INTRODUCTION, OVERVIEW, AND SUMMARY

1.1 INTRODUCTION

This report describes Arizona Public Service (APS) Company's reactor core physics method for Pressurized Water Reactor (PWR) analyses using the CASMO-4/SIMULATE-3 computer program package (References 1 through 5). STUDEVIK AB and STUDEVIK of America (currently Studsvik Scandpower, Inc.) developed the CASMO-4/SIMULATE-3 computer program package. This package is widely accepted within the nuclear industry.

Yankee Atomic Electric Company (YAEC) provided the theoretical basis and validation of The CASMO-3/SIMULATE-3 computer program package to the NRC (References 6 and 7). In these reports YAEC provided detailed descriptions of the computer programs and a general method for performing reactor physics analyses. The method for CASMO-4 is described in Reference 2, and verification and validation information is given in References 20 and 21. This report demonstrates Arizona Public Service's competence in implementing these programs and provides the appropriate biases and uncertainties to be applied when they are used for reload design. As more data becomes available, and if proved necessary, APS will revise and update the biases and uncertainties.

1.2 OVERVIEW

The data demonstrating the applicability of APS's method for PWR core physics analyses are documented in Sections 2.0 through 8.0 of this report.

Section 2.0, "DESCRIPTION OF METHOD", on page 19, presents a brief description of the CASMO-4/SIMULATE-3 computer program package.

Section 3.0, "DESCRIPTION OF REACTORS USED IN THE BENCHMARK", on page 25, describes the PWRs used in the benchmarks.

Section 4.0, "BENCHMARK COMPARISONS", on page 28, details the benchmark of key PWR core physics parameters listed in Table 1-1. For each parameter, the calculated data is compared with plant measurements, the sample mean and standard deviation are quantified, and a 95/95 tolerance limit (bias \pm uncertainty) is determined.

Section 5.0, "POWER PEAKING FACTOR UNCERTAINTY", on page 105, presents the derivation of the numerical uncertainties associated with the use of the CECOR system with fixed in-core detectors and the numerical uncertainties associated with the use of the SIMULATE-3 code in inferring the core power peaking factors listed in Table 1-1.

Section 6.0, "COLD MODEL AND NET (N - 1) ROD WORTH", on page 190, provides a benchmark comparison of the "cold model" developed using the CASMO-4/TABLES-3/SIMULATE-3 program package. The cold model represents a combination of cross section data produced by CASMO-4 at specific cold core temperatures (i.e., temperatures between hot operating conditions and cold shutdown) and a TABLES-3 functionalization which is designed specifically for cold conditions.

Section 7.0, "CONCLUSIONS", on page 197, presents the conclusions of this report and the range of applications for which APS will use this method.

Section 8.0, "REFERENCES", on page 198, presents documents referenced in this report.

1.3 SUMMARY

Table 1-2 summarizes the 95/95 tolerance limits calculated in Sections 4, 5, and 6. The tolerance limits are such that, when applied to the CASMO-4/SIMULATE-3 results, there is a 95 percent probability, with a 95 percent confidence that the calculated values will conservatively bound the “true” values.

APS concludes that this method is acceptable for the performance of all steady-state PWR core physics analyses, including:

- reload design
- physics input to safety analyses
- physics input to fuel and clad performance
- physics input to mechanical design
- physics input to thermal-hydraulic analysis
- input to LOCA/Non-LOCA transient analysis
- CECOR coefficients
- startup test predictions
- core physics data books
- Shutdown Margin
- inputs to reactor protection system and monitoring system (COLSS/CPC) functions and set-point and uncertainty updates
- other safety related physics parameters in support of refueling, safety analysis, and operation

Table 1-1 List of Key PWR Physics Parameters

- Core Reactivity
 - Hot Zero Power (HZP)
 - Hot Full Power (HFP)
- Inverse Boron Worth (IBW)
- Doppler Only Power Coefficient (DOPC)
- Fuel Temperature Coefficient (FTC)
- Isothermal Temperature Coefficient (ITC)
- Control Rod (CEA) Worth
- Local Pin Power (Pin-to-Box)
- Assembly Power Peaking
 - F_q (box)
 - F_{xy} (box)
 - F_r (box)
- Pin Peaking
 - F_q (pin)
 - F_{xy} (pin)
 - F_r (pin)

Table 1-2 List of 95/95 Tolerance Limits (Bias ± Uncertainty)

Parameter	Bias	95/95 Uncertainty	Units*
HFP Core Reactivity (pcm)	331.5	226.8	Absolute
HZP Core Reactivity (pcm) (BOC only)	Bias = $(0.157 \times \alpha) - (60.136 \times \beta) + 322.427$ Where, α = Number of Fresh Erbium Rods β = BOC Core Average BU in GWD/MT	621.7	Absolute
Isothermal Temperature Coefficient (pcm/°F)	-0.28	1.52	Absolute
Control Rod Worth - Bank Worth - Total Worth - Dropped Worth - Ejected Worth - Net (N - 1) Worth	0.8% 1.0% []% -1.3% 1.0%	8.3% 7.1% [] [] 7.1%	Relative
Inverse Boron Worth (ppm/ %Δk/k)	-3.16%	13.49%	Relative
Doppler Power Coefficient (pcm/% power)	Bias = $-5.704 + 1.115 \times \text{CAB}(\text{GWD/MT}) + 3.87\text{E-}03 \times \text{P}(\%)$, where CAB is the core average burnup	20.6%	Relative
Fuel Temperature Coefficient (pcm/°F)	-0.8%	16.4%	Relative
Local Pin Power (Pin-to-Box)	[]	[]	Relative
Calculated Assembly Peaking - F_q (box) - F_r (box) - F_{xy} (box)	0% 0% 0%	5.34% 3.25% 3.69%	Relative

Table 1-2 List of 95/95 Tolerance Limits (Bias ± Uncertainty)

Parameter	Bias	95/95 Uncertainty	Units*
Measured Instrumented Assembly Peaking 61 Detector Strings - F_q (box) - F_r (box) - F_{xy} (box) 50 Detector Strings - F_q (box) - F_r (box) - F_{xy} (box)	 0% 0% 0% 0% 0% 0%	 2.49% 2.49% 2.71% 2.57% 2.85% 2.87%	Relative
Calculated Pin Peaking - F_q (pin) - F_r (pin) - F_{xy} (pin)	 [] [] []	 [] [] []	Relative
Measured Pin Peaking 61 Detector Strings - F_q (pin) - F_r (pin) - F_{xy} (pin) 50 Detector Strings - F_q (pin) - F_r (pin) - F_{xy} (pin)	 [] [] [] [] [] []	 [] [] [] [] [] []	Relative

*For those parameters with differences expressed in relative units:

$$\text{Predicted} = \text{Calculated} * (1 + (\text{Bias} \pm \text{Uncertainty})/100)$$

*For parameters with differences in absolute units, the following equation applies:

$$\text{Predicted} = \text{Calculated} + \text{Bias} \pm \text{Uncertainty}$$

*For target Keff calculations:

$$K_{eff} = 1 / (1 - \rho \times 10^{-5})$$

where target ρ = -bias

2.0 DESCRIPTION OF METHOD

2.1 INTRODUCTION

This section provides a brief description of the CASMO-4/SIMULATE-3 method. Yankee Atomic Electric Company (YAEC) has already presented the theoretical bases and validation of CASMO-3 and SIMULATE-3 before the Nuclear Regulatory Commission (NRC). The computer program package has received NRC approval for use in core physics calculations (References 8 and 9). Arizona Public Service (APS) Company's reactor core physics method uses CASMO-4 rather than CASMO-3. The method for CASMO-4 is described in Reference 2, and verification and validation information is given in References 20 and 21.

2.2 COMPUTER PROGRAM DESCRIPTIONS

The CASMO-4/SIMULATE-3 computer program package (References 1 through 5) was developed by STUDSVIK of America (currently Studsvik Scandpower, Inc.), Inc., Newton, Massachusetts and STUDSVIK Core Analysis AB, Nykoping, Sweden. The computer program package consists of four computer programs:

- CASMO-4,
- CASLIB,
- TABLES-3/CMS-LINK, and
- SIMULATE-3

Additionally, APS uses the APS CECORLIB (References 22 and 37) and the ABB CECOR (Reference 25) computer programs to process measured power distribution data.

The computer program sequence flow chart is shown in Figure 2-1.

2.2.1 CASMO-4

CASMO-4 is a multigroup, two-dimensional transport theory computer program (References 1 and 2) for burnup calculations on assemblies or pin cells. The code handles a geometry consisting of cylindrical fuel rods of varying composition in a square pitch array. CASMO-4 can model fuel rods, burnable absorber rods, control rods, guide tubes, in-core instruments, water gaps, and reflectors.

New features of CASMO-4 over CASMO-3 are the incorporation of the microscopic depletion of burnable absorbers into the main calculation, and the introduction of a heterogeneous model for the two-dimensional calculation. Also new in CASMO-4 is the use of the characteristics form for solving the transport equation.

CASMO-4 generates all cross section data for SIMULATE-3. APS typically uses CASMO-4 in a single assembly format with reflective boundary conditions, with a 70-energy group cross section

library. The homogeneous pin cell calculations use 40 groups, and the 2D (heterogeneous across entire lattice) calculations use 12 groups.

2.2.2 CASLIB

CASLIB (Reference 3) produces a binary neutron cross section library for input to CASMO-4 from a card-image, formatted library. The card-image, formatted library, supplied with CASMO-4 from STUDSVIK, is based mainly on data from ENDF/B-IV, although some data come from other sources. Both forty- and seventy-group cross section data are available for over 100 materials.

2.2.3 TABLES-3/CMS-LINK

TABLES-3 (Reference 4) is a data processing program that links CASMO-4 to SIMULATE-3. The program processes the following types of data from CASMO-4:

- two-group cross sections,
- discontinuity factors,
- fission product data,
- in-core instrument response data,
- pin power reconstruction data,
- kinetics data, and
- isotopics data.

TABLES-3 reads the CASMO-4 card image files and produces a master binary cross section library for SIMULATE-3. CMS-LINK (References 18 and 19) is a modern version of TABLES-3, which performs all of the above functions in a more automated manner. In addition, CMS-LINK processes additional CASMO data for (future) use with space-time kinetics calculations.

2.2.4 SIMULATE-3

SIMULATE-3 is a two- or three-dimensional (2-D or 3-D), two-group coarse mesh diffusion theory reactor simulator program (Reference 5). The program explicitly models the baffle/reflector region, eliminating the need to normalize to higher-order fine mesh calculations such as PDQ. Homogenized cross sections and discontinuity factors are applied to the coarse mesh nodal model to solve the two-group diffusion equation using the QPANDA neutronics model. QPANDA employs fourth order polynomial representations of the intra-nodal flux distributions in both the fast and thermal groups.

The nodal thermal hydraulic properties are calculated based on the inlet temperature, RCS pressure, coolant mass flow rate, and the heat addition along the channels.

The pin-by-pin power distributions, on a 2-D or 3-D basis, are constructed from the inter- and intra-assembly information from the coarse mesh solution and the pin-wise assembly power distribution from CASMO-4.

The SIMULATE-3 program performs a macroscopic depletion. Individual Uranium, Plutonium, and lumped fission product isotopic concentrations are not computed. However, microscopic depletion of Iodine, Xenon, Promethium, and Samarium is included to model typical reactor transients.

2.2.5 CECORLIB

The APS CECORLIB code is a computer program developed at Southern California Edison (SCE) Company (Reference 22) and modified by APS (Reference 37). CECORLIB prepares libraries of signal-to-box-power conversion factors, single pin power peaking factors, coupling coefficients, azimuthal tilt functions, and axial fitting parameters from SIMULATE-3 summary files. These libraries are referred to collectively as CECOR coefficients and are input to the ABB CECOR System.

A more detailed description of the APS CECORLIB code is given in Reference 37.

2.2.6 CECOR

The ABB CECOR System synthesizes detailed three dimensional assembly and peak pin power distributions from the signals of a limited number of fixed, self-powered neutron sensitive in-core detectors. The actual synthesis is done in the CECOR program using libraries of pre-calculated coefficients generated by the CECORLIB code. The system is used to fulfill the required startup testing, monitoring, and surveillance functions as well as to provide the basis of measurement information for core-follow and methods verification.

A more detailed description of the ABB CECOR System is given in Section II.1 of Reference 25.

2.3 MODEL DESCRIPTIONS

2.3.1 CASMO-4 FUEL ASSEMBLY AND REFLECTOR MODELS

Each unique PWR fuel assembly type (defined by geometry, enrichment, and burnable poison pins) is separately modeled in CASMO-4 using octant symmetry. Enrichment zoning among fuel pins, burnable poison pins, and guide tubes are explicitly modeled. The water gap between assemblies in the reactor core is included in the CASMO-4 model. The spacer grid material is also included. Design bases documents such as the Updated Final Safety Analysis Report (FSAR), reload reports, and as-built drawings provide the necessary data to develop the CASMO-4 assembly models.

Several depletion cases are needed to generate each fuel assembly type's average cross section data. First, the fuel assembly is depleted at hot full power, no control rods, reactor average conditions. Moderator temperature, fuel temperature, and soluble boron concentration are set to constant average values for the complete depletion. Next, depletions called history depletions are performed at various other moderator temperatures, fuel temperatures, and boron concentrations. Each fuel assembly type is depleted to burnups which bracket licensed burnup limits.

Branch cases are performed to calculate instantaneous effects. The branch cases are executed from the hot full power reactor average conditions and from the history conditions discussed above at a selection of exposures. Branch cases are run for a range of boron concentrations, moderator temperatures, control rod conditions, and fuel temperatures. Both isothermal and non-isothermal cases are performed.

CASMO-4 also generates top, bottom, and radial reflector cross sections. The radial reflector consists of the stainless steel core baffle followed by about 15 centimeters (cm) of water. The top reflector extends from the top of the active fuel to the top of the zircaloy end tips of the fuel pins. The bottom reflector extends from the bottom of the active fuel to about 11 cm below the surface of the core support plate. Reflector cross sections are typically modeled as a function of soluble boron concentration and moderator temperature.

2.3.2 TABLES-3/CMS-LINK MODEL

The TABLES-3 (or CMS-LINK) program generates a one-, two-, or three-dimensional cross section set for SIMULATE-3. Typically, data from the following CASMO-4 card image files are combined into binary cross section libraries for input to SIMULATE-3:

- HFP Reactor Average Depletion + Branches + History Depletions,
 - Fuel Temperature Branches
 - Moderator Temperature Branches
 - Soluble Boron Concentration Branches
 - Control Rod Insertion Branches
 - Cold Branches ($293\text{ K} < T < 569\text{ K}$)
 - Boron History
 - Fuel Temperature History
 - Moderator Temperature History
- Bottom Reflector
- Top Reflector
- Radial Reflector

Cross sections are typically calculated for cycle specific assembly lattice configurations and enrichments.

2.3.3 SIMULATE-3 MODEL

The APS SIMULATE-3 model divides the active fuel region into 25 axial nodes and four radial nodes per assembly. A pseudo-assembly, consisting of reflector material, surrounds the core and

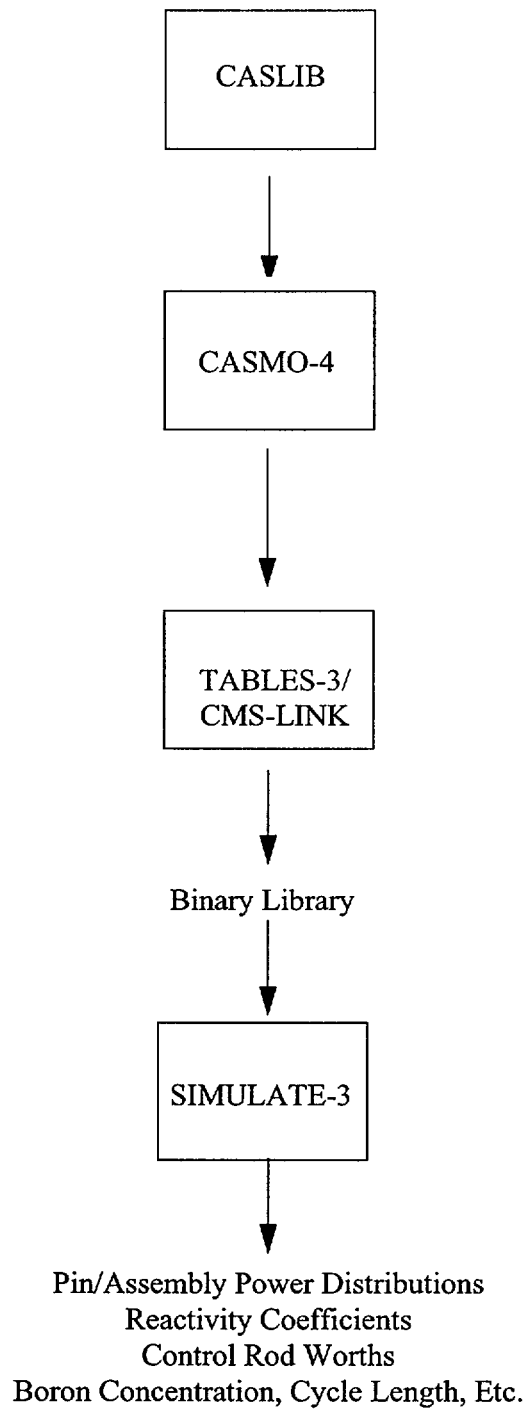
is divided into one radial and 25 axial nodes. Axially, the fuel is divided into a single bottom reflector node, 25 nodes for the active fuel region, and a single top reflector node.

Additional model input data are the:

- Full core assembly serial number map,
- Quarter core fuel assembly type map,
- Fuel assembly axial zone definition, including reflectors,
- Control rod locations,
- Grouping of control rods into banks,
- Axial zone definitions for control rods,
- In-core instrumentation locations,
- Fuel temperature versus power level and burnup correlation
- Core MW-thermal output at 100% power,
- Assembly pitch and core height,
- Assembly grid locations and compositions,
- Uranium loading in fuel,
- Detector data,
- Core pressure, power density, and coolant mass flow rate at 100% power conditions,
- Coolant inlet temperature versus power level,
- Input restart files, and
- Output restart files.

After the cycle base model is set up, the user can specify the percent power level, coolant inlet temperature and flow, rod bank positions (percent withdrawn), output and edit options, and the type of calculation: depletion, xenon transient, coefficient calculation, e.g., ITC, IBW, FTC, etc.

Figure 2-1 Program Sequence Flow Chart



3.0 DESCRIPTION OF REACTORS USED IN THE BENCHMARK

This report compares the CASMO-4/SIMULATE-3 predictions of key physics parameters against measured plant data. Data from Palo Verde Nuclear Generating Station (PVNGS) Units 1, 2, and 3 and from critical experiments were used.

The following sections provide a brief description of the Palo Verde reactor cores. Detailed descriptions can be found in Reference 10. A brief description of the core used in the RPI Critical experiment is included in Section 5.2. The cores used in the B&W critical experiments are described in Reference 31.

Each of the 3 PVNGS units is a Combustion Engineering (CE) pressurized water reactor using two reactor coolant loops. Each unit currently produces 3876 megawatts-thermal at 100% power. Unit 1 began commercial operation on January 23, 1986, Unit 2 on September 19, 1986, and Unit 3 on January 8, 1988.

The PVNGS reactors have operated at a variety of operating conditions. Each unit began commercial operation producing 3800 megawatts-thermal at 100% power. Between March, 1993 and Spring of 1994 all three units changed from a fixed inlet temperature (565°F) to a variable inlet temperature ranging from 555°F at 100% power to 565°F at <20% power. During this time period, each unit also had a brief period of operation at 85% power. After several cycles, all three units were stretched to 3876 megawatts-thermal. Unit 1 was stretched starting with Cycle 7, Unit 2 was stretched during Cycle 7, and Unit 3 was stretched during Cycle 6. To facilitate the stretch, the inlet temperature at 100% power was decreased from 555°F to 554°F.

There has also been a wide range of cycle lengths. The shortest cycle was Unit 1 Cycle 2, at 284 EFPD, whereas recent cycle lengths have been as long as ~525 to 530 EFPD.

The reactor core is composed of 241 fuel assemblies and 89 control element assemblies (CEAs) as shown in Figure 3-1. The fuel assemblies are arranged to approximate a right circular cylinder with an equivalent diameter of 143.6 inches and an active length of 150 inches. Each fuel assembly, which provides for 236 fuel rod positions (16 X 16 array), consists of 5 guide tubes welded to spacer grids and is closed at the top and bottom by end fittings. The guide tubes each displace four fuel rod positions and provide channels which guide the CEAs over their entire length of travel. In-core instrumentation is installed in the central guide tube of selected fuel assemblies. The in-core instrumentation is routed into the bottom of the fuel assemblies through the bottom head of the reactor vessel.

There are 9 Zircaloy spacer grids in the active fuel region. There is also a lower Inconel spacer grid that affects power at the base of the fuel if the assembly is not Guardian Grid fuel. For fuel assemblies with the Guardian Grid, the active fuel region is higher in the core relative to the grids, ICIs, CEAs, excore detectors, etc. Therefore, the lower Inconel grid is below the active fuel region. For simplicity, the non-Guardian Grid models were modeled in CASMO-4 as 10 Zircaloy grids smeared along the 150 inch (381 cm) active length of the fuel. In the Guardian Grid model, 9 Zircaloy grids are smeared along the active length of the fuel. The explicit grids are modeled in SIMULATE-3 at a later time.

The first batches of Guardian Grid fuel occurred in Unit 1 Cycle 5, Unit 3 Cycle 5, and then Unit 2 Cycle 6. The first cycles in which all of the fuel (except a few reinserts) used the Guardian Grid were Unit 1 Cycle 7, Unit 3 Cycle 7, and then Unit 2 Cycle 8.

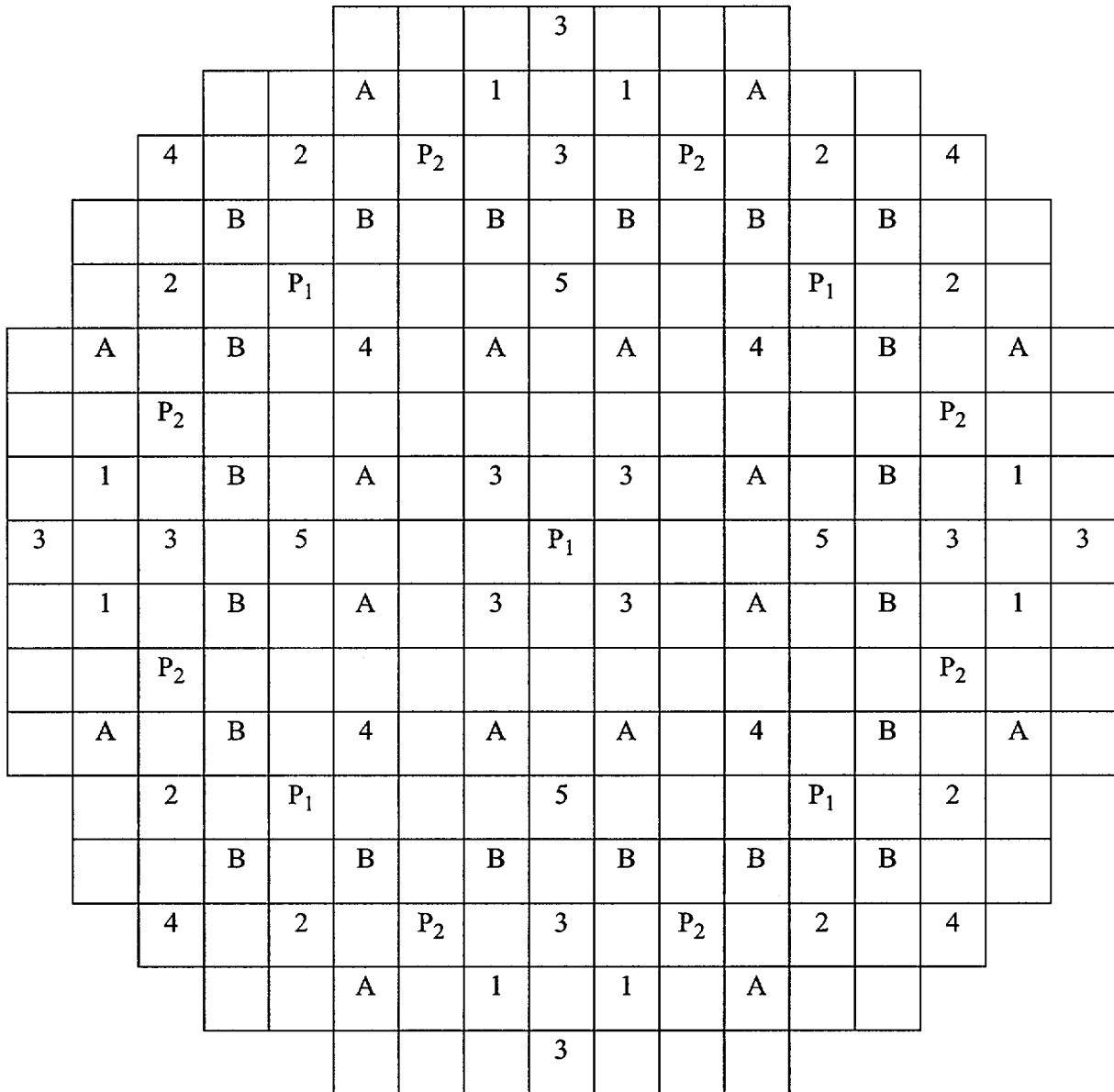
Each fuel rod consists of slightly enriched uranium in the form of sintered uranium dioxide pellets, enclosed in pressurized Zircaloy cladding. When used, discrete burnable absorber rods are provided in selected fuel assembly locations, and are mechanically similar to fuel rods. The original design of PVNGS fuel assemblies used aluminum oxide-boron carbide pellets for the discrete burnable absorber, whereas current reload designs have used the integral burnable absorber, erbium oxide. The erbium oxide is admixed with slightly enriched uranium. The current erbium oxide loading is 2.1 w/o. The first batches of erbium oxide fuel occurred in Unit 3 Cycle 5, Unit 2 Cycle 6, and then Unit 1 Cycle 6. The first cycles in which all of the fuel (except a few reinserts) used erbium oxide as a burnable absorber were Unit 3 Cycle 7, Unit 2 Cycle 8, and then Unit 1 Cycle 8.

The Value-Added pellet design was introduced in Palo Verde Unit 2 Cycle 5 as a design improvement. The Value-Added pellet is distinguished from prior pellet designs in operation at Palo Verde by a higher stack density, slightly greater diameter, and reduced chamfer and dish volume. The Value-Added pellet was introduced in the other Palo Verde units in Unit 1 Cycle 5 and Unit 3 Cycle 5. The Value-Added pellet design has been used in all subsequent and current cycles at Palo Verde.

Currently, there are 1 or 2 pin enrichments per assembly and 2 or three per reload. The intra-assembly enrichment split is typically between 0.0 w/o U-235 and 0.5 w/o U-235. When three enrichments per feed batch are used, the high and low enrichment pins are typically separated by an enrichment difference between 0.0 w/o U-235 and 0.8 w/o U-235.

Both conventional out-in and a variety of low leakage fuel management patterns have been used. A limited number of lead test assemblies that have not completed representative testing have occasionally been placed in non-limiting core regions.

Figure 3-1 Reactor Core and Control Rod Layout



4.0 BENCHMARK COMPARISONS

4.1 INTRODUCTION

This section provides comparisons of calculated and measured data resulting from Arizona Public Service's benchmark analysis used to verify the adequacy of the APS CASMO-4/SIMULATE-3 model. Comparisons are provided to measured data from zero power physics testing and operating data for Palo Verde Nuclear Generating Station Units 1, 2, and 3. Seven or eight cycles were analyzed for each unit for a total of 23 cycles, including both initial and reload cores, covering a wide variety of fuel types, operating conditions, and core loading patterns. The various fuel types, operating conditions, and core loading patterns are described in Section 3.0. For each parameter compared, a brief description of the measurement technique, statistical comparison technique, and the results obtained is given. Where applicable, the sample mean and standard deviation of the observed differences were calculated. The differences include both measurement and calculational differences. When measurement uncertainty data was available, a calculational uncertainty was calculated. Otherwise, for conservatism, all differences were assumed to be due only to CASMO-4/SIMULATE-3 calculational uncertainties. Based on the mean, standard deviation, and the sample size, a conservative 95/95 tolerance limit (bias \pm uncertainty) was calculated.

4.2 REACTIVITY BIASES AND UNCERTAINTY

SIMULATE-3 Critical Boron Concentration (CBC) and reactivity predictions were compared to zero-power startup test measurements as well as to full power operating data. The comparisons are divided into two categories. They are:

- Beginning-of-cycle (BOC) hot-zero-power (HZP) bias and uncertainty
- Overall reactivity bias and uncertainty (including a correction for B_{10} depletion)

4.2.1 BOC HOT-ZERO-POWER REACTIVITY

Measurement Technique

Critical boron concentrations are measured at hot-zero-power and hot-full-power by an acid-base titration of a reactor coolant system sample. The measurement uncertainty for critical boron concentrations is due to (1) error in the titration method and (2) error due to differences between the sample concentration and the core average concentration.

Comparison of Results

The reactivity bias at BOC has changed since erbium was introduced as the burnable absorber. Before Erbium, B_4C was used as the burnable absorber. With B_4C , CASMO-4/SIMULATE-3 tended to overpredict the BOC CBC. As erbium was introduced, CASMO-4/SIMULATE-3 tended to underpredict the BOC CBC. The bias has increased with the number of batches of erbium in the core, so the BOC reactivity biases are calculated from cores that contain at least two batches of erbium fuel. APS does not expect to return to core loading patterns using only discrete B_4C poison rods. The cycles with at least two batches of erbium are:

- U1C7 (2 Batches)
- U2C7 (2 Batches)
- U3C6 (2 Batches)
- U1C8 (3 Batches)
- U2C8 (3 Batches)
- U3C7 (3 Batches)

For each of these cycles a SIMULATE-3 case was run that calculated a CBC and a boron worth. These calculated CBCs were subtracted from the measured CBCs from zero-power startup test measurements. The ppm differences were multiplied by the boron worth in order to calculate a reactivity difference. There are a total of 6 data points.

Table 4-1 shows the comparison of the SIMULATE-3 calculated values and the measured values for BOC HZP.

Statistical Analysis

It was determined that the HZP BOC reactivity bias is a function of the number of erbium pins and the core average burnup.

A general additive multiple regression model, which relates a dependent variable y to k predictor variables x_1, x_2, \dots, x_k , is given by the model equation,

$$y = \alpha + \beta_1 x_1 + \beta_2 x_2 + \dots + \beta_k x_k$$

The BOC HZP reactivity bias is based on the multiple regression model given by the model equation,

$$y = \alpha + \beta_1 x_1 + \beta_2 x_2$$

The BOC HZP reactivity bias uses two predictor variables, x_1 and x_2 . The reactivity difference, in pcm, is y and the x 's are (1) number fresh erbium rods and (2) BOC Core Average Burnup (GWD/MT).

Once the statistical model was developed, a determination was made on whether or not the model was useful. The initial items examined were: R^2 and s_e .

$$R^2 = 1 - (SSResid)/(SSTo)$$

$$s_e = \sqrt{s_e^2} = \sqrt{(SSResid)/(n - (k + 1))}$$

Where,

$$SSResid = \sum (y - \hat{y})^2$$

$$SSTo = \sum (y - \bar{y})^2$$

n = Number of Observations

k = Number of Predictor Variables x_1, x_2, \dots, x_k .

Where,

\hat{y} = the predicted value from the predicted variables x_1, x_2, \dots, x_k .

\bar{y} = the mean of the y observations in the sample.

These values are known by the following names:

- R^2 -- R Square
- s_e -- Standard Error
- $SSResid$ -- Intersection of Residual and SS in the ANOVA Table
- $SSTo$ -- Intersection of Total and SS in the ANOVA Table
- $SSRegr$ -- Intersection of Regression and SS in the ANOVA Table

In general terms, a desirable model is one that results in both a large R^2 value and a small s_e value. However, these two conditions can be achieved by fitting a model that contains a large number of predictors. Such a model may be successful in explaining y variation, but it almost always specifies a relationship that is unrealistic and difficult to interpret. So two additional tests were performed, they are:

- F Test for Model Utility
- P -Value for an F Test

The value of F is calculated by the following equation:

$$F = ((SSRegr) \div k) / ((SSResid) \div (n - (k + 1)))$$

Where,

$$SSRegr = SSTo - SSResid$$

F is compared to F_{crit} . Where, F_{crit} is based on k numerator df (degrees of freedom) and $n - (k + 1)$ denominator df, respectively. F_{crit} values for tests with significance level of 0.05 (95/95) can be found in most statistics books. If the calculated value of F is greater than F_{crit} , then the model is useful, and the null hypothesis, denoted by H_0 , can be rejected.

The P -value for an F test is the smallest level of significance at which H_0 can be rejected. The P -value is known as the *Significance F*. For a 95/95 confidence level the P -value must be less than 0.05.

The preceding discussion on statistics comes from Reference 11.

In summary, a successful linear regression model should meet the following criteria:

- R^2 as close to 1.0 as possible, at least greater than 0.75.
- s_e as small as possible.
- F as large as possible, but it must be greater than F_{crit} .
- P as small as possible, but it must be less than 0.05.

Statistical Results

Table 4-2 presents the statistics for the HZP BOC reactivity differences.

The following two equations can be used to calculate the K_{eff} that will be input to SIMULATE-3 at HZP BOC:

$$1) \text{ Bias} = (0.157 \times \alpha) - (60.136 \times \beta) + 322.427$$

Where,

α = Number of Fresh Erbium Rods

β = BOC Core Average BU in GWD/MT

$$2) K_{eff} = 1 / (1 - \rho \times 10^{-5})$$

Where, the target reactivity is $\rho = -\text{Bias}$

Tolerance Limits:

$$\rho = (-0.157 \times \alpha) + (60.136 \times \beta) - 322.427 \pm 621.7$$

Table 4-1 HZP BOC Reactivity Differences

Unit and Cycle	Core Average Burnup (GWD/MT)	Number of Fresh Erbium Pins	Calculated		Measured		
			CBC (ppm)	BW (pcm/ppm)	CBC (ppm)	CBC Diff (M-C)	Reactivity Diff ^a (M-C)
U1C7	16.12	5184	2,057	-7.10	2,070	13	92
U2C7	13.80	5632	1,739	-7.84	1,785	46	361
U3C6	17.04	3008	1,890	-7.40	1,862	-28	-207
U1C8	17.27	6112	2,184	-6.88	2,208	24	165
U2C8	14.61	5632	2,125	-7.05	2,176	51	360
U3C7	16.75	6144	2,092	-7.07	2,149	57	403

- a. The reactivity difference is opposite in sign to the CBC Difference multiplied by the BW. If measured CBC is greater than calculated, and measured reactivity is 0.0, the reactivity calculated at the measured CBC would be negative, hence the reactivity difference (M-C) would be positive.

Table 4-2 HZP BOC Reactivity Multiple Linear Regression Model Statistics

Functionalization (Independent Variable)	Dependent Variable -- Reactivity Difference in pcm			
	R ² (>0.75)	F Test (>F _{crit} = 9.55)	P Value (<0.050)	S _e (small as possible)
Fresh Erbium Rods and BOC Core Average Burnup (GWD/MT)	0.895	12.72	0.034	97.6

The following two equations can be used to calculate the best-estimate K_{eff} that will be input to SIMULATE-3 at HZP BOC:

1) $Bias = (0.157 \times \alpha) - (60.136 \times \beta) + 322.427$

Where,

α = Number of Fresh Erbium Rods

β = BOC Core Average BU in GWD/MT

2) $K_{eff} = 1 / (1 - \rho \times 10^{-5})$

Where, the target reactivity is $\rho = -Bias$

Table 4-3 HZP BOC Reactivity Multiple Linear Regression Model 95/95 Uncertainty

Number of Data Points	Degrees of Freedom	K _{95/95} ^a (95/95 Tolerance Factor)	K _{95/95} *S _e (S _e from Table 4-2) (ρ)
6	3	6.370	621.7

a. Reference 13

Tolerance Limits:

$$\rho = (-0.157 \times \alpha) + (60.136 \times \beta) - 322.427 \pm 621.7$$

4.2.2 HOT-FULL-POWER REACTIVITY COMPARISONS

Measurement Technique

The measurement technique for hot-full-power CBC is described in Section 4.2.1.

Comparison of Results

The overall reactivity comparisons were based on the same cycles as the BOC HZP comparisons. For each of these cycles a SIMULATE-3 depletion case was run. These cases were based on operational data supplied by Reactor Engineering. The SIMULATE-3 HFP CBCs were adjusted for B₁₀ depletion. Due to downpowers, the B₁₀ depleted calculated CBCs required adjustment since the downpowers cause fresh boron to be injected into the RCS. These adjusted CBCs were then compared to measurements. The following criteria were used to determine if a calculated and measured data point can be compared: The points should be essentially unrodded, within ± 1 EFPD, within $\pm 0.75\%$ power, and be at a power level greater than 99%. There are a total of 279 data points in the distribution.

Table 4-4 lists the significant power reductions for cycles with at least 2 batches of erbium.

Table 4-5 shows the comparisons of the SIMULATE-3 calculated CBCs with the measured CBCs and the reactivity differences. The SIMULATE-3 calculated values have been corrected for B₁₀ depletion and downpowers.

Statistical Analysis

A statistical analysis was performed on the measured and SIMULATE-3 calculated reactivity differences. First, the bias (sample mean) and standard deviation were calculated. Secondly, the D' test (Reference 12) for normality was performed. The normality test is needed because the 95/95 tolerance limit assumes that the population has a normal distribution.

Statistical Results

Table 4-6 shows the reactivity difference statistics for the pooled data for all of the cycles with at least 2 batches of erbium.

The following two equations can be used to calculate the best-estimate K_{eff} that will be input to SIMULATE-3 at HFP:

$$1) \text{ Bias} = 331.5 \text{ pcm}$$

$$2) K_{\text{eff}} = 1 / (1 - \rho \times 10^{-5}), \text{ Where, the target reactivity is } \rho = -\text{Bias}$$

Tolerance Limits:

$$\rho = -331.5 \pm 226.8 \quad \text{pcm}$$

Table 4-4 Significant Downpowers for Cycles with at Least 2 Batches of Erbium

Unit and Cycle	Description
Unit 1 Cycle 7	<ul style="list-style-type: none"> • May 27, 1997; at 205 EFPD; reduced to 0% power; returning to full power on June 2, 1997. (PPM correction applied to the calculated CBC was -20.8.) • February 22, 1998; at 471 EFPD; reduced to 0% power; returning to full power on March 2, 1998. Since this occurred late in cycle there is no impact on the calculated CBC.
Unit 2 Cycle 8	<ul style="list-style-type: none"> • An early in life downpower occurred at ~5 EFPD. Since the B₁₀ concentration is fresh at BOL, the early downpower will not affect the B₁₀ concentration.
Unit 3 Cycle 6 ^a	<ul style="list-style-type: none"> • June 10, 1996; at 191 EFPD; reduced to 34.1% power; returning to full power on June 12, 1996. • June 25, 1996; at 205 EFPD; reduced to 26.9% power; returning to full power on June 28, 1996. <p>(PPM correction applied to the calculated CBC was -17.4.)</p>
Unit 3 Cycle 7	<ul style="list-style-type: none"> • June 1, 1997; at 58 EFPD; reduced to 0% power; returning to full power on June 6, 1997. Since this occurred early in cycle there is no impact on the calculated CBC. • November 7, 1997; at 215 EFPD; reduced to 40.0% power; returning to full power on November 10, 1997. (PPM correction applied to the calculated CBC was -11.3.)

a. These two events were treated as a single downpower, since they happened so close together.

Table 4-5 HFP Critical Boron/Reactivity Comparisons

Unit	Cycle	Power (%)	Burnup (EFPD)	Measured Boron (ppm)	Calculated Boron (ppm)	Calculated Boron Worth (pcm/ppm)	Difference Meas - Calc (ppm)	Difference ^a Meas - Calc (pcm)
1	7	99.97	6.91	1469	1448	-6.89	21	144.7
1	7	99.96	10.91	1456	1428	-6.89	28	192.9
1	7	99.99	14.90	1452	1417	-6.89	35	241.2
1	7	99.99	18.90	1441	1408	-6.89	33	227.4
1	7	99.98	27.90	1429	1394	-6.89	35	241.2
1	7	99.99	35.90	1420	1383	-6.89	37	254.9
1	7	99.96	41.90	1408	1366	-6.90	42	289.8
1	7	99.97	46.90	1405	1368	-6.90	37	255.3
1	7	99.99	51.90	1401	1358	-6.90	43	296.7
1	7	99.99	58.89	1386	1345	-6.91	41	283.3
1	7	99.99	66.89	1363	1330	-6.92	33	228.4
1	7	99.98	73.89	1357	1316	-6.94	41	284.5
1	7	99.92	76.89	1353	1309	-6.94	44	305.4
1	7	99.98	81.89	1350	1298	-6.95	52	361.4
1	7	99.35	89.88	1332	1281	-6.96	51	355.0
1	7	99.94	96.87	1321	1265	-6.98	56	390.9
1	7	99.98	103.87	1305	1248	-7.00	57	399.0
1	7	99.96	110.85	1285	1231	-7.01	54	378.5
1	7	99.93	117.85	1263	1213	-7.03	50	351.5
1	7	99.99	125.85	1250	1192	-7.05	58	408.9
1	7	99.99	140.85	1214	1150	-7.09	64	453.8
1	7	99.99	147.51	1193	1132	-7.12	61	434.3
1	7	99.99	155.51	1167	1112	-7.13	55	392.2
1	7	99.98	163.51	1152	1089	-7.16	63	451.1
1	7	99.99	170.50	1122	1070	-7.18	52	373.4

Table 4-5 HFP Critical Boron/Reactivity Comparisons

Unit	Cycle	Power (%)	Burnup (EFPD)	Measured Boron (ppm)	Calculated Boron (ppm)	Calculated Boron Worth (pcm/ppm)	Difference Meas - Calc (ppm)	Difference ^a Meas - Calc (pcm)
1	7	99.98	178.50	1101	1045	-7.21	56	403.8
1	7	99.99	185.50	1081	1025	-7.23	56	404.9
1	7	99.95	193.50	1055	1001	-7.26	54	392.0
1	7	99.99	204.50	1021	967	-7.30	54	394.2
1	7	99.99	212.55	976	921	-7.32	55	401.0
1	7	99.99	219.55	954	900	-7.35	54	398.9
1	7	99.99	227.55	926	875	-7.38	51	373.8
1	7	99.98	234.55	899	853	-7.41	46	341.8
1	7	99.99	242.55	872	827	-7.44	45	331.2
1	7	99.99	250.55	840	800	-7.47	40	298.1
1	7	99.99	257.54	819	779	-7.50	40	302.8
1	7	99.98	265.53	794	753	-7.53	41	306.9
1	7	99.87	281.47	738	698	-7.60	40	300.5
1	7	99.94	289.47	712	671	-7.64	41	312.7
1	7	99.99	296.47	689	648	-7.67	41	317.5
1	7	99.99	305.46	661	616	-7.71	45	344.7
1	7	99.99	312.45	631	592	-7.74	39	303.3
1	7	99.99	319.45	610	568	-7.77	42	323.6
1	7	99.99	326.45	584	542	-7.80	42	328.5
1	7	99.98	334.44	556	514	-7.84	42	325.4
1	7	99.91	342.44	527	487	-7.88	40	314.4
1	7	99.98	348.44	507	464	-7.92	43	344.0
1	7	99.99	357.01	468	433	-7.95	35	276.5
1	7	99.98	365.01	438	405	-8.00	33	265.4
1	7	99.99	379.92	387	352	-8.07	35	282.8
1	7	99.99	386.92	361	325	-8.11	36	287.9

Table 4-5 HFP Critical Boron/Reactivity Comparisons

Unit	Cycle	Power (%)	Burnup (EFPD)	Measured Boron (ppm)	Calculated Boron (ppm)	Calculated Boron Worth (pcm/ppm)	Difference Meas - Calc (ppm)	Difference ^a Meas - Calc (pcm)
1	7	99.99	394.92	332	296	-8.15	36	292.5
1	7	99.99	402.91	304	268	-8.20	36	297.5
1	7	99.99	410.91	273	238	-8.24	35	285.7
1	7	99.99	417.91	247	213	-8.28	34	282.7
1	7	99.99	423.91	226	191	-8.31	35	288.2
1	7	99.99	431.91	198	164	-8.35	34	285.2
1	7	99.99	436.91	180	142	-8.39	38	316.2
1	7	99.99	442.91	159	121	-8.42	38	321.9
1	7	99.96	448.90	134	98	-8.46	36	302.6
1	7	99.96	455.90	109	74	-8.50	35	299.5
1	7	99.89	462.90	83	46	-8.54	37	313.5
1	7	99.98	469.90	57	18	-8.59	39	335.9
1	7	99.99	480.27	26	-16	-8.65	42	366.6
1	7	99.71	485.27	6	-35	-8.68	41	355.9
1	8	99.99	9.16	1586	1534	-6.62	52	344.2
1	8	99.99	17.16	1567	1513	-6.62	54	357.5
1	8	99.99	25.16	1563	1502	-6.62	61	403.8
1	8	99.99	33.15	1556	1494	-6.62	62	410.4
1	8	99.99	40.15	1548	1486	-6.62	62	410.4
1	8	99.99	55.14	1534	1466	-6.64	68	451.5
1	8	99.99	62.14	1527	1455	-6.64	72	478.1
1	8	99.99	70.14	1512	1441	-6.65	71	472.2
1	8	99.79	77.12	1502	1428	-6.67	74	493.6
1	8	99.99	85.12	1469	1412	-6.68	57	380.8
1	8	99.98	93.09	1459	1393	-6.70	66	442.2
2	7	99.71	18.79	1221	1157	-7.64	64	489.0

Table 4-5 HFP Critical Boron/Reactivity Comparisons

Unit	Cycle	Power (%)	Burnup (EFPD)	Measured Boron (ppm)	Calculated Boron (ppm)	Calculated Boron Worth (pcm/ppm)	Difference Meas - Calc (ppm)	Difference ^a Meas - Calc (pcm)
2	7	99.94	23.79	1202	1146	-7.64	56	427.8
2	7	99.95	32.79	1182	1137	-7.64	45	343.8
2	7	99.94	36.78	1180	1131	-7.64	49	374.4
2	7	99.99	49.78	1165	1116	-7.65	49	374.9
2	7	99.95	62.77	1153	1096	-7.66	57	436.6
2	7	99.98	70.77	1143	1082	-7.67	61	467.9
2	7	99.98	73.76	1137	1077	-7.68	60	460.8
2	7	99.95	78.76	1119	1065	-7.69	54	415.3
2	7	99.98	85.76	1105	1054	-7.70	51	392.7
2	7	99.99	93.75	1087	1039	-7.72	48	370.6
2	7	99.99	101.73	1074	1023	-7.73	51	394.2
2	7	99.98	108.73	1062	1007	-7.75	55	426.3
2	7	99.72	117.70	1047	990	-7.77	57	442.9
2	7	99.98	124.70	1025	972	-7.79	53	412.9
2	7	99.98	132.70	1008	953	-7.81	55	429.6
2	7	99.99	139.70	984	937	-7.83	47	368.0
2	7	99.99	146.70	963	919	-7.85	44	345.4
2	7	99.99	154.69	946	900	-7.88	46	362.5
2	7	99.99	162.69	929	880	-7.90	49	387.1
2	7	99.99	170.69	909	859	-7.93	50	396.5
2	7	99.98	176.69	885	840	-7.95	45	357.8
2	7	99.96	185.69	866	818	-7.98	48	383.0
2	7	99.96	193.69	842	797	-8.01	45	360.5
2	7	99.25	199.68	828	777	-8.04	51	410.0
2	7	99.98	207.65	800	758	-8.07	42	338.9
2	7	99.99	215.65	770	735	-8.10	35	283.5

Table 4-5 HFP Critical Boron/Reactivity Comparisons

Unit	Cycle	Power (%)	Burnup (EFPD)	Measured Boron (ppm)	Calculated Boron (ppm)	Calculated Boron Worth (pcm/ppm)	Difference Meas - Calc (ppm)	Difference^a Meas - Calc (pcm)
2	7	99.99	223.65	749	712	-8.13	37	300.8
2	7	99.99	231.65	726	688	-8.16	38	310.1
2	7	99.99	238.65	706	667	-8.19	39	319.4
2	7	99.98	246.65	678	643	-8.23	35	288.1
2	7	99.99	254.65	650	619	-8.26	31	256.1
2	7	99.99	261.64	631	598	-8.29	33	273.6
2	7	99.99	269.64	602	573	-8.33	29	241.6
2	7	99.99	276.64	580	550	-8.36	30	250.8
2	7	99.98	283.64	551	528	-8.39	23	193.0
2	7	99.98	290.64	528	506	-8.43	22	185.5
2	7	99.99	297.64	510	483	-8.46	27	228.4
2	7	99.99	304.64	493	461	-8.50	32	272.0
2	7	99.99	311.63	470	438	-8.53	32	273.0
2	7	99.99	321.63	436	405	-8.58	31	266.0
2	7	99.99	328.63	413	381	-8.61	32	275.5
2	7	99.99	335.63	394	358	-8.65	36	311.4
2	7	99.98	343.62	363	331	-8.69	32	278.1
2	7	99.99	350.62	342	307	-8.73	35	305.6
2	7	99.99	358.62	311	280	-8.78	31	272.2
2	7	99.99	366.62	283	252	-8.82	31	273.4
2	7	99.99	374.62	256	225	-8.86	31	274.7
2	7	99.99	381.62	233	201	-8.90	32	284.8
2	7	99.94	389.62	208	173	-8.95	35	313.3
2	7	99.79	397.61	174	145	-9.00	29	261.0
2	7	99.98	404.22	148	122	-9.03	26	234.8
2	7	99.99	412.22	120	94	-9.08	26	236.1

Table 4-5 HFP Critical Boron/Reactivity Comparisons

Unit	Cycle	Power (%)	Burnup (EFPD)	Measured Boron (ppm)	Calculated Boron (ppm)	Calculated Boron Worth (pcm/ppm)	Difference Meas - Calc (ppm)	Difference ^a Meas - Calc (pcm)
2	7	99.99	418.82	97	71	-9.12	26	237.1
2	7	99.99	426.82	70	43	-9.17	27	247.6
2	7	99.99	434.82	43	15	-9.22	28	258.2
2	7	99.98	441.82	19	-9	-9.26	28	259.3
2	7	99.9	445.81	5	-27	-9.29	32	297.3
2	8	99.98	4.57	1587	1517	-6.82	70	477.4
2	8	99.97	15.11	1556	1482	-6.83	74	505.4
2	8	99.96	22.11	1547	1468	-6.82	79	538.8
2	8	99.99	30.11	1532	1457	-6.82	75	511.5
2	8	99.97	37.11	1522	1449	-6.82	73	497.9
2	8	99.99	41.11	1519	1446	-6.82	73	497.9
2	8	99.99	52.10	1507	1430	-6.83	77	525.9
2	8	99.98	60.10	1484	1412	-6.83	72	491.8
2	8	99.99	68.10	1472	1397	-6.84	75	513.0
2	8	99.99	74.10	1456	1387	-6.85	69	472.7
2	8	99.99	80.10	1440	1375	-6.86	65	445.9
2	8	99.99	87.10	1432	1360	-6.87	72	494.6
2	8	99.94	93.09	1417	1348	-6.88	69	474.7
2	8	99.99	99.09	1401	1334	-6.89	67	461.6
2	8	99.24	106.08	1387	1318	-6.90	69	476.1
2	8	99.99	113.08	1365	1302	-6.92	63	436.0
2	8	99.99	120.08	1354	1285	-6.93	69	478.2
2	8	99.99	127.08	1338	1268	-6.95	70	486.5
2	8	99.99	134.08	1314	1250	-6.97	64	446.1
2	8	99.99	140.08	1297	1234	-6.98	63	439.7
2	8	99.99	146.08	1283	1219	-7.00	64	448.0

Table 4-5 HFP Critical Boron/Reactivity Comparisons

Unit	Cycle	Power (%)	Burnup (EFPD)	Measured Boron (ppm)	Calculated Boron (ppm)	Calculated Boron Worth (pcm/ppm)	Difference Meas - Calc (ppm)	Difference ^a Meas - Calc (pcm)
2	8	99.99	152.08	1266	1203	-7.02	63	442.3
2	8	99.99	158.08	1250	1186	-7.03	64	449.9
2	8	99.99	165.08	1234	1167	-7.05	67	472.4
2	8	99.99	173.08	1202	1145	-7.07	57	403.0
2	8	99.98	180.07	1184	1125	-7.10	59	418.9
2	8	99.99	188.07	1165	1103	-7.12	62	441.4
2	8	100	196.07	1145	1082	-7.14	63	449.8
2	8	99.99	204.07	1116	1058	-7.17	58	415.9
2	8	99.96	212.07	1095	1034	-7.20	61	439.2
2	8	99.96	219.07	1069	1013	-7.22	56	404.3
2	8	99.99	227.07	1039	987	-7.25	52	377.0
2	8	100	234.07	1017	965	-7.27	52	378.0
2	8	99.99	241.07	998	943	-7.30	55	401.5
2	8	100	249.07	971	917	-7.33	54	395.8
2	8	99.99	256.06	939	896	-7.36	43	316.5
2	8	99.99	264.06	914	869	-7.39	45	332.6
3	6	99.98	9.13	1304	1297	-7.23	7	50.6
3	6	99.99	16.13	1298	1274	-7.23	24	173.5
3	6	100.00	23.13	1260	1258	-7.24	2	14.5
3	6	99.99	40.09	1245	1223	-7.26	22	159.7
3	6	99.99	53.08	1213	1194	-7.28	19	138.3
3	6	99.95	61.08	1200	1175	-7.29	25	182.3
3	6	99.99	68.08	1187	1158	-7.31	29	212.0
3	6	99.98	75.08	1167	1140	-7.33	27	197.9
3	6	99.96	83.08	1157	1119	-7.35	38	279.3
3	6	99.94	89.34	1140	1103	-7.37	37	272.7

Table 4-5 HFP Critical Boron/Reactivity Comparisons

Unit	Cycle	Power (%)	Burnup (EFPD)	Measured Boron (ppm)	Calculated Boron (ppm)	Calculated Boron Worth (pcm/ppm)	Difference Meas - Calc (ppm)	Difference ^a Meas - Calc (pcm)
3	6	99.99	99.34	1109	1075	-7.39	34	251.3
3	6	99.99	106.34	1091	1055	-7.42	36	267.1
3	6	99.98	113.33	1068	1035	-7.44	33	245.5
3	6	99.98	120.33	1047	1013	-7.46	34	253.6
3	6	99.98	128.33	1025	990	-7.49	35	262.2
3	6	99.98	132.33	1015	979	-7.50	36	270.0
3	6	99.98	141.32	981	951	-7.53	30	225.9
3	6	99.99	149.32	960	924	-7.56	36	272.2
3	6	99.98	157.32	929	902	-7.59	27	204.9
3	6	99.98	166.32	904	874	-7.62	30	228.6
3	6	99.97	174.32	875	845	-7.66	30	229.8
3	6	99.98	180.31	852	821	-7.69	31	238.4
3	6	99.88	190.31	813	791	-7.72	22	169.8
3	6	99.99	196.44	773	755	-7.76	18	143.1
3	6	99.90	208.92	732	714	-7.81	18	143.9
3	6	99.92	215.92	706	690	-7.84	16	124.5
3	6	99.99	222.92	680	667	-7.87	13	104.9
3	6	99.98	229.92	661	644	-7.90	17	132.6
3	6	99.96	234.92	648	627	-7.92	21	169.4
3	6	99.98	239.92	629	609	-7.94	20	158.8
3	6	99.99	245.91	611	589	-7.97	22	171.6
3	6	99.98	260.43	556	541	-8.05	15	123.9
3	6	99.99	269.43	524	509	-8.09	15	118.8
3	6	99.86	276.43	501	485	-8.12	16	131.0
3	6	99.99	287.42	463	447	-8.18	16	133.1
3	6	99.98	299.39	421	407	-8.24	14	118.1

Table 4-5 HFP Critical Boron/Reactivity Comparisons

Unit	Cycle	Power (%)	Burnup (EFPD)	Measured Boron (ppm)	Calculated Boron (ppm)	Calculated Boron Worth (pcm/ppm)	Difference Meas - Calc (ppm)	Difference ^a Meas - Calc (pcm)
3	6	99.99	306.39	393	382	-8.28	11	89.2
3	6	100.00	314.39	368	353	-8.32	15	126.1
3	6	99.98	322.38	342	323	-8.36	19	154.9
3	6	99.98	329.38	317	297	-8.41	20	167.3
3	6	99.98	336.37	294	275	-8.44	19	163.9
3	6	99.98	344.37	265	247	-8.48	18	151.0
3	6	99.82	352.37	239	219	-8.53	20	172.1
3	6	99.76	360.37	206	190	-8.57	16	133.3
3	6	99.99	368.36	183	161	-8.62	22	189.0
3	6	99.99	376.36	155	131	-8.66	24	210.4
3	6	99.99	384.36	128	104	-8.71	24	206.1
3	6	99.99	391.36	102	80	-8.76	22	193.8
3	6	99.96	399.36	74	52	-8.80	22	197.9
3	6	99.99	407.36	46	22	-8.85	24	211.2
3	6	99.99	412.36	29	4	-8.88	25	226.2
3	6	99.86	418.35	6.2	-18	-8.92	24	215.9
3	7	100.00	12.49	1503	1442	-6.82	61	416.0
3	7	99.99	19.48	1498	1430	-6.81	68	463.1
3	7	99.98	34.48	1492	1414	-6.81	78	531.2
3	7	99.98	38.48	1491	1411	-6.81	80	544.8
3	7	99.98	50.48	1477	1398	-6.82	79	538.8
3	7	99.99	58.48	1471	1385	-6.82	86	586.5
3	7	99.94	70.41	1442	1366	-6.84	76	519.8
3	7	100.00	78.41	1435	1352	-6.85	83	568.6
3	7	99.98	85.41	1408	1339	-6.86	69	473.3
3	7	99.98	93.09	1399	1324	-6.88	75	516.0

Table 4-5 HFP Critical Boron/Reactivity Comparisons

Unit	Cycle	Power (%)	Burnup (EFPD)	Measured Boron (ppm)	Calculated Boron (ppm)	Calculated Boron Worth (pcm/ppm)	Difference Meas - Calc (ppm)	Difference ^a Meas - Calc (pcm)
3	7	99.99	100.09	1375	1309	-6.89	66	454.7
3	7	99.99	108.09	1366	1291	-6.90	75	517.5
3	7	99.76	116.08	1346	1273	-6.92	73	505.2
3	7	99.99	131.25	1306	1239	-6.96	67	466.3
3	7	99.99	176.25	1174	1118	-7.09	56	397.0
3	7	99.69	184.21	1160	1096	-7.11	64	455.0
3	7	99.98	192.21	1125	1073	-7.14	52	371.3
3	7	99.99	199.21	1106	1052	-7.16	54	386.6
3	7	99.88	207.21	1077	1027	-7.18	50	359.0
3	7	99.99	214.21	1055	1006	-7.21	49	353.3
3	7	99.99	221.42	1021	973	-7.23	48	349.5
3	7	99.96	229.42	997	948	-7.26	49	355.3
3	7	99.95	236.42	974	927	-7.29	47	339.9
3	7	99.98	244.42	942	902	-7.32	40	294.7
3	7	99.99	252.42	924	877	-7.35	47	344.7
3	7	99.99	260.42	892	851	-7.38	41	299.1
3	7	99.99	267.42	874	828	-7.41	46	342.5
3	7	99.99	273.42	850	808	-7.43	42	311.7
3	7	99.99	280.41	826	784	-7.46	42	310.5
3	7	99.92	286.41	807	764	-7.49	43	324.7
3	7	99.98	292.41	785	743	-7.51	42	316.1
3	7	99.98	298.41	766	723	-7.54	43	322.8
3	7	99.99	305.41	743	700	-7.57	43	329.3
3	7	99.99	312.41	719	674	-7.60	45	343.4
3	7	99.99	319.41	696	650	-7.63	46	350.0
3	7	99.99	326.41	669	625	-7.66	44	333.6

Table 4-5 HFP Critical Boron/Reactivity Comparisons

Unit	Cycle	Power (%)	Burnup (EFPD)	Measured Boron (ppm)	Calculated Boron (ppm)	Calculated Boron Worth (pcm/ppm)	Difference Meas - Calc (ppm)	Difference ^a Meas - Calc (pcm)
3	7	99.99	334.28	623	602	-7.70	21	163.5
3	7	99.99	339.28	621	580	-7.72	41	316.3
3	7	99.98	345.27	601	559	-7.75	42	323.1
3	7	99.99	351.27	584	537	-7.78	47	369.0
3	7	99.99	357.27	560	514	-7.81	46	360.5
3	7	99.99	365.27	535	487	-7.85	48	375.2
3	7	99.99	373.27	506	456	-7.89	50	397.9
3	7	99.99	380.27	481	432	-7.93	49	389.5
3	7	99.99	387.27	455	405	-7.96	50	396.4
3	7	100.00	395.27	424	377	-8.00	47	379.5
3	7	99.99	403.27	396	347	-8.04	49	394.6
3	7	99.99	411.27	364	317	-8.09	47	377.9
3	7	99.98	418.26	340	291	-8.12	49	401.1
3	7	99.96	426.26	309	261	-8.16	48	391.9
3	7	99.97	433.26	282	236	-8.20	46	374.8
3	7	99.97	440.26	254	210	-8.24	44	365.8
3	7	99.99	448.26	224	180	-8.29	44	365.1
3	7	100.00	455.17	193	154	-8.33	39	322.6
3	7	99.99	463.17	164	124	-8.37	40	337.8
3	7	99.99	471.16	135	93	-8.41	42	353.2

a. The reactivity difference is opposite in sign to the CBC Difference multiplied by the BW. If measured CBC is greater than calculated, and measured reactivity is 0.0, the reactivity calculated at the measured CBC would be negative, hence the reactivity difference (M-C) would be positive.

Table 4-6 Full Power Reactivity Difference Statistics

	pcm
Bias (Meas - Calc)	331.5
Standard Deviation (S)	107.4
Number of Data Points	279
Degrees of Freedom	278
D' Value	1,317.7
Critical Value(s)	1,295.1 1,328.0
Normal Distribution?	Yes
$K_{95/95}^a$ (95/95 Tolerance Factor)	2.112
$K_{95/95} * S$	226.8
Tolerance Limit^b	-331.5 ± 226.8

- a. Reference 13
- b. The bias, based on (M-C) is positive. The measured reactivity is 0.0, and the calculated reactivity at the measured critical ppm is negative since the measured ppm is always larger. The target reactivity (ρ) which controls K_{eff} is equal to -bias, because the standard K_{eff} definition of $1/(1-\rho)$ must be less than unity for the core to be critical.

4.3 ITC BIAS AND UNCERTAINTY

Measurement Technique

The isothermal temperature coefficient (ITC) is the change in the reactivity due to a 1°F change in the core average moderator and fuel temperature. There are two different methods used in measuring ITC. At hot zero power (HZP), the temperature is decreased/increased by increasing/decreasing steam bypass. The resulting change in reactivity is read from the reactivity computer, based on the change in flux. The measurement of at-power ITC is done with coordinated changes in control rod position and turbine load while maintaining power constant and noting the change in reactor coolant system temperature. The resulting change in temperature is then used in conjunction with the predicted rod worth to determine ITC.

The measurement uncertainty for HZP ITCs is due to (1) measured core inlet moderator temperature uncertainty and (2) calculated reactivity computer data uncertainty. The measurement uncertainty for HFP ITCs is due to (1) measured core inlet moderator temperature uncertainty, (2) measured control rod position uncertainty, (3) measured core power uncertainty (4) calculated control rod worth uncertainty, (5) calculated ratio of core average moderator temperature to core inlet moderator temperature uncertainty, and (6) calculated power coefficient uncertainty.

Comparison of Results

Table 4-7 and Table 4-8 list the HZP and at-power comparisons of the calculated ITC's with measurements at PVNGS Units 1, 2, and 3. ITCs were calculated at numerous points in core life; BOC HZP, ~40 EFPD HFP, 2/3 cycle HFP for Cycles 1 - 7, and miscellaneous points early in core life for Cycles 1 - 3 of all Units. The power level, control rod position, and core exposure (EFPD) are also included. There are a total of 70 measurements from 21 cycles of operation.

Statistical method

The data were initially grouped according to power level, core exposure, Unit 1, Unit 2, and Unit 3. The data were also all grouped together (all power levels, Units, and times-in-life). For each grouping of data, a bias and standard deviation was calculated, along with a determination of normality, and whether or not the ITC differences were a function of boron concentration. The data showed that none of the groupings had a significant dependence on boron concentration except the Unit 3 data grouping. Rather than have a unit based bias, and because the "all data" grouping displays normality and has the most data points, it was used to determine the ITC bias and 95/95 uncertainty. Because the distribution has more than 50 points, the *D'* test (Reference 12) for normality was used.

Statistical Results

Table 4-9 shows the results of the statistical analysis for the ITC differences.

The tolerance limits for ITC at any power level or time-in-life are:

$$-0.28 \pm 1.517 \text{ pcm/}^{\circ}\text{F}$$

Table 4-7 HZP ITC Comparisons

Unit	Cycle	Control Rod Position	ITC Measurement (pcm/°F)	ITC Calculation (pcm/°F)	ITC Difference (M-C) (pcm/°F)
1	1	ARO	-4.40	-3.22	-1.18
1	2	ARO	+1.52	+2.23	-0.71
1	3	ARO	+1.35	+1.51	-0.16
1	4	ARO	-2.081	-1.76	-0.32
1	5	ARO	-1.28	-1.38	+0.10
1	6	ARO	-0.44	-0.23	-0.21
1	7	ARO	-0.38	-0.19	-0.19
2	1	ARO	-4.28	-3.41	-0.87
2	2	ARO	-0.48	-0.37	-0.11
2	3	ARO	+0.65	+1.10	-0.45
2	4	ARO	+1.759	+1.91	-0.15
2	5	ARO	-0.671	-0.55	-0.12
2	6	ARO	-0.70	-0.29	-0.41
2	7	ARO	-1.26	-0.99	-0.27
3	1	ARO	-3.79	-3.27	-0.52
3	2	ARO	+0.62	+1.36	-0.74
3	3	ARO	+0.87	+1.08	-0.21
3	4	ARO	+0.41	+0.56	-0.15
3	5	ARO	+1.01	+0.90	+0.11
3	6	ARO	-2.85	-1.15	-1.70
3	7	ARO	0.76	0.62	+0.14

Table 4-8 At-Power ITC Comparisons

Unit	Cycle	Power (%)	EFPD	Measurement (pcm/°F)	Calculation (pcm/°F)	Difference (M-C) (pcm/°F)
1	1	20	3	-6.722	-6.29	-0.43
1	1	50	7	-9.200	-8.78	-0.42
1	1	80	26	-9.506	-9.95	+0.44
1	1	100	56	-10.581	-11.17	+0.59
1	2	100	40	-9.672	-9.25	-0.42
1	2	100	223	-23.197	-23.35	+0.15
1	3	100	10	-8.691	-8.42	-0.27
1	3	100	41	-8.590	-9.07	+0.48
1	3	100	336	-22.703	-22.12	-0.58
1	4	100	41	-14.748	-14.23	-0.52
1	4	100	295	-28.126	-27.23	-0.90
1	5	85	43	-10.912	-11.13	+0.22
1	5	100	292	-21.013	-21.47	+0.46
1	6	100	42	-10.767	-11.61	+0.84
1	6	100	295	-25.211	-25.31	+0.10
1	7	100	41	-11.276	-11.08	-0.20
2	1	50	14	-7.965	-8.52	+0.56
2	1	100	28	-11.103	-11.68	+0.58
2	1	100	289	-18.036	-16.97	-1.07
2	2	100	15	-10.194	-10.17	-0.02
2	2	100	44	-10.436	-11.21	+0.77
2	2	100	282	-24.042	-22.56	-1.48
2	3	100	11	-9.706	-9.36	-0.35
2	3	100	43	-11.223	-10.82	-0.40
2	3	100	287	-23.571	-22.54	-1.03

Table 4-8 At-Power ITC Comparisons

Unit	Cycle	Power (%)	EFPD	Measurement (pcm/°F)	Calculation (pcm/°F)	Difference (M-C) (pcm/°F)
2	4	100	42	-10.140	-10.10	-0.04
2	4	100	267	-23.905	-24.98	+1.08
2	5	85	42	-9.413	-9.37	-0.04
2	5	100	247	-19.312	-18.96	-0.35
2	6	100	42	-11.662	-12.61	+0.95
2	6	100	217	-23.623	-24.02	+0.40
2	7	100	43	-12.073	-12.32	+0.25
2	7	100	314	-26.08	-24.53	-1.55
3	1	100	17	-13.081	-12.30	-0.78
3	1	100	41	-11.987	-11.60	-0.39
3	1	100	274	-17.653	-16.56	-1.09
3	2	100	28	-10.477	-9.02	-1.46
3	2	100	42	-10.946	-9.68	-1.27
3	2	100	276	-23.750	-21.72	-2.03
3	3	100	6	-10.105	-10.08	-0.03
3	3	100	40	-11.614	-11.52	-0.09
3	3	100	301	-26.015	-25.12	-0.90
3	4	100	42	-11.537	-11.62	+0.08
3	4	100	280	-24.190	-22.69	-1.50
3	5	100	43	-9.335	-9.71	+0.38
3	5	100	299	-23.234	-22.78	-0.45
3	6	100	43	-12.376	-12.91	+0.53
3	6	100	289	-25.93	-25.41	-0.52
3	7	100	41	-10.33	-10.61	+0.28

Table 4-9 ITC Difference Statistics

	pcm/°F
Bias (Meas - Calc)	-0.28
Standard Deviation (S)	0.66
Number of Data Points	70
Degrees of Freedom	69
<i>D</i> ' Value	163.9
Critical Value(s)	159.6 167.7
Normal Distribution?	Yes
$K_{95/95}^a$ (95/95 Tolerance Factor)	2.299
$K_{95/95} * S$	1.517
95/95 Tolerance Limit	-0.28 ± 1.517

a. Reference 13

4.4 CONTROL ROD WORTH BIAS AND UNCERTAINTY

Measurement Technique

Control rod bank worths are measured at BOC, HZP conditions as part of each cycle's startup physics testing. There are two basic ways this is done. The first is by the dilution technique. This technique involves a continuous decrease in boron concentration together with an insertion of the control rods in small, discrete steps. The change in reactivity due to each insertion is determined from reactivity computer readings before and after the insertion. The worth of each rod bank is the sum of all the reactivity changes for that bank.

The second method of measuring control rod bank worths is the rod swap technique. In this technique the reference bank worth is measured by the dilution technique. The reference bank can involve one or more rod banks, and they are typically chosen so that their predicted worth is larger than the predicted worths of each test bank. As the other banks are inserted and withdrawn, their reactivity is compensated by movement of the reference bank. Worths of these banks may then be inferred relative to the reference bank worth.

Dilution was the primary means for measuring rod worths for Unit 1 Cycle 1 and Unit 2 Cycle 1. After these two cycles dilution was only used for determining the worth of the reference bank used in the rod swap test. Starting with Unit 3 Cycle 1 rod swap was the primary means of calculating rod worths.

Measurement uncertainty for control rod worths is due to (1) measured boron concentration errors, (2) beta-effective data used in the reactivity computer, (3) control rod position uncertainty, and (4) the effect of spatial flux redistribution on the flux incident on the excore detectors. Another source of uncertainty is the applicability of the measured reference bank insertion curve to the determination of the test bank worth. The reference bank is measured under decreasing boron concentration, and is then used at constant boron to trade against a test bank. For heavy bank worth, the ppm can change enough to induce a radial shift which can affect the worth, such that the worth of the reference bank during withdrawal can deviate from the curve measured during insertion.

Comparison of Results

Calculated and measured control rod worths are compared in Table 4-10, Table 4-11, and Table 4-12, for PVNGS Units 1, 2, and 3, respectively. The comparisons are divided into 2 groups. All of the swap and dilution data is pooled together for a total of 190 data points, and the total rod worth data is pooled for a total of 21 data points.

Statistical Analysis

Observed Difference Uncertainty

Two means (biases) and standard deviations have been calculated. One mean and standard deviation is for the rod bank worth, based on swap and dilution data pooled together and the other

mean and standard deviation is for the total rod worth data.

Two different tests for normality were used based on the number of data points in the distribution. For the swap plus dilution distribution, with greater than 50 points, the D' test (Reference 12) was used. For the total rod worth distribution, with fewer than 51 points, the W test (Reference 12) was used. Also, a test for outliers was performed, and a determination of whether the percent differences depend on calculated rod worths was performed.

As Table 4-13 shows, the Unit 1 and Unit 3 data displays nonnormality. Both have D' values that are less than the lower critical value. According to Section A3 of Reference 12, this condition indicates that the underlying distribution has greater than normal kurtosis.

Reference 14 describes the T_n test, a method to detect outliers. Performing the T_n test indicated that two data points were outliers. The Unit 1 Cycle 4 data point at $1 \rightarrow A(19)$ (see Table 4-10) had a 27.17% observed difference. Performing the T_n^1 test indicated that this was an outlier data point. Elimination of this data point creates a normal distribution and a smaller standard deviation. The Unit 3 Cycle 2 data point at $3 \rightarrow 2$ (see Table 4-12) had a 20.47% observed difference. Performing the T_n^1 test indicated that this was an outlier data point. Elimination of this data point creates a normal distribution and a smaller standard deviation. Both of these points were also eliminated from the pooled data (all units, swap plus dilution).

The PLCEA dilutions for U1C1 and U2C1, and U2C1's dilution of Groups 1-5 in overlap were not included in the calculation of the rod worth biases and uncertainties. The PLCEAs were excluded since they are not entirely B_4C and because there were only two data points. The dilution of Group 1-5 in overlap was excluded because it was only measured once.

The bias, standard deviation, results of normality and T_n tests, and the 95/95 tolerance factor are presented in Table 4-13 for the observed differences between measured and calculated rod worths.

The swap plus dilution data for each unit and for all units pooled together indicates that there is no compelling reason to have a bias and uncertainty for each unit. By pooling the data from all three units the K-Factor is reduced by ~10%.

The all units (pooled) swap plus dilution data did not show a dependence on the calculated rod worth. The pooled total rod worth data shows a slight dependence on calculated rod worth, but in the range of expected upcoming total rod worths this slight dependence is not significant.

The observed difference uncertainty presented in Table 4-13 for the pooled swap plus dilution data for all units will be used to derive the calculational uncertainty for individual rod banks. The observed difference uncertainty presented in Table 4-13 for the pooled total rod worth data for all units will be used to derive the calculational uncertainty for total rod worth.

-
1. The T_n test should be performed on data that displays normality. The data for both Unit 1 and Unit 3 doesn't display normality, but the D' test indicates that the data is quite close to normal. Therefore, the T_n test can be used.

Measurement Uncertainty

If the same banks are measured on two identical reactors, it is assumed that differences in measured worths are the results of the measurement uncertainties. The measurement uncertainties for Palo Verde was determined by comparing the Unit 1 Cycle 1 and Unit 2 Cycle 1 dilutions and by comparing the Unit 1 Cycle 1 and Unit 3 Cycle 1 exchanges.

Table 4-14 shows the comparison of the Unit 1 and Unit 2 bank worth (by dilution) data, including the % differences, mean, and standard deviation. Table 4-15 shows a comparison of the Unit 1 and Unit 3 data (by rod exchange).

The Percent Differences are calculated in the following manner:

$$((\text{Reactor A} - \text{Reactor B}) / (\text{Reactor A} + \text{Reactor B})) * 2 * 100$$

The standard deviations for the measurement data for dilution (Table 4-14) and rod swap (Table 4-15) are calculated about zero rather than about the mean, and n is used in the denominator instead of $n - 1$. The standard deviations for each set of data are compared, and the smallest is used for the individual bank worth uncertainty (S_M). The total rod worth measurement uncertainty is determined by choosing the smallest absolute total rod worth percent difference from Table 4-14 and Table 4-15. Minimizing the measurement uncertainty is conservative in that it maximizes the calculational uncertainty.

The lowest standard deviation for individual bank measurement is 1.46% (from Table 4-14 and Table 4-15). Thus, this becomes the individual bank measurement uncertainty. The smallest absolute percent difference total measured worth is 1.18%, thus this becomes the total worth measurement uncertainty.

Calculational Uncertainty

The calculational uncertainty (S_C) is obtained from the total observed uncertainty (S_D) as follows:

$$S_C^2 = S_D^2 - S_M^2$$

Using the method discussed above, the calculational uncertainties for individual banks becomes:

$$S_C = \sqrt{4.7^2 - 1.46^2} = 4.5\%$$

where:

$$S_D = 4.7\% \quad (\text{observed standard deviation of differences, all units swap plus dilution from Table 4-13})$$

$$S_M = 1.46\% \quad (\text{lowest standard deviation of measurements for individual bank measurement from Table 4-14 and Table 4-15})$$

and for the total worth:

$$S_C = \sqrt{3.2^2 - 1.18^2} = 3.0\%$$

where:

$S_D = 3.2\%$ (observed standard deviation of differences, all units total rod worth from Table 4-13)

$S_M = 1.18\%$ (smallest absolute percent difference in total measured worth from Table 4-14 and Table 4-15)

Statistical Results

Table 4-16 show the results of the statistical analysis for calculational uncertainties of individual rod banks (swap plus dilution) and total rod worth.

All Units Swap plus Dilution

The tolerance limits for individual rod bank worth for all PVNGS units are:

$$0.8 \pm 8.3\%$$

All Units Total Rod Worth

The tolerance limits for total rod worth for all PVNGS units are:

$$1.0 \pm 7.1\%$$

Table 4-10 Unit 1 Rod Worth Comparisons

Cycle	Measurement Method	Rod Group	Measurement	Calculation	Difference	Percent Difference ^a
1	Dilution	5+4+3+2+1	-1225.24	-1168.00	-57.2	4.90
1	Dilution	5+4+3+2	-1032.15	-970.00	-62.2	6.41
1	Dilution	5+4+3	-786.30	-766.40	-19.9	2.60
1	Dilution	5+4	-442.92	-422.80	-20.1	4.76
1	Dilution	5	-275.70	-272.20	-3.5	1.29
1	Dilution	B	-2732.20	-2586.10	-146.1	5.65
1	Dilution	PLCEA	-263.76	-240.50	-23.3	9.67
1	Swap	3 → 1	-748.51	-707.89	-40.6	5.74
1	Swap	3 → 2	-565.37	-530.64	-34.7	6.54
1	Swap	3 → 4	-460.85	-436.01	-24.8	5.70
1	Swap	3 → 5	-236.90	-229.65	-7.3	3.16
1	Swap	B → A	-2520.00	-2358.30	-161.7	6.86
1	Swap	Total ^b	-7263.83	-6994.69	-269.1	3.85
2	Dilution	1	-866.16	-860.40	-5.8	0.67
2	Dilution	B	-2822.10	-2812.00	-10.1	0.36
2	Swap	1 → 2	-416.81	-386.91	-29.9	7.73
2	Swap	1 → 3	-799.06	-821.80	22.7	-2.77
2	Swap	1 → 4	-387.33	-386.84	-0.5	0.13
2	Swap	1 → 5	-239.92	-248.17	8.3	-3.32
2	Swap	B → A	-2200.98	-2102.19	-98.8	4.70
2	All	Total	-7732.36	-7618.31	-114.0	1.50
3	Dilution	3	-779.60	-804.70	25.1	-3.12
3	Dilution	B	-2557.00	-2586.20	29.2	-1.13
3	Swap	3 → 1	-759.31	-765.87	6.6	-0.86
3	Swap	3 → 2	-303.72	-325.75	22.0	-6.76

Table 4-10 Unit 1 Rod Worth Comparisons

Cycle	Measurement Method	Rod Group	Measurement	Calculation	Difference	Percent Difference^a
3	Swap	3 → 4	-313.85	-331.79	17.9	-5.41
3	Swap	3 → 5	-232.85	-249.14	16.3	-6.54
3	Swap	B → A	-2105.81	-2039.34	-66.5	3.26
3	All	Total	-7052.14	-7102.79	50.6	-0.71
4	Dilution	1	-730.00	-740.30	10.3	-1.39
4	Swap	1 → 2	-470.00	-423.20	-46.8	11.06
4	Swap	1 → 3	-690.00	-703.51	13.5	-1.92
4	Swap	1 → 4	-340.00	-318.25	-21.8	6.83
4	Swap	1 → 5	-270.00	-279.91	9.9	-3.54
4	Swap	1 → A(2)	-570.00	-553.28	-16.7	3.02
4	Swap	1 → A(3)	-590.00	-553.28	-36.7	6.64
4	Swap	1 → A(19) ^c	-350.00	-275.22	-74.8	27.17
4	Swap	1 → A(20)	-310.00	-275.22	-34.8	12.64
4	Swap	1 → B(6)	-610.00	-616.20	6.2	-1.01
4	Swap	1 → B(7)	-600.00	-616.20	16.2	-2.63
4	Swap	1 → B(9)	-660.00	-594.49	-65.5	11.02
4	Swap	1 → B(10)	-630.00	-594.49	-35.5	5.97
4	Swap	1 → B(16)	-520.00	-466.20	-53.8	11.54
4	All	Total	-6990.00	-6734.53	-255.5	3.79
5	Dilution	3	-782.50	-796.50	14.0	-1.76
5	Swap	3 → 5 & A(20)	-571.57	-579.01	7.4	-1.28
5	Swap	3 → B(9)	-665.42	-634.78	-30.6	4.83
5	Swap	3 → 2 & 4	-658.79	-641.89	-16.9	2.63
5	Swap	3 → A(19) & B(16)	-686.36	-647.43	-38.9	6.01
5	Swap	3 → 1	-703.05	-661.57	-41.5	6.27
5	Swap	3 → B(10)	-653.76	-631.46	-22.3	3.53

Table 4-10 Unit 1 Rod Worth Comparisons

Cycle	Measurement Method	Rod Group	Measurement	Calculation	Difference	Percent Difference ^a
5	Swap	3 → A(3)	-591.46	-591.56	0.1	-0.02
5	Swap	3 → B(6)	-748.05	-716.53	-31.5	4.40
5	Swap	3 → A(2)	-597.96	-591.78	-6.2	1.04
5	Swap	3 → B(7)	-744.68	-715.36	-29.3	4.10
5	All	Total	-7403.60	-7207.87	-195.7	2.72
6	Dilution	3 & 4	-1069.50	-1067.60	-1.9	0.18
6	Swap	3 & 4 → 1 & 2	-982.90	-956.55	-26.4	2.75
6	Swap	3 & 4 → B(6) & 5	-853.20	-822.18	-31.0	3.77
6	Swap	3 & 4 → B(7)	-657.10	-654.75	-2.4	0.36
6	Swap	3 & 4 → B(9)	-737.30	-740.29	3.0	-0.40
6	Swap	3 & 4 → B(10&16)	-990.30	-964.94	-25.4	2.63
6	Swap	3 & 4 → A(2&20)	-920.80	-922.11	1.3	-0.14
6	Swap	3 & 4 → A(3&19)	-917.50	-917.63	0.1	-0.01
6	All	Total	-7128.60	-7046.05	-82.6	1.17
7	Dilution	3 & 4	-1025.20	-1051.50	26.3	-2.50
7	Swap	3 & 4 → 1 & 2	-981.50	-940.90	-40.6	4.32
7	Swap	3 & 4 → B(6) & 5	-865.00	-879.59	14.6	-1.66
7	Swap	3 & 4 → B(7)	-648.80	-690.32	41.5	-6.01
7	Swap	3 & 4 → B(9)	-676.50	-704.00	27.5	-3.91
7	Swap	3 & 4 → B(10&16)	-911.20	-897.10	-14.1	1.57
7	Swap	3 & 4 → A(2&20)	-848.10	-907.40	59.3	-6.54
7	Swap	3 & 4 → A(3&19)	-836.70	-903.10	66.4	-7.35
7	All	Total	-6793.00	-6973.91	180.9	-2.59

a. $((\text{Meas} - \text{Calc}) / \text{Calc}) * 100$

b. The total includes all of the swap cases plus group B dilution (does not include PLCEAs are regulating group dilution cases).

c. This measurement is an outlier and is not included in the total.

Table 4-11 Unit 2 Rod Worth Comparisons

Cycle	Measurement Method	Rod Group	Measurement	Calculation	Difference	Percent Difference ^a
1	Dilution	5+4+3+2+1	-1260.61	-1167.80	-92.8	7.95
1	Dilution	5+4+3+2	-1033.06	-969.90	-63.2	6.51
1	Dilution	5+4+3	-788.36	-766.40	-22.0	2.87
1	Dilution	5+4	-449.81	-422.70	-27.1	6.41
1	Dilution	5	-275.08	-272.30	-2.8	1.02
1	Dilution	PLCEA	-270.82	-240.60	-30.2	12.56
1	Dilution	1 - 5 Overlap	-3843.92	-3563.68	-280.2	7.86
1	Dilution	Total (1 - 5)	-3806.92	-3599.10	-207.8	5.77
2	Dilution	1	-752.67	-715.90	-36.8	5.14
2	Dilution	B	-3179.28	-3054.80	-124.5	4.07
2	Swap	1 → 2	-562.59	-510.10	-52.5	10.29
2	Swap	1 → 3	-602.78	-579.33	-23.4	4.05
2	Swap	1 → 4	-401.85	-381.25	-20.6	5.40
2	Swap	1 → 5	-241.11	-239.78	-1.3	0.55
2	Swap	B → A	-2373.59	-2257.16	-116.4	5.16
2	All	Total	-8113.87	-7738.32	-375.6	4.85
3	Dilution	3	-805.84	-845.20	39.4	-4.66
3	Dilution	A	-2450.94	-2486.30	35.4	-1.42
3	Swap	3 → 1	-578.70	-574.34	-4.4	0.76
3	Swap	3 → 2	-414.08	-409.18	-4.9	1.20
3	Swap	3 → 4	-375.70	-389.13	13.4	-3.45
3	Swap	3 → 5	-201.99	-232.43	30.4	-13.10
3	Swap	A → B	-2090.58	-1987.55	-103.0	5.18
3	All	Total	-6917.83	-6924.13	6.3	-0.09

Table 4-11 Unit 2 Rod Worth Comparisons

Cycle	Measurement Method	Rod Group	Measurement	Calculation	Difference	Percent Difference^a
4	Dilution	1	-854.27	-795.20	-59.1	7.43
4	Swap	1 → 2	-444.70	-409.83	-34.9	8.51
4	Swap	1 → 3	-654.45	-702.88	48.4	-6.89
4	Swap	1 → 4	-311.59	-292.56	-19.0	6.50
4	Swap	1 → 5	-223.86	-228.10	4.2	-1.86
4	Swap	1 → A(2)	-516.30	-529.39	13.1	-2.47
4	Swap	1 → A(3)	-516.30	-529.39	13.1	-2.47
4	Swap	1 → A(19)	-316.64	-307.48	-9.2	2.98
4	Swap	1 → A(20)	-318.65	-307.48	-11.2	3.63
4	Swap	1 → B(6)	-593.94	-611.89	17.9	-2.93
4	Swap	1 → B(7)	-595.96	-611.89	15.9	-2.60
4	Swap	1 → B(9)	-609.07	-581.24	-27.8	4.79
4	Swap	1 → B(10)	-609.07	-581.24	-27.8	4.79
4	Swap	1 → B(16)	-441.68	-411.18	-30.5	7.42
4	All	Total	-7006.48	-6899.75	-106.7	1.55
5	Dilution	A(2&3)	-782.48	-848.20	65.7	-7.75
5	Swap	A(2&3) → 1	-631.11	-679.61	48.5	-7.14
5	Swap	A(2&3) → 2	-490.99	-522.82	31.8	-6.09
5	Swap	A(2&3) → 3	-551.37	-601.86	50.5	-8.39
5	Swap	A(2&3) → 4 & 5	-482.27	-516.60	34.3	-6.65
5	Swap	A(2&3) → A(19&20)	-655.42	-699.29	43.9	-6.27
5	Swap	A(2&3) → B(6)	-668.29	-700.44	32.2	-4.59
5	Swap	A(2&3) → B(7)	-653.60	-700.44	46.8	-6.69
5	Swap	A(2&3) → B(9)	-672.34	-710.68	38.3	-5.39
5	Swap	A(2&3) → B(10)	-663.63	-710.68	47.1	-6.62
5	Swap	A(2&3) → B(16)	-480.35	-512.71	32.4	-6.31
5	All	Total	-6731.85	-7203.33	471.5	-6.55

Table 4-11 Unit 2 Rod Worth Comparisons

Cycle	Measurement Method	Rod Group	Measurement	Calculation	Difference	Percent Difference ^a
6	Dilution	A(2&3)	-973.00	-991.80	18.8	-1.90
6	Swap	A(2&3) → 1	-654.20	-677.19	23.0	-3.39
6	Swap	A(2&3) → 2	-435.30	-446.68	11.4	-2.55
6	Swap	A(2&3) → 3	-471.80	-504.89	33.1	-6.55
6	Swap	A(2&3) → 4 & 5	-519.90	-535.54	15.6	-2.92
6	Swap	A(2&3) → A(19&20)	-689.20	-694.25	5.0	-0.73
6	Swap	A(2&3) → B(6)	-651.80	-687.08	35.3	-5.13
6	Swap	A(2&3) → B(7)	-658.20	-687.08	28.9	-4.20
6	Swap	A(2&3) → B(9)	-697.30	-712.43	15.1	-2.12
6	Swap	A(2&3) → B(10)	-695.70	-712.43	16.7	-2.35
6	Swap	A(2&3) → B(16)	-491.50	-507.08	15.6	-3.07
6	All	Total	-6937.90	-7156.45	218.6	-3.05
7	Dilution	3 & 4	-1084.00	-1088.90	4.9	-0.45
7	Swap	3 & 4 → 1 & 2	-1084.00	-1046.90	-37.1	3.54
7	Swap	3 & 4 → B(6) & 5	-964.60	-891.80	-72.8	8.16
7	Swap	3 & 4 → B(7)	-669.80	-715.50	45.7	-6.39
7	Swap	3 & 4 → B(9)	-662.00	-679.90	17.9	-2.63
7	Swap	3 & 4 → B(10&16)	-900.80	-912.30	11.5	-1.26
7	Swap	3 & 4 → A(2&20)	-952.40	-972.30	19.9	-2.05
7	Swap	3 & 4 → A(3&19)	-971.30	-977.10	5.8	-0.59
7	All	Total	-7288.90	-7284.70	-4.2	0.06

a. $((\text{Meas} - \text{Calc}) / \text{Calc}) * 100$

Table 4-12 Unit 3 Rod Worth Comparisons

Cycle	Measurement Method	Rod Group	Measurement	Calculation	Difference	Percent Difference^a
1	Dilution	3	-727.51	-724.50	-3.0	0.42
1	Dilution	B	-2694.73	-2586.00	-108.7	4.20
1	Swap	3 → 1	-721.12	-710.41	-10.7	1.51
1	Swap	3 → 2	-555.99	-531.51	-24.5	4.61
1	Swap	3 → 4	-455.56	-435.60	-20.0	4.58
1	Swap	3 → 5	-228.73	-228.74	0.0	0.00
1	Swap	B → A	-2514.21	-2358.32	-155.9	6.61
1	All	Total	-7897.85	-7575.08	-322.8	4.26
2	Dilution	3	-673.41	-728.00	54.6	-7.50
2	Dilution	B	-2599.99	-2611.30	11.3	-0.43
2	Swap	3 → 1	-609.77	-592.30	-17.5	2.95
2	Swap	3 → 2 ^b	-508.14	-421.79	-86.4	20.47
2	Swap	3 → 4	-447.16	-443.59	-3.6	0.80
2	Swap	3 → 5	-254.07	-244.41	-9.7	3.95
2	Swap	B → A	-2489.89	-2509.74	19.8	-0.79
2	All	Total	-7074.29	-7129.34	55.1	-0.77
3	Dilution	3	-706.94	-726.30	19.4	-2.67
3	Dilution	B	-2725.29	-2754.10	28.8	-1.05
3	Swap	3 → 1	-655.99	-674.14	18.2	-2.69
3	Swap	3 → 2	-471.46	-461.15	-10.3	2.24
3	Swap	3 → 4	-298.08	-288.40	-9.7	3.36
3	Swap	3 → 5	-274.76	-257.10	-17.7	6.87
3	Swap	B → A	-2197.10	-2106.72	-90.4	4.29
3	All	Total	-7329.62	-7267.91	-61.7	0.85
4	Dilution	1	-716.90	-709.50	-7.4	1.04

Table 4-12 Unit 3 Rod Worth Comparisons

Cycle	Measurement Method	Rod Group	Measurement	Calculation	Difference	Percent Difference^a
4	Swap	1 → 2	-389.98	-389.03	-1.0	0.24
4	Swap	1 → 3	-706.65	-695.80	-10.9	1.56
4	Swap	1 → 4	-372.67	-362.94	-9.7	2.68
4	Swap	1 → 5	-278.99	-270.72	-8.3	3.05
4	Swap	1 → A(2)	-594.64	-570.84	-23.8	4.17
4	Swap	1 → A(3)	-594.64	-570.84	-23.8	4.17
4	Swap	1 → A(19)	-256.59	-248.04	-8.5	3.45
4	Swap	1 → A(20)	-256.59	-248.04	-8.5	3.45
4	Swap	1 → B(6)	-669.99	-676.39	6.4	-0.95
4	Swap	1 → B(7)	-688.32	-676.39	-11.9	1.76
4	Swap	1 → B(9)	-665.92	-655.42	-10.5	1.60
4	Swap	1 → B(10)	-661.84	-655.42	-6.4	0.98
4	Swap	1 → B(16)	-498.93	-492.54	-6.4	1.30
4	All	Total	-7352.65	-7221.91	-130.7	1.81
5	Dilution	A(2&3)	-796.50	-822.90	26.4	-3.21
5	Swap	A(2&3) → 1	-613.83	-643.01	29.2	-4.54
5	Swap	A(2&3) → 2	-488.02	-497.20	9.2	-1.85
5	Swap	A(2&3) → 3	-624.99	-648.37	23.4	-3.61
5	Swap	A(2&3) → 4 & 5	-543.83	-543.82	0.0	0.00
5	Swap	A(2&3) → A(19)	-335.83	-360.49	24.7	-6.84
5	Swap	A(2&3) → A(20)	-353.08	-360.49	7.4	-2.06
5	Swap	A(2&3) → B(6)	-565.13	-582.26	17.1	-2.94
5	Swap	A(2&3) → B(7)	-575.28	-582.26	7.0	-1.20
5	Swap	A(2&3) → B(9)	-634.13	-636.13	2.0	-0.31
5	Swap	A(2&3) → B(10)	-645.29	-636.13	-9.2	1.44
5	Swap	A(2&3) → B(16)	-529.62	-537.22	7.6	-1.41

Table 4-12 Unit 3 Rod Worth Comparisons

Cycle	Measurement Method	Rod Group	Measurement	Calculation	Difference	Percent Difference^a
5	All	Total	-6705.53	-6850.28	144.8	-2.11
6	Dilution	3 & 4	-1196.00	-1150.20	-45.8	3.98
6	Swap	3 & 4 → 1 & 2	-936.98	-847.31	-89.7	10.58
6	Swap	3 & 4 → B(6) & 5	-894.56	-827.50	-67.1	8.10
6	Swap	3 & 4 → B(7)	-673.72	-637.13	-36.6	5.74
6	Swap	3 & 4 → B(9)	-851.89	-793.75	-58.1	7.32
6	Swap	3 & 4 → B(10&16)	-1083.41	-998.28	-85.1	8.53
6	Swap	3 & 4 → A(2&20)	-980.02	-952.71	-27.3	2.87
6	Swap	3 & 4 → A(3&19)	-1002.64	-964.02	-38.6	4.01
6	All	Total	-7619.22	-7170.90	-448.3	6.25
7	Dilution	3 & 4	-1192.20	-1178.70	-13.5	1.15
7	Swap	3 & 4 → 1 & 2	-778.10	-782.20	4.1	-0.52
7	Swap	3 & 4 → B(6) & 5	-937.70	-934.60	-3.1	0.33
7	Swap	3 & 4 → B(7)	-705.90	-725.50	19.6	-2.70
7	Swap	3 & 4 → B(9)	-666.60	-679.90	13.3	-1.96
7	Swap	3 & 4 → B(10&16)	-801.90	-815.30	13.4	-1.64
7	Swap	3 & 4 → A(2&20)	-981.90	-1031.10	49.2	-4.77
7	Swap	3 & 4 → A(3&19)	-974.40	-1028.90	54.5	-5.30
7	All	Total	-7038.70	-7176.20	137.5	-1.92

a. $((\text{Meas} - \text{Calc}) / \text{Calc}) * 100$

b. This measurement is an outlier and will not be included in the total.

Table 4-13 Rod Worth Percent Difference Statistics

	Unit Swap plus Dilution					All Units Swap plus Dilution All Data (Except ^a)	All Units Total Rod Worth
	One All Data	One All Data (Except ^b)	Two All Data	Three All Data	Three All Data (Except ^c)		
Bias ((Meas - Calc) / Calc) * 100	2.2	1.8	-0.6	1.4	1.1	0.8	1.0
Standard Deviation	5.6	4.7	5.3	4.4	3.7	4.7	3.2
Number of Data Points	66	65	63	63	62	190	21
Degrees of Freedom	65	64	62	62	61	189	20
W or D' Value	141.4	148.5	142.0	132.0	137.5	744.8	0.979
Critical Value(s)	146.0 153.5	142.7 150.1	136.0 143.2	136.0 143.2	136.0 143.2	725.9 748.1	0.908
Normal Distribution?	no	yes	yes	no	yes	yes	yes
T_n Value	4.459 ^d	n/a	n/a	4.334 ^e	n/a	n/a	n/a
Critical Value	3.230	n/a	n/a	3.218	n/a	n/a	n/a
Outlier?	yes	n/a	n/a	yes	n/a	n/a	n/a
K_{95/95}^f (95/95 Tolerance Factor)	n/a	2.005	2.012	n/a	2.015	1.843	2.371

- a. Does not include Unit 1 Cycle 4's Data Point 1→A(19) nor Unit 3 Cycle 2's Data Point 3→2.
- b. Does not include Unit 1 Cycle 4's Data Point 1 → A(19)
- c. Does not include Unit 3 Cycle 2's Data Point 3 → 2
- d. $4.477 = (27.17 - 2.2) / 5.6$, where 27.17 is Unit 1 Cycle 4's Data Point 1 → A(19)
- e. $4.334 = (20.47 - 1.4) / 4.4$, where 20.47 is Unit 3 Cycle 2's Data Point 3 → 2
- f. Reference 27

Table 4-14 Palo Verde Measured Worths -- Dilution

Bank	Unit 1	Unit 2	% Difference ^a
5	-275.7	-275.1	0.225
4	-442.9	-449.8	-1.544
3	-786.3	-788.4	-0.262
2	-1,032.2	-1,033.1	-0.088
1	-1,225.2	-1,260.6	-2.846
Total	-3,762.3	-3,807.0	-1.179
Standard Deviation			1.457

a. $((U1 - U2) / (U1 + U2)) * 2 * 100$

Table 4-15 Palo Verde Measured Worths -- Rod Exchange

Bank	Unit 1	Unit 3	% Difference ^a
5	-236.9	-228.7	3.522
4	-460.9	-455.6	1.157
2	-565.4	-556.0	1.676
1	-748.5	-721.1	3.729
A	-2,520.0	-2,514.2	0.230
3	-729.6	-727.5	0.288
B	-2,732.2	-2,694.7	1.382
Total	-7,263.9	-7,170.3	1.204
Standard Deviation			2.155

a. $((U1 - U3) / (U1 + U3)) * 2 * 100$

Table 4-16 Summary of Statistics for Rod Worth for PVNGS Units 1, 2, and 3

Rod Group	Bias^a	Measurement Standard Deviation (S_M)	Calculational Standard Deviation^b (S_C)	K_{95/95}^c (95/95 Tolerance Factor)	K_{95/95}*S_C
Bank Worth	0.8%	1.46%	4.5%	1.843	8.3%
Total Worth	1.0%	1.18%	3.0%	2.371	7.1%

- a. from Table 4-13
- b. $S^2_C = S^2_D - S^2_M$
- c. Reference 27

4.5 INVERSE BORON WORTH BIAS AND UNCERTAINTY

Measurement Technique

The inverse boron worths (IBWs) were calculated at BOC hot zero power conditions for Cycles 1 through 7 of PVNGS Units 1, 2, and 3.

The measured IBW is calculated using:

$$IBW = (CBC_1 - CBC_2) / (\Delta Reactivity)$$

where,

CBC_1 is the critical boron concentration for state-point 1 (normally, ARO CBC)

CBC_2 is the critical boron concentration for state-point 2 (normally, reference bank full in CBC)

$\Delta Reactivity$ is the reactivity change from state-point 1 to 2. Normally, this reactivity change is accomplished by control rod insertion/withdrawal.

The measurement uncertainty includes boron titration errors and control rod worth measurement errors.

Comparison of Results

Calculated and measured inverse boron worths are compared in Table 4-17 for PVNGS Units 1 (7 data points), 2 (6 data points), and 3 (7 data points). The measured IBW for Unit 2 Cycle 7 is being treated as an outlier and is therefore not included in the calculation of the IBW bias and uncertainty. The measurement is in question because it was unusually low in magnitude (110.4 ppm/% $\Delta\rho$). For the high boron concentrations required for present core designs, it is unlikely that the IBW could be this low. The magnitude is typically 120 ppm/% $\Delta\rho$ or higher. See Reference 24 for further details.

Statistical Analysis

A mean (bias) and standard deviation have been calculated based on all of the data pooled together. The *W* test for normality was performed because there are fewer than 51 data points. Finally, a 95/95 tolerance factor was determined.

Statistical Results

The IBW difference statistics are presented in Table 4-18.

The tolerance limits for inverse boron worth are:

$$-3.16 \pm 13.49\%$$

Table 4-17 Units 1, 2, and 3 IBW Comparisons

Unit	Cycle	IBW Measurement (PPM/% ΔK/K)	IBW Calculation (PPM/% ΔK/K)	% Difference ^a
1	1	-87.87	-89.53	-1.85
1	2	-100.91	-102.99	-2.02
1	3	-117.65	-119.62	-1.65
1	4	-116.28	-120.05	-3.14
1	5	-121.36	-122.55	-0.97
1	6	-116.96	-124.22	-5.84
1	7	-134.6	-142.1	-5.28
2	1	-80.71	-88.42	-8.72
2	2	-98.14	-107.4	-8.62
2	3	-114.2	-116.0	-1.55
2	4	-105.4	-120.1	-12.24
2	5	-125.8	-122.1	+3.03
2	6	-128.5	-117.2	+9.64
3	1	-80.65	-85.47	-5.64
3	2	-107.18	-107.99	-0.75
3	3	-109.89	-112.36	-2.20
3	4	-102.88	-117.65	-12.55
3	5	-135.14	-125.79	7.43
3	6	-122.85	-132.70	-7.42
3	7	-139.9	-143.9	-2.78

a. $(100 * ((\text{measured IBW} - \text{calculated IBW (at the measured CBC)}) / \text{calculated IBW (at the measured CBC)}))$

Table 4-18 IBW Difference Statistics

	%
Bias ((Meas - Calc) / Calc) * 100	-3.16
Standard Deviation	5.63
Number of Data Points	20
Degrees of Freedom	19
W Value	0.945
Critical Value(s)	0.905
Normal Distribution?	yes
$K_{95/95}^a$ (95/95 Tolerance Factor)	2.396
$K_{95/95} * S$	13.49
95/95 Tolerance Limit	-3.16 ± 13.49

a. Reference 27

4.6 DOPPLER POWER COEFFICIENT

Measurement Technique

The power coefficient is defined as the change in reactivity due to a change in core power level. The Doppler power coefficient includes only the reactivity change due to the nuclear Doppler effect, excluding the reactivity effects of the change in moderator temperature after a power perturbation. To measure power coefficient, a reactivity insertion is made using control rods, resulting in a change in reactor power. Average coolant temperature is held nearly constant by changing the turbine load or adjusting the steam bypass system to match reactor power. The reactor settles out at a new power when the reactivity feedback due to change in power is equal and opposite to the control rod reactivity insertion. Because there is a change in the moderator axial temperature profile, there will be a change in average volumetric temperature. Reactivity due to changes in average volumetric temperature can be calculated using a calculated ITC. The reactivity due to moderator temperature change can then be subtracted from the control rod reactivity insertion, allowing a calculation of the Doppler power coefficient. The power coefficient was measured only in early cycles (Unit 1 Cycles 1 and 2, Unit 2 Cycles 1 and 2, and Unit 3 Cycle 3).

The measurement uncertainty for Doppler power coefficient is due to (1) core average temperature measurement uncertainty, (2) control rod position and calculated worth vs. position, (3) core average power measurement, (4) uncertainty in calculated ITC.

Comparison of Results

The comparison of the SIMULATE-3 calculated and the measured Doppler power coefficients are shown in Table 4-19. There are nine measured Doppler Only Power Coefficients (DOPCs); they are from the early cycles of PVNGS.

SIMULATE-3 calculates a power coefficient that includes the effects of the change in average moderator temperature. The Doppler power coefficient is derived from the SIMULATE-3 power coefficient using the following equation:

$$DOPC = PC - ITC \times \Delta(T_{avg}) / (\Delta Power)$$

where,

DOPC= Doppler power coefficient

PC= the SIMULATE-3 calculated power coefficient, including reactivity effects of changes in moderator temperature

ITC= SIMULATE-3 calculated isothermal temperature coefficient

ΔT_{avg} = calculated change in average volumetric moderator temperature after power perturbation

$\Delta Power$ = change in core power

Statistical Analysis

The *W* test for normality was performed on the DOPC observed differences, then a determination as to whether or not the DOPC is a function of power level or power level and core average burnup. Once that was determined a bias and uncertainty ($K(95/95)*S$) was calculated.

Table 4-20 shows the average, standard deviation (S), and $K(95/95)*S$.

Table 4-20 shows that the normally distributed DOPC relative difference data has a $K(95/95)*S$ of 23.12%. Since this is quite large a determination was made as to whether or not the DOPC is a function of power level or power level and core average burnup.

The data showed that the functionalization with the smallest uncertainty is against core average burnup, but it won't be used since the data is basically made up of beginning-of-life (BOL) data and is not entirely appropriate for reload cycles.

The next best was a combination of power and core average burnup. This one will be used since []. Table 4-21 shows the statistical results for DOPC.

By using the combination of power and core average burnup the uncertainty is reduced from 23.1% to 20.6%.

Statistical Results

The DOPC tolerance limits (from Table 4-21) are:

$-5.704 + 1.115*CAB(GWD/MT) + 3.87E-03*P(\%) \pm 20.6\%$,
where CAB is the core average burnup

Table 4-19 Doppler Power Coefficient Comparisons

Unit	Cycle	Core Average Burnup (GWD/MT)	Power (% HFP)	Measurement (pcm/%power)	SIMULATE-3 Calculation (pcm/%power)	% Difference $100*(M - C)/C$
1	1	0.125	18.4	-15.13	-15.01	0.799%
1	1	0.255	53.3	-11.60	-12.52	-7.348
1	1	0.988	80.5	-10.15	-10.56	-3.883
1	1	2.142	95.3	-9.11	-9.17	-0.654
1	2	12.718	95.0	-10.98	-9.86	11.359
2	1	0.541	50	-10.89	-12.61	-13.640
2	1	1.080	96.3	-7.86 ^a	-9.71	-19.053
2	2	9.543	94.4	-10.46	-10.29	1.652
3	1	0.658	96.0	-9.28	-9.43	-1.591

a. This point is abnormally low. Compare -7.86 to the other two Cycle 1 HFP data points of -9.11 and -9.28. This point is not negative enough and is eliminated from the data base.

Table 4-20 Doppler Power Coefficient Statistics for Relative Differences

	pcm/%power
Mean 100*(Meas - Calc)/Calc	-1.663%
Standard Deviation (S)	7.254
Number of Data Points	8
Degrees of Freedom	7
W Value	0.964
Critical Value(s)	0.818
Normal Distribution?	Yes
K_{95/95}^a (95/95 Tolerance Factor)	3.187
K_{95/95}*S	23.12%

a. Reference 27 for n = 8 and 95/95 confidence interval.

Table 4-21 Functionalization for the DOPC Relative Differences

Functionalization	R²	Standard Error (%)	Degrees of Freedom	K(95/95)^a	Uncertainty 95/95 (%)
Power and Core Average Burnup ^b	0.58	5.56	5	3.708	20.6%

a.Reference 27

b.Bias (%) = -5.704 + 1.115*CAB(GWD/MT) + 3.87E-03*P(%)

4.7 FUEL TEMPERATURE COEFFICIENT

Statistical Analysis

The fuel temperature coefficient (FTC) is related to the DOPC by the relationship:

$$\frac{d\rho}{dP} = \frac{d\rho}{dT_f} \times \frac{dT_f}{dP}$$

where

ρ = core reactivity

T_f = fuel temperature

P = core power

The term $d\rho/dP$ has been assigned a bias and an uncertainty, but neither $d\rho/dT_f$ nor dT_f/dP can be evaluated separately. One way of assigning biases and uncertainties is to assign biases and uncertainties equally to $d\rho/dT_f$ and dT_f/dP . The data base of DOPCs is used, without regression analysis versus power and core average burnup. The bias and uncertainty become:

$$\text{FTC Bias} = \text{Average} / 2$$

$$\text{FTC Uncertainty} = K(95/95) * S / \sqrt{2}$$

Another method is to assign a bias to dT_f/dP and uncertainty to $d\rho/dT_f$ (FTC) using the fit of $(\text{Meas} - \text{Calc})/\text{Calc}$ with respect to power and core average burnup. The FTC bias becomes zero and the uncertainty becomes $K(95/95) * S$ of the fit.

Assigning biases and uncertainties equally to $d\rho/dT_f$ and dT_f/dP is slightly more conservative, and []. Therefore biases and uncertainties were assigned equally to $d\rho/dT_f$ and dT_f/dP .

Assigning biases and uncertainties equally to $d\rho/dT_f$ and dT_f/dP yields the following:

$$\text{FTC Bias} = \text{Average} / 2 = -1.66^1 / 2 = -0.83\%$$

$$\text{FTC Uncertainty} = K(95/95) * S / \sqrt{2} = 23.12^1 / \sqrt{2} = 16.35\%$$

Statistical Results

The tolerance limits for fuel temperature coefficient are:

$$-0.8 \pm 16.4\%$$

1. From Table 4-20.

4.8 DROPPED ROD

Measurement Technique

The measurements were performed to measure the worth of the worst “dropped” control rod (CEA) from the all rods out condition. The worths of the following CEAs were measured:

- Worst dropped CEA (CEA 3 (Box 3))
- Next worst dropped CEA (CEA 9)
- Worst dropped part-length CEA (PLCEA) (CEA 31)
- Worst dropped PLCEA subgroup (P1)

The measurements were performed with the RCS at 565°F and 2250 psia. The measured dropped rod worths were required to be within $\pm 0.1\%$ of the predicted worths.

The worths of the dropped CEAs/PLCEAs were measured as follows. The changes in reactivity were recorded by a strip chart recorder.

PLCEA 31 (Box 31) - Due to its small worth, this CEA was simply inserted in one continuous motion to its fully inserted position (Lower Electrical Limit, or LEL), and then withdrawn to its fully withdrawn position (Upper Electrical Limit, or UEL). No changes in RCS boron concentration were made.

CEA 3 (Box 3) - Dilution of the RCS boron concentration was initiated and this CEA was inserted in discrete steps to its LEL.

Subgroup P1 - P1 insertion was traded with withdrawal of CEA 3 until P1 was at its LEL and CEA 3 was at its UEL.

CEA 9 (Box 9) - CEA 9 insertion was traded with P1 withdrawal until CEA 9 was at its LEL and P1 was at its UEL.

To determine the worths of the dropped CEAs, the reactivity data for the measurements was obtained from the strip chart recorder and analyzed in a manner similar to that used to determine the individual CEA group worths.

Measurement uncertainty for control rod worths is due to (1) beta-effective data used in the reactivity computer and (2) the effect of spatial flux redistribution on the flux incident on the excore detectors.

Calculational Method

Palo Verde measured four dropped rod worths at BOC of U1C1. Since there is a limited database the following method was used to determine the appropriate bias and uncertainty:

- Use SIMULATE-3 to calculate the four dropped rod worths measured at BOC U1C1.

- Use both SIMULATE-3 and ROCS to calculate the dropped rod worths for U1C8, U2C8, and U3C8.
- Compare the SIMULATE-3 and ROCS dropped rod worths and calculate a SIMULATE-3 to ROCS bias.
- Using this SIMULATE-3 to ROCS bias, adjust the existing dropped ROCS bias and use the adjusted bias as the SIMULATE-3 dropped bias.
- Use the ROCS dropped uncertainty

The reason the ROCS dropped rod uncertainty will be used is discussed below in the **Statistical Analysis** subsection.

Both codes were run in 3-D full core. Each rod in a core octant was dropped and the resulting reactivities were used to calculate dropped rod worths.

Comparison of Results

Table 4-22 shows the results of the ROCS and SIMULATE-3 calculations of the U1C1 measured dropped rod worths.

Table 4-23, Table 4-24, and Table 4-25 show the results from the ROCS dropped rod worth runs for Cycle 8 for Units 1, 2, and 3.

Table 4-26, Table 4-27, and Table 4-28 show the results from the SIMULATE-3 dropped rod worth runs for Cycle 8 for Units 1, 2, and 3.

Table 4-29 shows the differences between the U1C1 measured dropped rod worths and the calculations done by SIMULATE-3 and ROCS. All of the differences are within $\pm 0.1\%$ $\Delta K/K$ of the calculated worths.

Table 4-30 shows the differences between SIMULATE-3 and ROCS for Cycle 8 for each of Units 1, 2, and 3. All of the differences are within $\pm 0.1\%$ $\Delta K/K$ of the calculated worths.

Statistical Analysis

As Table 4-29 shows there are only three viable measurements. If the bias and uncertainty were based only on these three points they would be meaningless.

Table 4-30 shows that SIMULATE-3 and ROCS calculate similar dropped rod worths for Cycle 8 for Units 1, 2, and 3. In absolute units (ROCS - SIMULATE-3), the statistics (mean and standard deviation) are 3.4 ± 4.2 pcm. This shows that the relative differences between SIMULATE-3 and ROCS are small. Based on the results shown in Table 4-30, a SIMULATE-3 to ROCS bias was calculated, and then the existing ROCS dropped rod bias was adjusted in order to determine the SIMULATE-3 dropped rod bias. The relative difference between ROCS and SIMULATE-3 calculated dropped rod worths is $-0.0580 \pm 0.0712\%$ $\Delta\rho$, meaning SIMULATE-3 tends to overpredict dropped rod worths. Thus, ROCS dropped rod worth bias will be decreased by 5.80%. The present ROCS bias is [] (Reference 38), and the SIMULATE-3 dropped bias will be:

$$(([] / 1.0580) - 1) * 100 = []$$

Thus, ABB's dropped rod worth uncertainty of [] (Reference 38) will be used as the SIMULATE-3 dropped rod worth uncertainty. The reason the ROCS dropped rod uncertainty will be used is because there are only four dropped rod measurements. The bias and uncertainty based on these 4 data points would indicate the need for a large percentage uncertainty and would not be meaningful. []

[]. In absolute units, the SIMULATE-3 dropped and group worth uncertainties are similar and small. The SIMULATE-3 group worth uncertainty is 8.3% (from Section 4.4). Therefore, it is conservative to use [] for dropped rod worth uncertainty, and it is reasonable to assume that measurement uncertainty and the SIMULATE-3 calculational uncertainty are encompassed by this value. Thus, the ROCS dropped rod uncertainty of [] is conservative and will be used as the SIMULATE-3 dropped rod uncertainty.

Statistical Results

The tolerance limits for the SIMULATE-3 dropped rod worths are:

[]

Table 4-22 U1C1 Dropped Rod Worths from ROCS, SIMULATE-3, and Measurement

Dropped Rod Group and Full Core Box Number	Measurement (% $\Delta\rho$)	ROCS Dropped Rod Worth (%$\Delta\rho$)	SIMULATE-3 K_{eff}^a	SIMULATE-3 Dropped Rod Worth (%$\Delta\rho$)
Grp 3/Box 3	-0.073	-0.0871	0.9969723	-0.1071
Grp A/Box 9	-0.069	-0.0860	0.9970310	-0.1012
PLCEA/Box 31	-0.020	-0.0216	0.9978637	-0.0175
PLCEA Subgroup P1	-0.066	-0.1344	0.9971201	-0.0922

a. The ARO K_{eff} is 0.9980377 at a CBC of 1,025.2 PPM.

Table 4-23 U1C8 Dropped Rod Worths from ROCS

Dropped Rod Group and Full Core Box Number	Reactivity^a	Dropped Rod Worth (%$\Delta\rho$)
Grp 3/Box 4	0.2668	-0.0063
Grp A/Box 10	0.2403	-0.0328
Grp 1/Box 12	0.2131	-0.0600
Grp 4/Box 19	0.2719	-0.0012
Grp 2/Box 21	0.2509	-0.0222
Grp 3/Box 25	0.2241	-0.0490
Grp B/Box 34	0.2177	-0.0554
Grp B/Box 36	0.1848	-0.0883
Grp B/Box 38	0.1765	-0.0966
Grp 5/Box 54	0.2205	-0.0526
Grp 4/Box 67	0.2082	-0.0649
Grp A/Box 69	0.1468	-0.1263
Grp 3/Box 103	0.1306	-0.1425

a. The ARO ρ is 0.2731 at a CBC of 2,221 PPM.

Table 4-24 U2C8 Dropped Rod Worths from ROCS

Dropped Rod Group and Full Core Box Number	Reactivity^a	Dropped Rod Worth (%$\Delta\rho$)
Grp 3/Box 4	0.2637	-0.0089
Grp A/Box 10	0.2248	-0.0478
Grp 1/Box 12	0.2065	-0.0661
Grp 4/Box 19	0.2713	-0.0013
Grp 2/Box 21	0.2383	-0.0343
Grp 3/Box 25	0.2294	-0.0432
Grp B/Box 34	0.2176	-0.0550
Grp B/Box 36	0.1872	-0.0854
Grp B/Box 38	0.1780	-0.0946
Grp 5/Box 54	0.2183	-0.0543
Grp 4/Box 67	0.2213	-0.0513
Grp A/Box 69	0.1610	-0.1116
Grp 3/Box 103	0.1630	-0.1096

a. The ARO ρ is 0.2726 at a CBC of 2,175 PPM.

Table 4-25 U3C8 Dropped Rod Worths from ROCS

Dropped Rod Group and Full Core Box Number	Reactivity^a	Dropped Rod Worth (%$\Delta\rho$)
Grp 3/Box 4	0.2610	-0.0078
Grp A/Box 10	0.2238	-0.0450
Grp 1/Box 12	0.2074	-0.0614
Grp 4/Box 19	0.2621	-0.0067
Grp 2/Box 21	0.2301	-0.0387
Grp 3/Box 25	0.2189	-0.0499
Grp B/Box 34	0.2106	-0.0582
Grp B/Box 36	0.1827	-0.0861
Grp B/Box 38	0.1734	-0.0954
Grp 5/Box 54	0.2157	-0.0531
Grp 4/Box 67	0.2162	-0.0526
Grp A/Box 69	0.1560	-0.1128
Grp 3/Box 103	0.1417	-0.1271

a. The ARO ρ is 0.2688 at a CBC of 2,075 PPM.

Table 4-26 U1C8 Dropped Rod Worths from SIMULATE-3

Dropped Rod Group and Full Core Box Number	$K_{\text{eff}}^{\text{a}}$	Dropped Rod Worth (%$\Delta\rho$)
Grp 3/Box 4	0.9973592	-0.0069
Grp A/Box 10	0.9970939	-0.0336
Grp 1/Box 12	0.9968255	-0.0606
Grp 4/Box 19	0.9974113	-0.0017
Grp 2/Box 21	0.9972021	-0.0227
Grp 3/Box 25	0.9969386	-0.0492
Grp B/Box 34	0.9968670	-0.0564
Grp B/Box 36	0.9965168	-0.0917
Grp B/Box 38	0.9964223	-0.1012
Grp 5/Box 54	0.9968692	-0.0562
Grp 4/Box 67	0.9967467	-0.0685
Grp A/Box 69	0.9960581	-0.1379
Grp 3/Box 103	0.9958254	-0.1613

a. The ARO K_{eff} is 0.9974280 at a CBC of 2,221 PPM.

Table 4-27 U2C8 Dropped Rod Worths from SIMULATE-3

Dropped Rod Group and Full Core Box Number	K_{eff}^a	Dropped Rod Worth (%Δρ)
Grp 3/Box 4	0.9964157	-0.0094
Grp A/Box 10	0.9960291	-0.0484
Grp 1/Box 12	0.9958344	-0.0680
Grp 4/Box 19	0.9964886	-0.0021
Grp 2/Box 21	0.9961666	-0.0345
Grp 3/Box 25	0.9960693	-0.0443
Grp B/Box 34	0.9959406	-0.0573
Grp B/Box 36	0.9956220	-0.0894
Grp B/Box 38	0.9955196	-0.0998
Grp 5/Box 54	0.9959374	-0.0576
Grp 4/Box 67	0.9959738	-0.0539
Grp A/Box 69	0.9953056	-0.1214
Grp 3/Box 103	0.9952956	-0.1224

a. The ARO K_{eff} is 0.9965092 at a CBC of 2,175 PPM.

Table 4-28 U3C8 Dropped Rod Worths from SIMULATE-3

Dropped Rod Group and Full Core Box Number	$K_{\text{eff}}^{\text{a}}$	Dropped Rod Worth (%$\Delta\rho$)
Grp 3/Box 4	0.9980146	-0.0081
Grp A/Box 10	0.9976362	-0.0461
Grp 1/Box 12	0.9974657	-0.0632
Grp 4/Box 19	0.9980274	-0.0068
Grp 2/Box 21	0.9977101	-0.0387
Grp 3/Box 25	0.9975900	-0.0507
Grp B/Box 34	0.9975028	-0.0595
Grp B/Box 36	0.9972037	-0.0896
Grp B/Box 38	0.9970983	-0.1002
Grp 5/Box 54	0.9975405	-0.0557
Grp 4/Box 67	0.9975515	-0.0546
Grp A/Box 69	0.9968888	-0.1213
Grp 3/Box 103	0.9967110	-0.1392

a. The ARO K_{eff} is 0.9980953 at a CBC of 2,075 PPM.

Table 4-29 Differences Between U1C1 Measured Dropped Rod Worths and the SIMULATE-3 and ROCS Calculations

Dropped Rod Group and Full Core Box Number	ROCS Difference		SIMULATE-3 Difference	
	M - C Absolute ($\% \Delta \rho$)	(M - C) / C Relative	M - C Absolute ($\% \Delta \rho$)	(M - C) / C Relative
Grp 3/Box 3	0.0141	-0.1619	0.0341	-0.3178
Grp A/Box 9	0.0170	-0.1977	0.0322	-0.3175
PLCEA/Box 31	0.0016	-0.0741	-0.0025	0.1494
PLCEA Subgroup P1	NA ^a			
Average	0.0109	-0.1446	0.0213	-0.1618
Standard Deviation	0.0082	0.0636	0.0206	0.2696

a.Measurement is too small. Subgroup P1 has 5 rods, one of which is P31 so P1 should be at least 5 times larger than P31.

**Table 4-30 Differences Between SIMULATE-3 and ROCS Dropped Rod Worths
for Cycle 8 for Units 1, 2, and 3**

Dropped Rod Group and Full Core Box Number	Difference	
	ROCS - SIM Absolute ($\% \Delta \rho$)	(ROCS - SIM) / SIM Relative
U1C8		
Grp 3/Box 4	0.0006	-0.0870
Grp A/Box 10	0.0008	-0.0238
Grp 1/Box 12	0.0006	-0.0099
Grp 4/Box 19	0.0005	-0.2941
Grp 2/Box 21	0.0005	-0.0220
Grp 3/Box 25	0.0002	-0.0041
Grp B/Box 34	0.0010	-0.0177
Grp B/Box 36	0.0034	-0.0371
Grp B/Box 38	0.0046	-0.0455
Grp 5/Box 54	0.0036	-0.0641
Grp 4/Box 67	0.0036	-0.0526
Grp A/Box 69	0.0116	-0.0841
Grp 3/Box 103	0.0188	-0.1166
U2C8		
Grp 3/Box 4	0.0005	-0.0532
Grp A/Box 10	0.0006	-0.0124
Grp 1/Box 12	0.0019	-0.0279
Grp 4/Box 19	0.0008	-0.3810
Grp 2/Box 21	0.0002	-0.0058
Grp 3/Box 25	0.0011	-0.0248
Grp B/Box 34	0.0023	-0.0401
Grp B/Box 36	0.0040	-0.0447
Grp B/Box 38	0.0052	-0.0521
Grp 5/Box 54	0.0033	-0.0573
Grp 4/Box 67	0.0026	-0.0482

Table 4-30 Differences Between SIMULATE-3 and ROCS Dropped Rod Worths for Cycle 8 for Units 1, 2, and 3

Dropped Rod Group and Full Core Box Number	Difference	
	ROCS - SIM Absolute ($\% \Delta \rho$)	(ROCS - SIM) / SIM Relative
Grp A/Box 69	0.0098	-0.0807
Grp 3/Box 103	0.0128	-0.1046
U3C8		
Grp 3/Box 4	0.0003	-0.0370
Grp A/Box 10	0.0011	-0.0239
Grp 1/Box 12	0.0018	-0.0285
Grp 4/Box 19	0.0001	-0.0147
Grp 2/Box 21	0.0000	0.0000
Grp 3/Box 25	0.0008	-0.0158
Grp B/Box 34	0.0013	-0.0218
Grp B/Box 36	0.0035	-0.0391
Grp B/Box 38	0.0048	-0.0479
Grp 5/Box 54	0.0026	-0.0467
Grp 4/Box 67	0.0020	-0.0366
Grp A/Box 69	0.0085	-0.0701
Grp 3/Box 103	0.0121	-0.0869
Average	0.0034	-0.0580
Standard Deviation	0.0042	0.0712

4.9 EJECTED ROD

Measurement Technique

The measurements were performed to measure the worth of the worst “ejected” control rod (CEA) from the zero power dependent insertion limit (ZPDIL). The worths of the following CEAs were measured:

- Worst ejected CEA (CEA 87 (Box 87))
- Next worst ejected CEA (CEA 19 (Box 19))

The measurements were performed with the RCS at 565°F and 2250 psia. The measured ejected rod worths were required to be within $\pm 0.1\%$ of the predicted worths.

With CEA groups 5 and 4 at the lower Lower Electrical Limit (LEL), and group 3 partially inserted, the worths of the ejected CEAs were measured as follows. All changes in reactivity were recorded by a strip chart recorder.

CEA 87 (Box 87) - CEA 87 withdrawal was traded with group 3 insertion until group 3 reached its LEL (“near” ZPDIL). At that point, boration of the RCS was initiated and CEA 87 was withdrawn in discrete steps to its Upper Electrical Limit (UEL).

CEA 19 (Box 19) - CEA 19 withdrawal was exchanged with CEA 87 insertion until CEA 19 reached its UEL and CEA 87 reached its LEL.

To determine the worths of the ejected CEAs, the reactivity data for the measurements was obtained from the strip chart recorder and analyzed in a manner similar to that used to determine the individual CEA group worths.

Measurement uncertainty for control rod worths is due to (1) beta-effective data used in the reactivity computer and (2) the effect of spatial flux redistribution on the flux incident on the excore detectors.

Calculational Method

Palo Verde measured two ejected rod worths at BOC of U1C1. Since there is a limited database the following method will be used to determine the appropriate bias and uncertainty.

- SIMULATE-3 will be used to calculate the two ejected rod worths measured at BOC U1C1.
- Both SIMULATE-3 and ROCS will be used to calculate ejected rod worths for U1C8, U2C8, and U3C8.
- Compare the SIMULATE-3’s and ROCS’s ejected rod worths and calculate a SIMULATE-3 to ROCS bias.
- Using this SIMULATE-3 to ROCS bias adjust the existing ejected ROCS biases and use the adjusted bias as SIMULATE-3’s ejected bias.
- Use the ROCS ejected uncertainties.

Table 4-39 shows the ejected worth results. In absolute units (ROCS - SIMULATE-3), the statistics are -1.1 ± 5.1 pcm. This shows that the differences between SIMULATE-3 and ROCS are small. Thus, the ROCS ejected uncertainty of [] will be used as SIMULATE-3's ejected uncertainty. (NOTE: The conservatism in the ABB (ROCS) ejected uncertainty helps to make up for the limited amount of PVNGS measured data.)

Statistical Results

The tolerance limits for the SIMULATE-3 ejected rod worths are:

[]

Table 4-31 U1C1 Ejected Rod Worths from ROCS, SIMULATE-3, and Measurement

Ejected Rod Group and Full Core Box Number	Measurement (% $\Delta\rho$)	ROCS Ejected Rod Worth (%$\Delta\rho$)	SIMULATE-3 K_{eff}^a	SIMULATE-3 Ejected Rod Worth (%$\Delta\rho$)
Grp 4/Box 87	0.147 SIMULATE-3: 0.146 ^b	0.1346	0.9993922	0.120
Grp 4/Box 19	0.138 SIMULATE-3: 0.1375	0.1092	0.9994314	0.124

a. The ARO K_{eff} is 0.9981950 at a CBC of 893 PPM.

b. The measured value was corrected for the difference in B_{eff} between SIMULATE-3 and ROCS. This correction factor is 0.995334.

Table 4-32 U1C8 Ejected Rod Worths from ROCS

Ejected Rod Group and Full Core Box Number	Reactivity^a	Ejected Rod Worth (%$\Delta\rho$)
Grp 3/Box 4	0.2827	0.0098
Grp 4/Box 19	0.2773	0.0044
Grp 3/Box 25	0.4531	0.1802
Grp 5/Box 54	0.3426	0.0697
Grp 4/Box 67	0.4403	0.1674
Grp 3/Box 103	0.3358	0.0629

a. The Banks 3-5 All-rods-in ρ is 0.2729, at a CBC of 2,017 PPM.

Table 4-33 U2C8 Ejected Rod Worths from ROCS

Ejected Rod Group and Full Core Box Number	Reactivity^a	Ejected Rod Worth (%$\Delta\rho$)
Grp 3/Box 4	0.2883	0.0148
Grp 4/Box 19	0.2776	0.0041
Grp 3/Box 25	0.3961	0.1226
Grp 5/Box 54	0.3455	0.0720
Grp 4/Box 67	0.3742	0.1007
Grp 3/Box 103	0.3199	0.0464

a. The Banks 3-5 All-rods-in ρ is 0.2735, at a CBC of 2,012 PPM.

Table 4-34 U3C8 Ejected Rod Worths from ROCS

Ejected Rod Group and Full Core Box Number	Reactivity^a	Ejected Rod Worth (%$\Delta\rho$)
Grp 3/Box 4	0.2774	0.0110
Grp 4/Box 19	0.2866	0.0202
Grp 3/Box 25	0.4194	0.1530
Grp 5/Box 54	0.3305	0.0641
Grp 4/Box 67	0.3711	0.1047
Grp 3/Box 103	0.3121	0.0457

a. The Banks 3-5 All-rods-in ρ is 0.2664, at a CBC of 1,900 PPM.

Table 4-35 U1C8 Ejected Rod Worths from SIMULATE-3

Ejected Rod Group and Full Core Box Number	K_{eff}^a	Ejected Rod Worth ($\% \Delta \rho$)
Grp 3/Box 4	0.9968283	0.0109
Grp 4/Box 19	0.9967728	0.0053
Grp 3/Box 25	0.9983904	0.1679
Grp 5/Box 54	0.9974602	0.0745
Grp 4/Box 67	0.9983600	0.1648
Grp 3/Box 103	0.9974561	0.0741

a. The Banks 3-5 All-rods-in K_{eff} is 0.9967198, at a CBC of 2,017 PPM.

Table 4-36 U2C8 Ejected Rod Worths from SIMULATE-3

Ejected Rod Group and Full Core Box Number	$K_{\text{eff}}^{\text{a}}$	Ejected Rod Worth ($\% \Delta \rho$)
Grp 3/Box 4	0.9964157	0.0154
Grp 4/Box 19	0.9961014	0.0048
Grp 3/Box 25	0.9971346	0.1194
Grp 5/Box 54	0.9966924	0.0750
Grp 4/Box 67	0.9969505	0.1009
Grp 3/Box 103	0.9964855	0.0541

a. The Banks 3-5 All-rods-in K_{eff} is 0.9959484 at a CBC of 2,012 PPM.

Table 4-37 U3C8 Ejected Rod Worths from SIMULATE-3

Ejected Rod Group and Full Core Box Number	$K_{\text{eff}}^{\text{a}}$	Ejected Rod Worth (%$\Delta\rho$)
Grp 3/Box 4	0.9980146	0.0119
Grp 4/Box 19	0.9975910	0.0201
Grp 3/Box 25	0.9989575	0.1491
Grp 5/Box 54	0.9981485	0.0679
Grp 4/Box 67	0.9985111	0.1043
Grp 3/Box 103	0.9979955	0.0526

a. The Banks 3-5 All-rods-in K_{eff} is 0.9974723 at a CBC of 1,900 PPM.

Table 4-38 Differences Between UIC1 Measured Ejected Rod Worths and the SIMULATE-3 and ROCS Calculations

Ejected Rod Group and Full Core Box Number	ROCS Difference in%		SIMULATE-3 Difference	
	M - C Absolute ($\% \Delta \rho$)	(M - C) / C Relative	M - C Absolute ($\% \Delta \rho$)	(M - C) / C Relative
Grp 4/Box 87	0.0124	0.0921	0.0260	0.2167
Grp 4/Box 19	0.0288	0.2637	0.0130	0.1048
Average	0.0206	0.1779	0.0195	0.1608
Standard Deviation	0.0116	0.1213	0.0092	0.0791

Table 4-39 Differences Between SIMULATE-3 and ROCS Ejected Rod Worths for Cycle 8 for Units 1, 2, and 3

Ejected Rod Group and Full Core Box Number	Difference	
	ROCS - SIM Absolute ($\% \Delta \rho$)	(ROCS - SIM) / SIM Relative
U1C8		
Grp 3/Box 4	-0.0011	-0.1009
Grp 4/Box 19	-0.0009	-0.1698
Grp 3/Box 25	0.0123	0.0733
Grp 5/Box 54	-0.0048	-0.0644
Grp 4/Box 67	0.0026	0.0158
Grp 3/Box 103	-0.0112	-0.1511
U2C8		
Grp 3/Box 4	-0.0006	-0.0390
Grp 4/Box 19	-0.0007	-0.1458
Grp 3/Box 25	0.0032	0.0268
Grp 5/Box 54	-0.0030	-0.0400
Grp 4/Box 67	-0.0002	-0.0020
Grp 3/Box 103	-0.0077	-0.1423
U3C8		
Grp 3/Box 4	-0.0009	-0.0756
Grp 4/Box 19	0.0001	0.0050
Grp 3/Box 25	0.0039	0.0262
Grp 5/Box 54	-0.0038	-0.0560
Grp 4/Box 67	0.0004	0.0038
Grp 3/Box 103	-0.0069	-0.1312
Average	-0.0011	-0.0537
Standard Deviation	0.0051	0.0734

5.0 POWER PEAKING FACTOR UNCERTAINTY

5.1 INTRODUCTION

The purpose of this section is to quantify the numerical uncertainties associated with the use of the CECOR system with fixed in-core detectors and the numerical uncertainties associated with the use of the SIMULATE-3 code in inferring the following pin power peaking factors:

- (1) $F_q(\text{pin})$, the ratio of the peak local pin power to the average local pin power,
- (2) $F_r(\text{pin})$, the ratio of the peak axially integrated pin power to the average axially integrated pin power, and
- (3) $F_{xy}(\text{pin})$, the ratio of the planar peak pin power to the planar average pin power.

The numerical uncertainties associated with the use of the CECOR system with fixed in-core detectors will be referred to as the measurement uncertainties while those associated with the use of the SIMULATE-3 code will be referred to as the calculational uncertainties.

The measurement uncertainties consist of the following four components:

- (1) $F_{pC}\left(\frac{\text{pin}}{\text{box}}\right)$, the pin-to-box power peaking factor calculational uncertainty (Section 5.2),
- (2) $F_{BM}(\text{box})$, the instrumented box power peaking factor measurement uncertainty (Section 5.3.7 and 5.3.8),
- (3) $F_{pS}\left(\frac{\text{pin}}{\text{box}}\right)$, the pin-to-box power peaking factor synthesis uncertainty (Section 5.4),
and
- (4) $F_{BS}(\text{box})$, the uninstrumented box power peaking factor synthesis uncertainty (Section 5.4).

The calculational uncertainties consist of the following two components:

- (1) $F_{pC}\left(\frac{\text{pin}}{\text{box}}\right)$, the pin-to-box power peaking factor calculational uncertainty (Section 5.2) and
- (2) $F_{BC}(\text{box})$, the instrumented box power peaking factor calculational uncertainty (Section 5.3.6).

The box power peaking factor calculational uncertainty was quantified with the historical pattern of 61 in-core detector strings while the box power peaking factor measurement uncertainty was quantified with both the historical pattern of 61 detector strings and a proposed future pattern of 50 detector strings.

5.2 PIN PEAKING CALCULATION UNCERTAINTY

Yankee Atomic Electric Company (YAEC) verified the pin power reconstruction capabilities of SIMULATE-3 in extensive benchmarking (Reference 7). The Southern California Edison Company CASMO-3/SIMULATE-3 topical (Reference 22) and the Duke Power Company CASMO-3/SIMULATE-3P topical (Reference 23) both cite YAECs SIMULATE-3 validation as a basis for their pin power uncertainties. Reference 20 presents results of benchmarking CASMO-4 against critical experiments.

This section describes the development of pin-to-box uncertainty for the CASMO-4/SIMULATE-3 code group. Section 5.2.1 describes the comparison of pin fission rates calculated in CASMO-4 and DOT (Reference 15) with measurements from the RPI Critical Experiments (Reference 17). Section 5.2.1 also describes a comparison of the CASMO-4/DOT method with DIT/DOT and CASMO-3/DORT methods. Section 5.2.2 describes the computation of the CASMO-4 component of the combined CASMO-4/SIMULATE-3 uncertainty, Section 5.2.3 describes the computation of the SIMULATE-3 component, and Section 5.2.4 describes the computation of the combined CASMO-4/SIMULATE-3 uncertainty from the CASMO-4 and SIMULATE-3 components. (The pin-to-box calculation error is a combination of the CASMO-4 absolute pin power error and the SIMULATE-3 pin power reconstruction algorithm error.)

5.2.1 CASMO-4/DOT UNCERTAINTY FROM RPI CRITICALS

In order to establish a pin power calculational uncertainty for CASMO-4, this section compares the predicted pin-by-pin power distributions with the measured data from the RPI critical experiment. The core configurations compared were the 0/468, 20/468, 44/468, and the 56/468 core configurations (corresponding to 0, 20, 44, and 56 erbium pins) described in Reference 17.

The cross sections for each lattice type were calculated in CASMO-4. A preliminary comparison was performed by comparing the CASMO-4 calculated pin powers on a single, infinite lattice type with the same single lattice modeled in DOT. The preliminary comparison showed that the pin powers calculated with CASMO-4 and DOT were within a small calculational uncertainty. The entire core was then modeled in DOT (Reference 15), and the calculated pin powers were compared with the measured results from the RPI critical experiment. The CASMO-4/DOT calculational uncertainty therefore includes the calculational uncertainty of DOT. The CASMO-4/DOT pin power uncertainty was calculated using the same method as for the DIT/DOT pin power uncertainty, as described in Reference 17.

Measurement Technique

The measurements were obtained by counting delayed fission product gammas in the test lattices used in the RPI critical experiment. The count rate was proportional to the fission rate. Details of the RPI critical experiment, including a description of the cores used and the measurement technique are included in References 16 and 17. The test lattice configurations used in the RPI critical experiment (pin dimensions, water hole, burnable absorber) are similar to lattices used at PVNGS.

Comparison of Results

Figure 5-1 through Figure 5-4 show the CASMO-4/DOT pin power distributions and the measurements. The data on the figures have been normalized. Both the measured and calculated data were normalized to the average value of the distribution for each eighth core. The differences were then based on the normalized data. The differences are percent differences, given by

$$100\% \times \frac{(\text{Calculated} - \text{Measured})}{\text{Measured}}$$

Also included on each figure is the standard deviation for each lattice configuration.

Statistical Analysis

A mean and standard deviation were calculated for each core configuration, and for the pooled data. The mean is negligibly small and negative, so it will be assumed to be 0. Figure 5-1 through Figure 5-4 show the standard deviations for the observed differences between the CASMO-4/DOT pin fission rates and the measured pin fission rates for the four core configurations.

The W test (Reference 12), a test for normality, was performed on the distribution of observed differences from each of the four cores. The W test can be used when the number of data points is small ($n < 50$). Table 5-1 presents the results of the W test.

The method used in deriving the calculational uncertainty for the CASMO-4/DOT pin fission rates is the same method used in Reference 17. The variance in the observed difference (D) is related to the measurement (M) and calculational (C) variances by:

$$s_D^2 = s_C^2 + s_M^2$$

The equation given above yields the calculational standard deviation for pin fission rates calculated by CASMO-4/DOT. Table 5-2 presents the CASMO-4/DOT calculational standard deviations for the four core configurations and for the pooled data.

The method used in deriving the calculational degrees of freedom for the CASMO-4/DOT pin fission rates is the same method used in Reference 25. The degrees of freedom in the observed difference is related to the measurement and calculational degrees of freedom by:

$$\frac{s_D^4}{f_D} = \frac{s_C^4}{f_C} + \frac{s_M^4}{f_M}$$

The equation given above yields the calculational degrees of freedom for pin powers calculated by CASMO-4/DOT. Table 5-2 presents the CASMO-4/DOT calculational degrees of freedom for the pooled data.

Comparison with DIT/DOT and CASMO-3/DORT Methods

Reference 30 describes analyses that have been performed by ABB-CE using the DIT and DOT codes and Southern California Edison (SCE) using CASMO-3 and DORT (References 32 through

35). Both analyses compared calculated pin powers with measurements from the RPI critical experiments. Table 5-3 shows a comparison of sample standard deviations of the observed differences (C-M) for the ABB-CE's DIT/DOT calculations, SCE's CASMO-3/DORT calculations, and APS's CASMO-4/DOT calculations.

The data in Table 5-3 show that the three methods are close in their ability to calculate cores with erbia.

5.2.2 CASMO-4 UNCERTAINTY FROM RPI AND B&W CRITICALS

CASMO-4 Uncertainty from RPI Erbium Criticals

To make direct comparisons between CASMO-4 results and the RPI Critical Experiments, the latter were taken for the centrally located assembly in the core where effects of the global distribution are a minimum. Quarter core and single assembly CASMO-4/DOT calculations were performed for each RPI lattice type. The experimental results were then reduced to remove the global component using the CASMO-4/DOT calculations for the quarter core and for the central assembly. The experimental results thus obtained were compared directly to the CASMO-4 calculations. The resulting differences are a measure of the CASMO-4 pin fission rate calculation uncertainty. The method for removing the global component introduced an additional uncertainty in the experimental values. This uncertainty component is automatically retained in the final estimate of the uncertainty of the calculational method since it is part of the standard deviation. The method used to remove the global component is analogous to the method used in Section 3.3.3.3 of Reference 25.

The variance of the RPI sample of the CASMO-4 error distribution is given by

$$S_{rpi}^2 = S_{diff}^2 - S_{meas}^2$$

The degrees of freedom of the sample is given by

$$\frac{S_{rpi}^4}{f_{rpi}} = \frac{S_{diff}^4}{f_{diff}} - \frac{S_{meas}^4}{f_{meas}}$$

where S denotes the sample standard deviation, f denotes the sample degrees of freedom,

$diff$ denotes the difference between measurement and calculation, and $meas$ denotes measurement.

Table 5-4 presents the standard deviation and degrees of freedom of the RPI sample of the CASMO-4 error distribution.

The sample has a standard deviation of [] and [] degrees of freedom.

CASMO-4 Uncertainty from B&W Gadolinium Criticals

Reference 20 describes the SOA benchmarking of CASMO-4 against the Babcock and Wilcox (B&W) critical experiments. The B&W critical experiments are described in Reference 31. A typical B&W critical geometry consists of a single B&W or CE type fuel assembly embedded in an array of B&W or CE type fuel assemblies surrounded by a water reflector.

Because the KRAM two-dimensional heterogeneous transport solution within CASMO-4 is incapable of modeling such large problems, the critical experiments were modeled outside of CASMO-4 using a stand-alone version of the characteristics solution, capable of modeling large problems. All cross sections for the stand-alone model were generated by CASMO-4. The stand-alone code gives identical results to the CASMO-4 code for smaller problems that can be modeled by both codes. Hence, we shall refer to the stand-alone model results as stand-alone CASMO-4 results and treat them as CASMO-4 results. See Reference 20 for further details.

Reference 20 gives results for the comparison of stand-alone CASMO-4 calculated fission rates to measured fission rates from the B&W criticals. The results are reproduced in Table 5-5. The results presented in Table 5-5 show good agreement between the stand-alone CASMO-4 fission rates and the measured fission rates from the B&W critical experiments.

CASMO-4 Uncertainty from RPI and B&W Criticals

We now pool the RPI and B&W samples of the CASMO-4 error distribution to obtain the RPI + B&W sample of the CASMO-4 error distribution. The sample includes the effects of both erbium and gadolinium. The variance of the RPI + B&W sample is given by

$$S_{rpi + baw}^2 = \frac{f_{rpi} \times S_{rpi}^2 + f_{baw} \times S_{baw}^2}{f_{rpi} + f_{baw}}$$

The degrees of freedom of the sample is given by

$$f_{rpi + baw} = f_{rpi} + f_{baw}$$

where *baw* denotes the B&W sample and *rpi + baw* denotes the RPI + B&W sample of the CASMO-4 error distribution.

Table 5-4 gives the standard deviation and degrees of freedom of the RPI sample of the CASMO-4 error distribution. Table 5-5 gives the standard deviation and degrees of freedom of the B&W sample of the CASMO-4 error distribution. The results of pooling these two samples are shown in Table 5-6.

The RPI + B&W sample has a standard deviation of [] and [] degrees of freedom.

5.2.3 SIMULATE-3 UNCERTAINTY FROM B&W CRITICALS

CASMO-4/SIMULATE-3 Uncertainty from B&W Criticals

Table 5-5 also shows the results of APS benchmarking of CASMO-4/SIMULATE-3 against Babcock and Wilcox (B&W) critical experiments. A large number of different fuel assembly designs were used in the experiments, including a variety of enrichments, small (15x15 B&W) and large (16x16 CE) water holes, and with and without gadolinia pins.

Assembly-homogenized cross sections, discontinuity factors, and pin power form functions required by SIMULATE-3 were generated using single-assembly CASMO-4 calculations of each assembly type. Reflector data for SIMULATE-3 was generated using the CASMO-4 reflector option, and cross sections were tabulated as functions of the boron concentration, fuel temperature, and moderator temperature. The CASMO-4/SIMULATE-3 models of the B&W cores were essentially the same as those used by the Studsvik code system to analyze power reactors.

The results demonstrate that uncertainties in the CASMO-4/SIMULATE-3 pin fission rates are slightly greater than the uncertainties in the stand-alone CASMO-4 pin fission rates.

SIMULATE-3 Uncertainty from B&W Criticals

The variance of the B&W sample of the SIMULATE-3 component of the CASMO-4/SIMULATE-3 error distribution is given by

$$S_{sim}^2 = S_{cas \cdot sim}^2 - S_{baw}^2$$

The degrees of freedom of the sample can be computed from the equation

$$\frac{S_{sim}^4}{f_{sim}} = \frac{S_{cas \cdot sim}^4}{f_{cas \cdot sim}} - \frac{S_{baw}^4}{f_{baw}}$$

where *sim* denotes the SIMULATE-3 component of the CASMO-4/SIMULATE-3 calculation error and *cas · sim* denotes the CASMO-4/SIMULATE-3 error.

Table 5-5 gives the standard deviation and degrees of freedom of the differences between the stand-alone CASMO-4 pin fission rate calculations and the B&W pin fission rate measurements and Table 5-5 also gives the standard deviations and degrees of freedom of the differences between the CASMO-4/SIMULATE-3 pin fission rate calculations and the same B&W pin fission rate measurements. The results of combining these results to obtain the standard deviation and degrees of freedom of the B&W sample of the SIMULATE-3 component of the CASMO-4/SIMULATE-3 pin-to-box power peaking factor error distribution are shown in Table 5-7.

The sample has a standard deviation of [] and [] degrees of freedom.

5.2.4 CASMO-4/SIMULATE-3 UNCERTAINTY FROM RPI AND B&W CRITICALS

We now combine the RPI + B&W sample of the CASMO-4 calculation error distribution with the B&W sample of the SIMULATE-3 component of the CASMO-4/SIMULATE-3 calculation error distribution to obtain the (RPI + B&W)/B&W sample of the CASMO-4/SIMULATE-3 calculation error distribution. This sample includes the effects of both erbium and gadolinium.

The variance of the sample is given by

$$S_{(baw + rpi) \cdot sim}^2 = S_{baw + rpi}^2 + S_{sim}^2$$

The degrees of freedom of the sample can be computed from the equation

$$\frac{S_{(baw + rpi) \cdot sim}^4}{f_{(baw + rpi) \cdot sim}} = \frac{S_{baw + rpi}^4}{f_{baw + rpi}} + \frac{S_{sim}^4}{f_{sim}}$$

where $(baw + rpi) \cdot sim$ denotes the combination of the RPI + B&W sample of the CASMO-4 pin-to-box power peaking factor error distribution with the B&W sample of the SIMULATE-3 component of the CASMO-4/SIMULATE-3 pin-to-box power peaking factor error distribution.

Table 5-6 gives the standard deviation and degrees of freedom of the RPI + B&W sample of the CASMO-4 pin-to-box power peaking factor error distribution, and Table 5-7 gives the standard deviation and degrees of freedom of the B&W sample of the SIMULATE-3 component of the CASMO-4/SIMULATE-3 pin-to-box power peaking factor error distribution. The result of combining these results to obtain the standard deviation and degrees of freedom of the (RPI + B&W)/B&W sample of the CASMO-4/SIMULATE-3 pin-to-box power peaking factor error distribution is shown in Table 5-8.

The sample has a standard deviation of [] and [] degrees of freedom.

Table 5-1 RPI Criticals - W Test for Normality of CASMO-4/DOT Pin Peaking Data

Core (# of Erbium Pins)	Number of Data Points	Calculated W	W from Table^a	Normal?
0	32	0.976	0.930	Yes
20	32	0.933		Yes
44	32	0.971		Yes
56	32	0.963		Yes

a. From Table 2 of Reference 12 for the 5th percentage point (0.05)

Table 5-2 RPI Criticals - CASMO-4/DOT Uncertainty

Core	Difference	Difference	Measure- ment	Measure- ment	Calcula- tion	Calcula- tion
# of Erbium Pins	Standard Deviation	Degrees of Freedom	Standard Deviation	Degrees of Freedom	Standard Deviation	Degrees of Freedom
0	1.50%	31	[]	[]		
20	2.18	31	[]	[]		
44	1.51	31	[]	[]		
56	0.96	31	[]	[]		
Pooled Values	1.59	124	[]	[]	[]	[]

Table 5-3 RPI Criticals - DIT/DOT, CASMO-3/DORT, and CASMO-4/DOT Uncertainty

Core	ABB-CE	SCE	APS
(# of Erbium Pins)	DIT/ DOT	CASMO-3/ DORT	CASMO-4/ DOT
0	2.1%	2.0%	1.5%
20	2.5	1.9	2.2
44	1.3	1.5	1.5
56	1.1	1.9	1.0
Pooled Values	1.9	1.7	1.6

Table 5-4 RPI Criticals - CASMO-4 Uncertainty

Core	Difference	Difference	Measure- ment	Measure- ment	Calcula- tion	Calcula- tion
# of Erbium Pins	Standard Deviation	Degrees of Freedom	Standard Deviation	Degrees of Freedom	Standard Deviation	Degrees of Freedom
0	1.33%	31	[]	[]		
20	2.07	31	[]	[]		
44	1.23	31	[]	[]		
56	1.14	31	[]	[]		
Pooled Values	1.49	124	[]	[]	[]	[]

Table 5-5 B&W Criticals - CASMO-4 and CASMO-4/SIMULATE-3 Uncertainty

B&W Core	Description	Degrees of Freedom	Stand-Alone CASMO-4 Standard Deviation	CASMO-4/SIMULATE-3 Standard Deviation
I	Base B&W, no absorbers	31	0.50	0.55
V	28 Gd rods, 12 in center assy	31	0.48	0.60
XII	Split enrichment B&W, no absorbers	31	0.75	0.77
XIV	28 Gd rods, 12 in center assy	31	0.84	0.86
XVIII	Base CE, no absorbers	31	0.72	1.07
XX	32 Gd rods, 16 in center assy	31	0.84	1.09
Pooled		186	0.71	0.85

Table 5-6 RPI and B&W Criticals - CASMO-4 Uncertainty

Source	Description	Degrees of Freedom	Standard Deviation
RPI	CASMO-4	[]	[]
B&W	CASMO-4	186	0.71
RPI + B&W	CASMO-4	[]	[]

Table 5-7 B&W Criticals - SIMULATE-3 Uncertainty

Source	Description	Degrees of Freedom	Standard Deviation
B&W	CASMO-4/SIMULATE-3	186	0.85%
B&W	CASMO-4	186	0.71
B&W	SIMULATE-3	34	0.47

Table 5-8 RPI and B&W Criticals - CASMO-4/SIMULATE-3 Uncertainty

Source	Description	Degrees of Freedom	Standard Deviation
RPI + B&W	CASMO-4	[]	[]
B&W	SIMULATE-3	34	0.47
RPI + B&W	CASMO-4/SIMULATE-3	[]	[]

Figure 5-1 Central 1/4 Assembly of RPI Critical 0 Erbium Pin Core

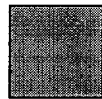
Measured (Normalized)
 Calculated (Normalized)
 % Difference $100\% * (\text{Calculated} - \text{Measured}) / \text{Measured}$

							[] 0.68 []
						[] 0.78 []	[] 0.72 []
					[] 0.98 []	[] 0.85 []	[] 0.77 []
					[] 1.17 []	[] 0.91 []	[] 0.81 []
					[] 1.20 []	[] 0.94 []	[] 0.84 []
		[] 1.19 []	[] 1.31 []	[] 1.27 []	[] 1.07 []	[] 0.93 []	[] 0.85 []
	[] 1.24 []	[] 1.14 []	[] 1.11 []	[] 1.06 []	[] 0.99 []	[] 0.92 []	[] 0.86 []
	[] 1.41 []	[] 1.15 []	[] 1.07 []	[] 1.02 []	[] 0.97 []	[] 0.91 []	[] 0.86 []

H2O



ERBIA



UO2



Standard Deviation = 1.50%

Figure 5-2 Central 1/4 Assembly of RPI Critical 20 Erbium Pin Core

Measured (Normalized)
 Calculated (Normalized)
 % Difference 100%*(Calculated - Measured)/Measured

							[] 0.69 []
						[] 0.75 []	[] 0.73 []
					[] 0.99 []	[] 0.86 []	[] 0.78 []
					[] 1.19 []	[] 0.92 []	[] 0.82 []
					[] 1.22 []	[] 0.95 []	[] 0.85 []
		[] 1.18 []	[] 1.32 []	[] 1.28 []	[] 1.07 []	[] 0.89 []	[] 0.86 []
	[] 1.21 []	[] 1.07 []	[] 1.10 []	[] 1.07 []	[] 1.00 []	[] 0.92 []	[] 0.87 []
	[] 1.40 []	[] 1.14 []	[] 1.07 []	[] 1.03 []	[] 0.98 []	[] 0.93 []	[] 0.87 []

H2O



ERBIA



UO2



Standard Deviation = 2.18%

Figure 5-3 Central 1/4 Assembly of RPI Critical 44 Erbium Pin Core

Measured (Normalized)
 Calculated (Normalized)
 % Difference $100\% * (\text{Calculated} - \text{Measured}) / \text{Measured}$

							[] 0.73 []
						[] 0.83 []	[] 0.78 []
					[] 0.99 []	[] 0.88 []	[] 0.82 []
					[] 1.12 []	[] 0.93 []	[] 0.85 []
					[] 1.15 []	[] 0.96 []	[] 0.88 []
		[] 1.15 []	[] 1.23 []	[] 1.20 []	[] 1.07 []	[] 0.96 []	[] 0.90 []
	[] 1.12 []	[] 1.10 []	[] 1.09 []	[] 1.06 []	[] 1.01 []	[] 0.96 []	[] 0.90 []
	[] 1.28 []	[] 1.11 []	[] 1.06 []	[] 1.03 []	[] 1.00 []	[] 0.95 []	[] 0.91 []

H2O



ERBIA



UO2



Standard Deviation = 1.51%

Figure 5-4 Central 1/4 Assembly of RPI Critical 56 Erbium Pin Core

Measured (Normalized)
 Calculated (Normalized)
 % Difference $100\% * (\text{Calculated} - \text{Measured}) / \text{Measured}$

							[] 0.74 []
						[] 0.83 []	[] 0.78 []
					[] 0.94 []	[] 0.88 []	[] 0.82 []
					[] 1.11 []	[] 0.93 []	[] 0.86 []
					[] 1.14 []	[] 0.96 []	[] 0.89 []
		[] 1.16 []	[] 1.23 []	[] 1.20 []	[] 1.02 []	[] 0.95 []	[] 0.90 []
	[] 1.13 []	[] 1.11 []	[] 1.09 []	[] 1.06 []	[] 1.01 []	[] 0.96 []	[] 0.91 []
	[] 1.29 []	[] 1.12 []	[] 1.07 []	[] 1.04 []	[] 1.00 []	[] 0.96 []	[] 0.92 []

H2O



ERBIA



UO2



Standard Deviation = 0.96%

5.3 INSTRUMENTED BOX POWER UNCERTAINTY FOR F_q , F_r , and F_{xy}

5.3.1 INTRODUCTION

The box power peaking factor uncertainty can be obtained by comparing SIMULATE-3 calculations of the fuel assembly box powers with those inferred from in-core measurements with the CECOR system using fixed, in-core rhodium detectors. The resulting difference is a reflection of both measurement and calculational uncertainties and errors.

Comparisons of measured and calculated box powers have been made for PVNGS Units 1, 2, and 3 for cycles 4, 5, and 6. The data reflects a mixture of B4C and erbium burnable absorber core designs. It also reflects a mixture of conventional and guardian grid fuel assembly designs, a mixture of 85% and 100% HFP operation, a mixture of 565F and 555F inlet coolant temperature operation, and a mixture of initial HFP and stretch HFP operation.

5.3.2 DESCRIPTION OF MEASURED DATA

The measured data consist of the powers in assemblies with fixed in-core detectors. The fixed in-core detectors consist of self-powered rhodium neutron detectors. Each detector segment is 40 cm long and each instrumented assembly contains five segments. The segments are nominally centered at 10%, 30%, 50%, 70%, and 90% of the core height. A more complete description of the in-core instrument system is given in Section I.1 of Reference 25.

The conversion of detector signals to box powers by the CE CECOR fixed in-core detector analysis system uses signal to power conversion factors calculated as a function of assembly burnup by the SIMULATE-3 and CECORLIB codes. It also uses depletion dependent instrument sensitivity factors including initial calibration and background corrections. Calculational errors in these factors are therefore included when comparing the measured assembly power with the true power distribution. A more complete description is given in Section II.1 of Reference 25.

The CECOR code models the PVNGS cores in full core with one radial node and 51 axial planes per assembly.

5.3.3 OPERATING HISTORIES

PVNGS Unit 1 Cycle 4

- (1) operated at 100% HFP and 565°F from 0 to 13.021 GWD/MTU,
- (2) powered down to 40% HFP and 565°F from 13.021 to 13.074 GWD/MTU,
- (3) powered up to 100% HFP and 565°F from 13.074 to 13.226 GWD/MTU,
- (4) operated at 100% HFP and 565°F from 13.226 to 14.563 GWD/MTU,
- (5) powered down to 89% HFP and 56°F from 14.563 to 15.098 GWD/MTU,
- (6) powered and cooled down to 72% HFP and 560°F from 15.098 to 16.298 GWD/MTU,

- (7) powered down and heated up to 65% HFP and 564°F from 16.298 to 16.399 GWD/MTU,
- (8) operated at 65% HFP and 564°F from 16.399 to 16.598 GWD/MTU, and
- (9) shutdown for refueling at 16.598 GWD/MTU.

Rodded snapshots were taken at 0.152, 11.302, and 13.074 GWD/MTU.

The batch of fresh fuel assemblies loaded in PVNGS Unit 1 Cycle 4 had conventional grids and B4C burnable poison rods.

PVNGS Unit 1 Cycle 5

- (1) powered up to 98% HFP and 565°F from 0 to 0.238 GWD/MTU,
- (2) powered down to 85% HFP and 557°F from 0.238 to 0.373 GWD/MTU,
- (3) operated at around 85% HFP and 557°F from 0.373 to 6.960 GWD/MTU,
- (4) powered up to 100% HFP and 565°F from 6.960 to 7.184 GWD/MTU,
- (5) cooled down to 100% HFP and 555°F from 7.184 to 7.483 GWD/MTU,
- (6) operated at 100% HFP and 555°F from 7.483 to 16.526 GWD/MTU,
- (7) coasted down to 85% HFP and 556°F from 16.526 to 16.724 GWD/MTU,
- (8) operated at 85% HFP and 556°F from 16.724 to 16.982 GWD/MTU, and
- (9) shutdown for refueling at 16.982 GWD/MTU.

Rodded snapshots were taken at 1.736, 11.141, and 16.724 GWD/MTU.

The batch of fresh fuel assemblies loaded in PVNGS Unit 1 Cycle 5 had GUARDIAN grids and B4C burnable poison rods. GUARDIAN grids raise the fuel column 1.589 inches relative to conventional grids.

PVNGS Unit 1 Cycle 6

- (1) powered up to 100% HFP and 555°F from 0 to 0.485 GWD/MTU,
- (2) operated at 100% and 555°F from 0.485 to 15.635 GWD/MTU,
- (3) coasted down to 85% HFP and 554°F at 16.321 GWD/MTU, and
- (4) shutdown for refueling at 16.321 GWD/MTU.

A rodDED snapshot was taken at 10.957 GWD/MTU.

The batch of fresh fuel assemblies loaded in PVNGS Unit 1 Cycle 6 had GUARDIAN grids and erbium shims. GUARDIAN grids raise the fuel column 1.589 inches relative to conventional grids.

PVNGS Unit 2 Cycle 4

- (1) operated at 100% HFP and 565°F from 0 to 14.172 GWD/MTU,
- (1) coasted down to 97.5% HFP and 565°F from 14.172 to 15.729 GWD/MTU, and
- (1) shutdown for refueling at 15.729 GWD/MTU.

Rodded snapshots were taken at 10.198 and 15.348 GWD/MTU.

The batch of fresh fuel assemblies loaded in PVNGS Unit 2 Cycle 4 had conventional grids and B4C burnable poison rods.

PVNGS Unit 2 Cycle 5

- (1) powered up to 100% HFP and 565°F from 0 to 0.282 GWD/MTU,
- (2) powered down to 80% HFP and 565°F from 0.282 to 0.385 GWD/MTU,
- (3) powered up to 89% HFP and 562°F from 0.385 to 0.721 GWD/MTU.
- (4) powered down to 85% HFP and 562°F from 0.721 to 0.946 GWD/MTU,
- (5) operated at 85% HFP and 562°F from 0.946 to 1.396 GWD/MTU,
- (6) cooled down to 85% HFP and 557°F from 1.396 to 1.713 GWD/MTU,
- (7) operated at 85% HFP and 557°F from 1.713 to 6.850 GWD/MTU,
- (8) powered up to 100% HFP and 565°F from 6.850 to 6.888 GWD/MTU,
- (9) operated at 100% HFP and 565°F from 6.888 to 7.152 GWD/MTU,
- (10) coasted down to 88% HFP and 562°F from 7.152 to 7.384 GWD/MTU,
- (11) operated at 88% HFP and 562°F from 7.384 to 8.514 GWD/MTU,
- (12) powered up to 100% HFP and 555°F from 8.514 to 8.777 GWD/MTU,
- (13) operated at 100% HFP and 555°F from 8.777 to 13.546 GWD/MTU, and
- (14) shutdown for refueling at 13.546 GWD/MTU.

Rodded snapshots were taken at 1.584, 5.862, 6.888, 6.963, and 9.419 GWD/MTU.

The batch of fresh fuel assemblies loaded in PVNGS Unit 2 Cycle 5 had conventional grids and B4C burnable poison rods.

PVNGS Unit 2 Cycle 6

- (1) operated at 100% HFP and 555°F from 0 to 12.410 GWD/MTU,
- (2) coasted down to 92% HFP and 554°F from 12.410 to 12.755 GWD/MTU, and
- (3) shutdown for refueling at 12.755 GWD/MTU.

A rodDED snapshot was taken at 8.153 GWD/MTU.

The batch of fresh fuel assemblies loaded in PVNGS Unit 2 Cycle 6 had GUARDIAN grids and erbium shims. GUARDIAN grids raise the fuel column 1.589 inches relative to conventional grids.

PVNGS Unit 3 Cycle 4

- (1) powered up to 100% HFP and 565°F from 0 to 0.346 GWD/MTU,
- (2) operated at 100% HFP and 565°F from 0.346 to 11.075 GWD/MTU,
- (3) powered down to 85% HFP and 562°F from 11.075 to 11.197 GWD/MTU
- (4) operated at 85% HFP and 562°F from 11.197 to 12.039 GWD/MTU,
- (5) cooled down to 85% HFP and 556°F from 12.039 to 12.489 GWD/MTU,
- (6) operated at 85% HFP and 556°F from 12.489 to 15.745 GWD/MTU, and
- (7) shutdown for refueling at 15.745 GWD/MTU.

Rodded snapshots were taken at 1.676, 3.004, 3.508, 5.225, 6.969, 10.695, and 11.196 GWD/MTU.

The batch of fresh fuel assemblies loaded in PVNGS Unit 3 Cycle 4 had conventional grids and B4C burnable poison rods.

PVNGS Unit 3 Cycle 5

- (1) powered up to 100% HFP and 555°F from 0 to 0.256 GWD/MTU,
- (2) operated at 100% HFP and 555°F from 0.256 to 16.750 GWD/MTU, and
- (3) shutdown for refueling at 16.750 GWD/MTU.

The batch of fresh fuel assemblies loaded in PVNGS Unit 3 Cycle 5 had GUARDIAN grids and erbium shims. GUARDIAN grids raise the fuel column 1.589 inches relative to conventional grids.

PVNGS Unit 3 Cycle 6

- (1) operated at 3800 MWt and 555°F from 0 to 6.409 GWD/MTU,
- (2) stretched to 3876 MWt and 554°F from 6.409 to 6.633 GWD/MTU,
- (3) operated at 3876 MWt and 554°F from 6.633 to 14.464 GWD/MTU, and
- (4) shutdown for refueling at 14.464 GWD/MTU.

The batch of fresh fuel assemblies loaded in PVNGS Unit 3 Cycle 6 had GUARDIAN grids and erbium shims. GUARDIAN grids raise the fuel column 1.589 inches relative to conventional grids.

5.3.4 DESCRIPTION OF CALCULATIONS

Description of Basic Core Follow Models

The 3-D spatial calculations were performed with the SIMULATE-3 code. Each fuel assembly was represented by 4 nodes in the x-y direction. A quarter core model was used with rotational boundary conditions along the axes. The core was thus assumed to be quadrant symmetric in a rotational sense. Any asymmetries actually occurring were included in the full core power comparisons of instrumented boxes. The radial and axial reflectors were explicitly modeled.

Axially, the 150 inch high 241 assembly PVNGS cores were represented by 25 nodes. Each node was 6 inches long.

The 3-D SIMULATE-3 model for each reactor and cycle was depleted in a core follow mode, which simulated the actual core operation from BOC to EOC.

Correction of Calculation for Radial [] Shifts

Calculations were corrected for radial shifts in accordance with the method described in section 3.2.2 of Reference 25. [

]

5.3.5 STATISTICAL MODEL FOR CALCULATION OF INSTRUMENTED ASSEMBLY POWER DISTRIBUTION UNCERTAINTIES

Definitions

UC(i,L) Uncorrected calculated value of the assembly power in instrument location i at instrument level L.

M(i,L) Measured value of the assembly power in instrument location i at instrument level L. The measured values are always uncorrected.

CC(i,L) Corrected calculated value of the assembly power in instrument location i at instrument level L. [

]

D(i,L) Difference between corrected calculated and measured value of the assembly power in instrument location i at instrument level L.

UC(i) Uncorrected value of the axially summed uncorrected calculated assembly power from each level of the intact instrument string at location i;

$$\sum_{L=1}^5 UC(i, L)$$

M(i) Value of the axially summed measured assembly power from each level of the intact instrument string at location i;

$$\sum_{L=1}^5 M(i, L)$$

CC(i) Corrected value of the axially summed uncorrected calculated assembly power from each level of the intact instrument string at location i.

D(i) Difference between corrected value of the axially summed uncorrected calculated assembly power and the value of the axially summed measured assembly power in intact instrument location i.

N(L) Number of intact instruments at detector level L (L =1,..,5).

NS Number on intact instrument strings in the core.

NLEV Number of detector levels; = 5.

NDET Number of intact instruments in core.

NDEG Number of degrees of freedom.

NTOT Total number of data points.

σ_D The standard deviation of the difference between measurement and calculation.

σ_M The measurement standard deviation relative to the true power.

σ_C The calculation standard deviation relative to the true power.

The basic relation for σ_D is:

$$\sigma_D^2 = \sigma_M^2 + \sigma_C^2$$

This shows that

$$\sigma_M^2 \leq \sigma_D^2$$

and that

$$\sigma_C^2 \leq \sigma_D^2$$

Standard Measurement Uncertainty

The standard measurement uncertainty is based on the sample variance for the difference between the corrected calculation and the measurement.

Standard Fq Measurement Uncertainty: S_{DFq}

For the standard Fq measurement uncertainty the corrected calculated and measured assembly powers for all intact detector locations at all levels in the core (NDET) are compared. [

]

The differences, quoted as a fraction of peak assembly value, are given by

$$D(i, L) = \frac{CC(i, L) - M(i, L)}{M_{max}} \text{ for } i = 1, \dots, N(L), L = 1, \dots, 5$$

where $M_{max} = \text{maximum}[M(i, L)]$ over all $i = 1, \dots, N(L)$, and over all $L = 1, \dots, 5$.

The sample bias is given by

$$\bar{D} = \frac{1}{NDET} \sum_{L=1}^5 \sum_{i=1}^{N(L)} D(i, L)$$

The sample bias is zero because of the normalization. [

]

Standard Fr Measurement Uncertainty: S_{DFr}

For the standard Fr measurement uncertainty the corrected axially summed uncorrected calculated and the axially summed measured assembly powers in all the intact detector string locations (NS) are compared. The normalization is

$$\sum_{i=1}^{NS} M(i) = \sum_{i=1}^{NS} CC(i) = NS$$

The differences, quoted as a fraction of peak assembly value, are given by

$$D(i) = \frac{CC(i) - M(i)}{M_{max}} \text{ for } i = 1, \dots, NS$$

where $M_{max} = \text{maximum}[M(i)]$ over all $i = 1, \dots, NS$

The sample bias is given by

$$\bar{D} = \frac{1}{NS} \sum_{i=1}^{NS} D(i)$$

The sample bias is zero because of the normalization. The sample variance is then:

$$S_{DFr}^2 = \frac{1}{NS-2} \sum_{i=1}^{NS} D(i)^2$$

Standard Fxy Measurement Uncertainty: S_{DFxy}

For the standard Fxy measurement uncertainty the corrected calculated and measured assembly powers are compared at each level L for all intact detector location, N(L). The normalization is:

$$\sum_{i=1}^{N(L)} M(i, L) = \sum_{i=1}^{N(L)} CC(i, L) = N(L)$$

The differences, quoted as a fraction of peak assembly value, are given by:

$$D(i, L) = \frac{CC(i, L) - M(i, L)}{M_{max}(L)} \text{ for } i = 1, \dots, N(L)$$

where $M_{max}(L) = \text{maximum}[M(i, L)]$ over all $i = 1, \dots, N(L)$

The sample bias is given by

$$\bar{D} = \frac{1}{N(L)} \sum_{i=1}^{N(L)} D(i, L)$$

The sample bias is zero because of the normalization. The sample variance at level L is then

$$S_{DFxy}^2 = \frac{1}{N(L)-2} \sum_{i=1}^{N(L)} D(i, L)^2$$

Alternative Measurement Uncertainty

The alternative measurement uncertainty is based on the sample variance for the difference between the uncorrected calculation and the measurement.

Sometimes the sample variance for the difference between uncorrected calculation and measurement displays better poolability than the sample variance for the difference between corrected calculation and measurement. Since the sample variance for the difference between uncorrected calculation and measurement is an unbiased estimator of the sum of the uncorrected calculation

variance and the measurement variance, it can be used to compute an upper bound for the measurement variance.

Alternative Fq Measurement Uncertainty: S_{DFq}

For the alternative Fq measurement uncertainty the uncorrected calculated and measured assembly powers for all intact detector locations at all levels in the core (NDET) are compared. The normalization is:

$$\sum_{L=1}^5 \sum_{i=1}^{N(L)} M(i, L) = \sum_{L=1}^5 \sum_{i=1}^{N(L)} UC(i, L) = NDET$$

where the total number of intact detectors NDET is given by

$$NDET = \sum_{L=1}^5 N(L)$$

The differences, quoted as a fraction of peak assembly value, are given by

$$D(i, L) = \frac{UC(i, L) - M(i, L)}{M_{max}} \text{ for } i = 1, \dots, N(L), L = 1, \dots, 5$$

where $M_{max} = \text{maximum}[M(i, L)]$ over all $i = 1, \dots, N(L)$, and over all $L = 1, \dots, 5$.

The sample bias is given by

$$\bar{D} = \frac{1}{NDET} \sum_{L=1}^5 \sum_{i=1}^{N(L)} D(i, L)$$

The sample bias is zero because of the normalization. The sample variance is

$$S_{DFq}^2 = \frac{1}{NDET-1} \sum_{L=1}^5 \sum_{i=1}^{N(L)} D(i, L)^2$$

Alternative Fr Measurement Uncertainty: S_{DFr}

For the alternative Fr measurement uncertainty the uncorrected axially summed uncorrected calculated and the axially summed measured assembly powers in all the intact detector string locations (NS) are compared. The normalization is

$$\sum_{i=1}^{NS} M(i) = \sum_{i=1}^{NS} UC(i) = NS$$

The differences, quoted as a fraction of peak assembly value, are given by

$$D(i) = \frac{UC(i) - M(i)}{M_{max}} \text{ for } i = 1, \dots, NS$$

where $M_{max} = \text{maximum}[M(i)]$ over all $i = 1, \dots, NS$

The sample bias is given by

$$\bar{D} = \frac{1}{NS} \sum_{i=1}^{NS} D(i)$$

The sample bias is zero because of the normalization. The sample variance is then:

$$S_{DFr}^2 = \frac{1}{NS-1} \sum_{i=1}^{NS} D(i)^2$$

Alternative Fxy Measurement Uncertainty: S_{DFxy}

For the alternative Fxy measurement uncertainty the uncorrected calculated and the measured assembly powers are compared at each level L for all intact detector locations, N(L). The normalization is:

$$\sum_{i=1}^{N(L)} M(i, L) = \sum_{i=1}^{N(L)} UC(i, L) = N(L)$$

The differences, quoted as a fraction of peak assembly value, are given by:

$$D(i, L) = \frac{UC(i, L) - M(i, L)}{M_{max}(L)} \text{ for } i = 1, \dots, N(L)$$

where $M_{max}(L) = \text{maximum}[M(i, L)]$ over all $i = 1, \dots, N(L)$

The sample bias is given by

$$\bar{D} = \frac{1}{N(L)} \sum_{i=1}^{N(L)} D(i, L)$$

The sample bias is zero because of the normalization. The sample variance at level L is then

$$S_{DFxy}^2 = \frac{1}{N(L) - 1} \sum_{i=1}^{N(L)} D(i, L)^2$$

Standard Calculation Uncertainty

The standard calculation uncertainty is based on the sample variance for the difference between corrected calculation and uncorrected calculation

Standard Fq Calculation Uncertainty: S_{DFq}

For the standard Fq calculation uncertainty the corrected calculated and uncorrected calculated assembly powers for all intact detector locations at all levels in the core (NDET) are compared.

[

]

The differences, quoted as a fraction of peak assembly value, are given by

$$D(i, L) = \frac{CC(i, L) - UC(i, L)}{UC_{max}} \text{ for } i = 1, \dots, N(L), L = 1, \dots, 5$$

where $UC_{max} = \text{maximum}[UC(i, L)]$ over all $i = 1, \dots, N(L)$, and over all $L = 1, \dots, 5$.

The sample bias is given by

$$\bar{D} = \frac{1}{NDET} \sum_{L=1}^5 \sum_{i=1}^{N(L)} D(i, L)$$

The sample bias is zero because of the normalization. [

]

Standard Fr Calculation Uncertainty: S_{DFr}

For the standard Fr calculation uncertainty the corrected axially summed uncorrected calculated and the uncorrected axially summed uncorrected calculated assembly powers in all the intact detector string locations (NS) are compared. The normalization is

$$\sum_{i=1}^{NS} UC(i) = \sum_{i=1}^{NS} CC(i) = NS$$

The differences, quoted as a fraction of peak assembly value, are given by

$$D(i) = \frac{CC(i) - UC(i)}{UC_{max}} \text{ for } i = 1, \dots, NS$$

where $UC_{max} = \text{maximum}[UC(i)]$ over all $i = 1, \dots, NS$

The sample bias is given by

$$\bar{D} = \frac{1}{NS} \sum_{i=1}^{NS} D(i)$$

The sample bias is zero because of the normalization. The sample variance is then:

$$S_{DFr}^2 = \frac{1}{NS-2} \sum_{i=1}^{NS} D(i)^2$$

Standard Fxy Calculation Uncertainty: S_{DFxy}

For the standard Fxy calculation uncertainty the corrected calculated and uncorrected calculated assembly powers are compared at each level L for all intact detector location, N(L). The normalization is:

$$\sum_{i=1}^{N(L)} UC(i, L) = \sum_{i=1}^{N(L)} CC(i, L) = N(L)$$

The differences, quoted as a fraction of peak assembly value, are given by:

$$D(i, L) = \frac{CC(i, L) - UC(i, L)}{UC_{max}(L)} \text{ for } i = 1, \dots, N(L)$$

where $UC_{max}(L) = \text{maximum}[UC(i, L)]$ over all $i = 1, \dots, N(L)$

The sample bias is given by

$$\bar{D} = \frac{1}{N(L)} \sum_{i=1}^{N(L)} D(i, L)$$

The sample bias is zero because of the normalization. The sample variance at level L is then

$$S_{DFxy}^2 = \frac{1}{N(L)-2} \sum_{i=1}^{N(L)} D(i, L)^2$$

Alternative Calculation Uncertainty

The alternative calculation uncertainty is based on the sample variance for the difference between the measurement and the uncorrected calculation

Sometimes the sample variance for the difference between measurement and uncorrected calculation displays better poolability than the sample variance for the difference between corrected calculation and uncorrected calculation. Since the sample variance for the difference between measurement and uncorrected calculation is an unbiased estimator for the sum of the measurement variance and the uncorrected calculation variance, it can be used to compute an upper bound for the uncorrected calculation uncertainty.

Alternative Fq Calculation Uncertainty: S_{DFq}

For the alternative Fq calculation uncertainty the measured and uncorrected calculated assembly powers for all intact detector locations at all levels in the core (NDET) are compared. The normalization is:

$$\sum_{L=1}^5 \sum_{i=1}^{N(L)} M(i, L) = \sum_{L=1}^5 \sum_{i=1}^{N(L)} UC(i, L) = NDET$$

where the total number of intact detectors NDET is given by

$$NDET = \sum_{L=1}^5 N(L)$$

The differences, quoted as a fraction of peak assembly value, are given by

$$D(i, L) = \frac{M(i, L) - UC(i, L)}{UC_{max}} \quad \text{for } i = 1, \dots, N(L), L = 1, \dots, 5$$

where $UC_{max} = \text{maximum}[UC(i, L)]$ over all $i = 1, \dots, N(L)$, and over all $L = 1, \dots, 5$.

The sample bias is given by

$$\bar{D} = \frac{1}{NDET} \sum_{L=1}^5 \sum_{i=1}^{N(L)} D(i, L)$$

The sample bias is zero because of the normalization. The sample variance is

$$S_{DFq}^2 = \frac{1}{NDET-1} \sum_{L=1}^5 \sum_{i=1}^{N(L)} D(i, L)^2$$

Alternative Fr Calculation Uncertainty: S_{DFr}

For the alternative Fr calculation uncertainty the uncorrected axially summed measured and the uncorrected axially summed uncorrected calculated assembly powers in all the intact detector string locations (NS) are compared. The normalization is

$$\sum_{i=1}^{NS} M(i) = \sum_{i=1}^{NS} UC(i) = NS$$

The differences, quoted as a fraction of peak assembly value, are given by

$$D(i) = \frac{M(i) - UC(i)}{UC_{max}} \quad \text{for } i = 1, \dots, NS$$

where $UC_{max} = \text{maximum}[UC(i)]$ over all $i = 1, \dots, NS$

The sample bias is given by

$$\bar{D} = \frac{1}{NS} \sum_{i=1}^{NS} D(i)$$

The sample bias is zero because of the normalization. The sample variance is then:

$$S_{DFr}^2 = \frac{1}{NS-1} \sum_{i=1}^{NS} D(i)^2$$

Alternative Fxy Calculation Uncertainty: S_{DFxy}

For the alternative Fxy calculation uncertainty the measured and uncorrected calculated assembly powers are compared at each level L for all intact detector location, N(L). The normalization is:

$$\sum_{i=1}^{N(L)} M(i, L) = \sum_{i=1}^{N(L)} UC(i, L) = N(L)$$

The differences, quoted as a fraction of peak assembly value, are given by:

$$D(i, L) = \frac{M(i, L) - UC(i, L)}{UC_{max}(L)} \quad \text{for } i = 1, \dots, N(L)$$

where $UC_{max}(L) = \text{maximum}[UC(i, L)]$ over all $i = 1, \dots, N(L)$

The sample bias is given by

$$\bar{D} = \frac{1}{N(L)} \sum_{i=1}^{N(L)} D(i, L)$$

The sample bias is zero because of the normalization. The sample variance at level L is then

$$S_{DFxy}^2 = \frac{1}{N(L) - 1} \sum_{i=1}^{N(L)} D(i, L)^2$$

Procedure for Rejecting Snapshots

The CECORLIB code generated CECOR coefficients for ARO, equilibrium xenon depletion at a definite power level and at a definite inlet coolant temperature. If there was substantial operation at a reduced power level or at a different inlet coolant temperature, then two sets of CECOR coefficients were generated. Nevertheless, there were always a number of snapshots taken under conditions that did not match the conditions for which the CECOR coefficients were generated.

An initial attempt was made to pool the data from all of the snapshots used for the core follow depletion. If that failed, as it usually did, then snapshots were subject to be discarded from the statistical database if they met one or more of the following criteria:

- rodged
- power level mismatch with that used to generate CECOR coefficients, or
- inlet coolant temperature mismatch with that used to generate CECOR coefficients.

Measurement uncertainties clearly apply to ARO, HFP, nominal inlet temperature, nominal flow, equilibrium xenon conditions. Increasing judgement is required when using these uncertainties in other conditions. A new set of coefficients could easily be generated for cases of extended operation at other than nominal conditions. Nominal uncertainties continue to apply if the operating

conditions match those at which the coefficients were generated. Use of CECOR coefficients generated at HFP ARO conditions is consistent with the application of CECOR in Palo Verde Tech Spec surveillance tests and of measured peaking factors installed in COLSS and CPC.

Calculation uncertainties apply to any quasi-static, normal operating conditions.

Procedure for Testing Poolability

[

]

Procedure for Computing One-Sided Tolerance Limits

[

]

5.3.6 EVALUATION OF INSTRUMENTED BOX POWER PEAKING FACTOR CALCULATION UNCERTAINTY

Summary of Results

The estimates of uncertainty parameters for the F_q , F_r , and F_{xy} instrumented box power calculations are summarized in Table 5-9. Results include the standard deviation, number of degrees of freedom, the 95/95 tolerance factor, and the upper 95/95 tolerance limit.

Chi-Square Homogeneity Test Results

The results of the chi-square tests for k independent samples for the F_q , F_r , and F_{xy} instrumented box power calculations are given in Table 5-10, Table 5-11, and Table 5-12, respectively. Except for timepoints 49 through 69 in Unit 1 Cycle 5 in Table 5-10 and timepoints 50 through 58 in Unit

3 Cycle 4 in Table 5-10, none of the timepoints pool. It was necessary to resort to the alternative uncertainty calculation in order to get those timepoints to pool.

Normal Uncertainty Parameters

The normal uncertainty parameters for the F_q , F_r , and F_{xy} instrumented box power calculations are given in Table 5-13, Table 5-14, and Table 5-15, respectively. The normal uncertainty parameters are used if they are less favorable than the non-normal uncertainty parameters.

Non-Normal Uncertainty Parameters

The non-normal uncertainty parameters for the F_q , F_r , and F_{xy} instrumented box power calculations are given in Table 5-16, Table 5-17, and Table 5-18, respectively. The non-normal uncertainty parameters are used if they are less favorable than the normal uncertainty parameters.

Table 5-9 Summary of Uncertainties for the Calculation of Peak Assembly Power

Type	Mean	STD*	Degrees of Freedom	K	KSTD*
$F_{qC}(box)$	0.00%	2.69%	72	1.98	5.34%
$F_{rC}(box)$	0.00%	1.57%	47	2.08	3.25%
$F_{xyC}(box)$	0.00%	1.83%	58	2.03	3.69%

* Quoted in percent of peak assembly value.

Table 5-10 Chi-Square Test Results for Instrumented Box Fq Calculation

Cycle	Timepoints	DOF	chi-square	CHI-95	PASSED?
U1C4	1-56	2145	14304.23	2254.81	NO
U1C5	1-48	2021	11799.57	2126.89	NO
U1C5*	49-69	1000	1042.99	1074.70	YES
U1C6	1-57	2184	12755.98	2294.98	NO
U2C4	1-65	2368	15395.19	2484.10	NO
U2C5	1-56	2035	14807.26	2141.35	NO
U2C6	1-49	2016	13376.41	2121.73	NO
U3C4*	1-49	1680	1802.16	1780.24	NO
U3C4*	50-58	288	262.10	328.58	YES
U3C5	1-65	2624	11490.43	2746.14	NO
U3C6	1-53	2080	9374.72	2187.79	NO

* Alternate form for the Fq differences used in order to facilitate pooling.

Table 5-11 Chi-Square Test Results for Instrumented Box Fr Calculation

Cycle	Timepoints	DOF	chi-square	CHI-95	PASSED?
U1C4	1-56	330	3288.87	373.46	NO
U1C5	1-73	432	4847.80	481.52	NO
U1C6	1-57	336	2218.04	379.83	NO
U2C4	1-65	384	3211.57	430.77	NO
U2C5	1-56	385	3473.95	431.82	NO
U2C6	1-49	288	3137.25	328.58	NO
U3C4	1-58	285	847.58	325.38	NO
U3C5	1-65	448	1866.98	498.35	NO
U3C6	1-53	364	3025.39	409.55	NO

Table 5-12 Chi-Square Test Results for Instrumented Box Fxy Calculation

Cycle	Time-points	Levels	DOF	chi-square	CHI-95	PASSED?
U1C4	1-56	1	330	3160.64	373.46	NO
	1-56	2	330	2349.24	373.46	NO
	1-56	3	275	3003.21	314.70	NO
	1-56	4	330	3626.95	373.46	NO
	1-56	5	385	3920.74	431.82	NO
U1C5	1-73	1	432	3761.29	481.52	NO
	1-73	2	504	4957.17	557.37	NO
	1-73	3	648	4571.39	708.30	NO
	1-73	4	432	5301.35	481.52	NO
	1-73	5	648	5827.05	708.30	NO
U1C6	1-57	1	392	1902.33	439.21	NO
	1-57	2	336	1884.94	379.83	NO
	1-57	3	336	1554.36	379.83	NO
	1-57	4	336	3646.36	379.83	NO
	1-57	5	504	4006.58	557.37	NO
U2C4	1-65	1	448	3430.46	498.35	NO
	1-65	2	640	3585.53	699.96	NO
	1-65	3	576	3290.86	632.97	NO
	1-65	4	512	4448.98	565.80	NO
	1-65	5	384	4216.66	430.77	NO
U2C5	1-56	1	330	3474.08	373.46	NO
	1-56	2	440	3526.48	489.94	NO
	1-56	3	440	3629.82	489.94	NO
	1-56	4	495	4108.38	547.91	NO
	1-56	5	440	2903.02	489.94	NO
U2C6	1-49	1	288	2948.25	328.58	NO
	1-49	2	336	3562.81	379.83	NO
	1-49	3	384	3210.87	430.77	NO
	1-49	4	336	3048.95	379.83	NO
	1-49	5	432	4199.80	481.52	NO
U3C4	1-58	1	171	452.32	202.50	NO

Table 5-12 Chi-Square Test Results for Instrumented Box Fxy Calculation

Cycle	Time-points	Levels	DOF	chi-square	CHI-95	PASSED?
	1-58	2	285	944.42	325.38	NO
	1-58	3	342	935.59	386.17	NO
	1-58	4	285	1309.45	325.38	NO
	1-58	5	285	2073.52	325.38	NO
U3C5	1-65	1	448	1393.93	498.35	NO
	1-65	2	448	449.17	498.35	NO
	1-65	3	512	429.94	565.80	NO
	1-65	4	448	1765.44	498.35	NO
	1-65	5	448	2762.83	498.35	NO
U3C6	1-53	1	364	2557.63	409.55	NO
	1-53	2	416	2528.32	464.61	NO
	1-53	3	468	2885.11	519.49	NO
	1-53	4	364	3901.53	409.55	NO
	1-53	5	312	3474.94	354.27	NO

Table 5-13 Normal Uncertainties for Instrumented Box Fq Calculation

Cycle	Timepoints	STD*	DOF	K	KSTD*
U2C4	1-65	1.69%	291	1.80	3.05%
U3C6	1-53	2.14%	265	1.81	3.86%
U1C5	1-48	2.17%	283	1.80	3.91%
U2C6	1-49	2.18%	288	1.80	3.94%
U3C4#	1-49	2.15%	202	1.84	3.95%
U1C4	1-56	2.21%	281	1.80	3.98%
U1C6	1-57	2.25%	283	1.80	4.06%
U2C5	1-56	2.26%	288	1.80	4.06%
U3C5	1-65	2.52%	270	1.81	4.56%
U1C5#	49-69	2.74%	6127	1.68	4.59%
U3C4#	50-58	2.69%	1818	1.71	4.60%

* Quoted in percent of peak assembly value.

Alternate form for the Fq differences used in order to facilitate pooling.

Table 5-14 Normal Uncertainties for Instrumented Box Fr Calculation

Cycle	Timepoints	STD*	DOF	K	KSTD*
U3C4	1-58	0.40%	37	2.14	0.86%
U3C5	1-65	0.66%	49	2.07	1.36%
U1C6	1-57	0.94%	51	2.06	1.92%
U2C5	1-56	0.99%	53	2.05	2.03%
U2C4	1-65	1.03%	56	2.03	2.10%
U2C6	1-49	1.08%	54	2.04	2.21%
U1C4	1-56	1.09%	53	2.05	2.24%
U1C5	1-73	1.39%	51	2.06	2.86%
U3C6	1-53	1.57%	47	2.08	3.25%

* Quoted in percent of peak assembly value.

Table 5-15 Normal Uncertainties for Instrumented Box Fxy Calculation

Cycle	Time-points	Levels	STD*	DOF	K	KSTD*
U3C4	1-58	1-5	0.60%	39	2.13	1.27%
U2C4	1-65	1-5	1.12%	59	2.02	2.27%
U1C6	1-57	1-5	1.21%	58	2.03	2.46%
U2C5	1-56	1-5	1.30%	59	2.02	2.63%
U3C5	1-65	1-5	1.34%	54	2.04	2.74%
U2C6	1-49	1-5	1.49%	57	2.03	3.02%
U1C4	1-56	1-5	1.54%	56	2.03	3.14%
U3C6	1-53	1-5	1.69%	55	2.04	3.45%
U1C5	1-73	1-5	1.83%	58	2.03	3.69%

* Quoted in percent of peak assembly value.

Table 5-16 Non-Normal Uncertainties for Instrumented Box Fq Calculation

Cycle	Timepoints	STD*	DOF	K	KSTD*
U1C5	1-48	1.94%	infinite	1.63	3.16%
U1C4	1-56	2.21%	infinite	1.45	3.21%
U2C4	1-65	1.69%	45	2.09	3.53%
U2C5	1-56	2.26%	infinite	1.63	3.67%
U3C6	1-53	2.14%	102	1.92	4.10%
U2C6	1-49	2.18%	108	1.91	4.18%
U3C4#	1-49	1.88%	24	2.29	4.30%
U1C5#	49-69	2.74%	520	1.76	4.81%
U1C6	1-57	2.25%	29	2.22	4.99%
U3C5	1-65	2.52%	56	2.03	5.13%
U3C4#	50-58	2.69%	72	1.98	5.34%

* Quoted in percent of peak assembly value.

Alternate form for the Fq differences used in order to facilitate pooling.

:

Table 5-17 Non-Normal Uncertainties for Instrumented Box Fr Calculation

Cycle	Timepoints	STD*	DOF	K	KSTD*
U3C4	1-58	0.40%	80	1.96	0.79%
U2C5	1-56	0.99%	infinite	1.27	1.26%
U1C6	1-57	0.94%	infinite	1.37	1.28%
U1C4	1-56	1.09%	infinite	1.21	1.32%
U2C4	1-65	1.03%	infinite	1.29	1.34%
U2C6	1-49	1.08%	infinite	1.26	1.36%
U3C5	1-65	0.66%	37	2.14	1.41%
U1C5	1-73	1.39%	infinite	1.31	1.82%
U3C6	1-53	1.57%	infinite	1.27	1.99%

* Quoted in percent of peak assembly value.

Table 5-18 Non-Normal Uncertainties for Instrumented Box Fxy Calculation

Cycle	Time-points	Levels	STD*	DOF	K	KSTD*
U3C4	1-58	1-5	0.60%	66	2.00	1.19%
U1C6	1-57	1-5	1.21%	infinite	1.31	1.58%
U2C4	1-65	1-5	0.79%	55	2.04	1.61%
U2C6	1-49	1-5	1.49%	infinite	1.20	1.79%
U1C4	1-56	1-5	1.54%	infinite	1.24	1.90%
U3C6	1-53	1-5	1.69%	infinite	1.29	2.19%
U1C5	1-73	1-5	1.82%	infinite	1.24	2.27%
U2C5	1-56	1-5	1.19%	49	2.06	2.44%
U3C5	1-65	1-5	1.34%	34	2.17	2.90%

* Quoted in percent of peak assembly value.

5.3.7 EVALUATION OF INSTRUMENTED BOX POWER PEAKING FACTOR MEASUREMENT UNCERTAINTY WITH 61 DETECTOR STRINGS

Summary of Results

The estimates of uncertainty parameters for the F_q , F_r , and F_{xy} instrumented box power measurements with 61 detector strings are summarized in Table 5-19. Results include the mean, the standard deviation, the number of degrees of freedom, the 95/95 tolerance factor, and the upper 95/95 tolerance limit.

Chi-Square Homogeneity Test Results

The results of the chi-square tests for k independent samples for the F_q , F_r , and F_{xy} instrumented box power measurements with 61 detector strings are given in Table 5-20, Table 5-21, and Table 5-22, respectively.

Normal Uncertainty Parameters

The normal uncertainty parameters for the F_q , F_r , and F_{xy} instrumented box power measurements with 61 detector strings are given in Table 5-23, Table 5-24, and Table 5-25, respectively. The normal uncertainty parameters are used if they are less favorable than the non-normal uncertainty parameters.

Non-Normal Uncertainty Parameters

The non-normal uncertainty parameters for the F_q , F_r , and F_{xy} instrumented box power measurements with 61 detector strings are given in Table 5-26, Table 5-27, and Table 5-28, respectively. The non-normal uncertainty parameters are used if they are less favorable than the normal uncertainty parameters.

Table 5-19 Summary of Uncertainties for the Measurement of Peak Assembly Power with 61 Detector Strings

Type	Mean	STD*	DOF	K	KSTD*
$F_{qM}(box)$	0.0%	1.50%	16113	1.67	2.49%
$F_{rM}(box)$	0.0%	1.44%	857	1.73	2.49%
$F_{xyM}(box)$	0.0%	1.63%	16113	1.67	2.71%

* Quoted in percent of peak assembly value.

**Table 5-20 Chi-Square Test Results for Instrumented Box Fq Measurement
with 61 Detector Strings**

Cycle	Timepoints	DOF	chi-square	CHI-95	PASSED?
U1C4	1-56	2255	2362.46	2368.04	YES
U1C5	1-73	3240	2932.04	3374.41	YES
U1C6	1-57	2296	2303.02	2410.18	YES
U2C4	1-65	2816	2632.75	2941.83	YES
U2C5	1-56	2475	2266.57	2593.78	YES
U2C6	1-49	2160	2171.12	2270.26	YES
U3C4	1-58	1824	1490.28	1927.04	YES
U3C5	1-65	2624	2425.98	2746.14	YES
U3C6	1-23	792	845.57	858.57	YES
U3C6	24-53	928	786.78	1000.04	YES

**Table 5-21 Chi-Square Test Results for Instrumented Box Fr
Measurement with 61 Detector Strings**

Cycle	Timepoints	DOF	chi-square	CHI-95	PASSED?
U1C4	1-28	243	214.43	280.36	YES
U1C4	29-56	243	123.41	280.36	YES
U1C5	1-73	576	476.45	632.97	YES
U1C6	1-28	243	173.49	280.36	YES
U1C6	29-57	252	112.91	290.03	YES
U2C4	1-65	640	580.95	699.96	YES
U2C5	1-56	550	451.23	605.66	YES
U2C6	1-49	432	365.11	481.52	YES
U3C4	1-58	342	193.70	386.18	YES
U3C5	1-65	512	269.63	565.80	YES
U3C6	1-23	154	154.12	183.96	YES
U3C6	24-53	203	84.05	237.25	YES

**Table 5-22 Chi-Square Test Results for Instrumented Box Fxy
Measurement with 61 Detector Strings**

Cycle	Time-points	Levels	DOF	chi-square	CHI-95	PASSED?
U1C4	1-56	1-3	1670	1661.87	1770.02	YES
U1C4	1-56	3-5	1670	1614.53	1770.02	YES
U1C5	1-73	1-5	3640	3287.69	3782.41	YES
U1C6	1-28	1	243	268.79	280.36	YES
U1C6	1-28	2-3	550	427.66	605.66	YES
U1C6	1-28	3-5	830	795.20	898.14	YES
U1C6	29-57	1-5	1440	1519.53	1533.57	YES
U2C4	1-65	1-4	2849	2964.29	2975.40	YES
U2C4	1-65	2-5	2331	2304.22	2446.13	YES
U2C5	1-56	1-5	2790	2561.15	2915.37	YES
U2C6	1-49	1	480	438.77	532.14	YES
U2C6	1-49	2-5	2145	2187.90	2254.81	YES
U3C4	1-58	1-5	1881	1525.82	1984.89	YES
U3C5	1-65	1-5	3240	2744.29	3374.41	YES
U3C6	1-53	1	416	251.95	464.61	YES
U3C6	1-23	2	220	239.90	255.60	YES
U3C6	24-53	2	290	147.19	330.72	YES
U3C6	1-53	3-5	1422	1432.91	1514.96	YES

Table 5-23 Normal Uncertainties for Instrumented Box Fq Measurement with 61 Detector Strings

Cycle	Timepoints	STD*	DOF	K	KSTD*
U3C6	24-53	0.88%	7981	1.67	1.47%
U3C6	1-23	1.02%	6124	1.68	1.71%
U1C6	1-57	1.13%	16131	1.66	1.88%
U3C4	1-58	1.17%	11194	1.67	1.94%
U1C4	1-56	1.26%	15734	1.66	2.09%
U1C5	1-73	1.28%	20654	1.66	2.12%
U2C6	1-49	1.34%	14104	1.66	2.23%
U2C4	1-65	1.36%	18915	1.66	2.25%
U3C5	1-65	1.37%	17463	1.66	2.27%
U2C5	1-56	1.50%	16113	1.67	2.49%

* Quoted in percent of peak assembly value.

**Table 5-24 Normal Uncertainties for Instrumented Box Fr Measurement with 61
Detector Strings**

Cycle	Timepoints	STD*	DOF	K	KSTD*
U3C6	24-53	0.63%	1441	1.71	1.08%
U1C6	29-57	0.78%	1479	1.71	1.33%
U1C5	1-73	0.87%	3718	1.69	1.48%
U1C4	29-56	0.90%	1484	1.71	1.53%
U3C6	1-23	0.89%	1110	1.72	1.54%
U3C4	1-58	1.00%	2146	1.70	1.71%
U3C5	1-65	1.04%	3205	1.69	1.75%
U1C6	1-28	1.10	1428	1.71	1.89%
U1C4	1-28	1.18%	1484	1.71	2.02%
U2C4	1-65	1.26%	3640	1.69	2.12%
U2C6	1-49	1.29%	2736	1.69	2.19%
U2C5	1-56	1.44%	2953	1.69	2.43%

* Quoted in percent of peak assembly value.

Table 5-25 Normal Uncertainties for Instrumented Box Fxy Measurement with 61 Detector Strings

Cycle	Time-points	Levels	STD*	DOF	K	KSTD*
U3C6	24-53	2	0.78%	1620	1.71	1.34%
U3C6	1-53	1	0.94%	2710	1.70	1.60%
U1C6	1-28	1	1.00%	1540	1.71	1.70%
U3C6	1-53	3-5	1.06%	8533	1.67	1.78%
U1C6	29-57	1-5	1.07%	8207	1.67	1.78%
U3C6	1-23	2	1.10%	1242	1.72	1.89%
U1C6	1-28	2-3	1.20%	3164	1.69	2.03%
U1C4	1-56	1-3	1.21%	9464	1.67	2.03%
U3C4	1-58	1-5	1.26%	11194	1.67	2.09%
U2C6	1-49	1	1.32%	2793	1.69	2.24%
U1C5	1-73	1-5	1.38%	20654	1.66	2.29%
U2C4	1-65	1-4	1.43%	15145	1.66	2.38%
U2C6	1-49	2-5	1.45%	11311	1.67	2.42%
U3C5	1-65	1-5	1.46%	17463	1.66	2.42%
U1C6	1-28	3-5	1.47%	4788	1.68	2.47%
U1C4	1-56	3-5	1.49%	9350	1.67	2.48%
U2C4	1-65	2-5	1.50%	15145	1.66	2.50%
U2C5	1-56	1-5	1.63%	16113	1.67	2.71%

* Quoted in percent of peak assembly value.

**Table 5-26 Non-Normal Uncertainties for Instrumented Box Fq
Measurement with 61 Detector Strings**

Cycle	Timepoints	STD*	DOF	K	KSTD*
U3C6	24-53	0.88%	infinite	1.47	1.29%
U3C6	1-23	1.02%	infinite	1.36	1.39%
U1C6	1-57	1.13%	infinite	1.47	1.66%
U3C4	1-58	1.17%	infinite	1.48	1.73%
U3C5	1-65	1.37%	infinite	1.40	1.92%
U1C5	1-73	1.28%	infinite	1.55	1.99%
U1C4	1-56	1.26%	110149	1.65	2.07%
U2C4	1-65	1.36%	infinite	1.62	2.20%
U2C6	1-49	1.34%	2649	1.70	2.28%
U2C5	1-56	1.50%	infinite	1.63	2.44%

* Quoted in percent of peak assembly value.

**Table 5-27 Non-Normal Uncertainties for Instrumented Box Fr Measurement
with 61 Detector Strings**

Cycle	Timepoints	STD*	DOF	K	KSTD*
U3C6	24-53	0.63%	infinite	1.45	0.91%
U3C6	1-23	0.89%	infinite	1.34	1.20%
U1C6	29-57	0.78%	187	1.84	1.44%
U3C4	1-58	1.00%	infinite	1.46	1.47%
U1C5	1-73	0.87%	372	1.78	1.56%
U3C5	1-65	1.04%	infinite	1.57	1.63%
U1C6	1-28	1.10%	infinite	1.49	1.65%
U1C4	29-56	0.90%	38	2.13	1.91%
U2C4	1-65	1.26%	infinite	1.63	2.05%
U1C4	1-28	1.18%	342	1.79	2.11%
U2C6	1-49	1.29%	136	1.88	2.43%
U2C5	1-56	1.44%	857	1.73	2.49%

* Quoted in percent of peak assembly value.

**Table 5-28 Non-Normal Uncertainties for Instrumented Box Fxy Measurement
with 61 Detector Strings**

Cycle	Time-points	Levels	STD*	DOF	K	KSTD*
U3C6	24-53	2	0.78%	infinite	1.44	1.13%
U3C6	1-23	2	1.10%	infinite	1.29	1.43%
U3C6	1-53	1	0.94%	infinite	1.53	1.44%
U3C6	1-53	3-5	1.06%	infinite	1.42	1.51%
U1C6	29-57	1-5	1.07%	infinite	1.50	1.59%
U1C6	1-28	2-3	1.20%	infinite	1.50	1.80%
U1C6	1-28	1	1.00%	209	1.83	1.82%
U3C4	1-58	1-5	1.26%	infinite	1.46	1.84%
U1C4	1-56	1-3	1.21%	infinite	1.62	1.96%
U3C5	1-65	1-5	1.46%	infinite	1.37	2.00%
U1C6	1-28	3-5	1.47%	infinite	1.43	2.10%
U1C5	1-73	1-5	1.38%	infinite	1.53	2.12%
U2C4	1-65	2-5	1.50%	infinite	1.56	2.34%
U1C4	1-56	3-5	1.49%	infinite	1.58	2.35%
U2C4	1-65	1-4	1.43%	24656	1.66	2.37%
U2C6	1-49	2-5	1.45%	1476	1.71	2.49%
U2C6	1-49	1	1.32%	75	1.97	2.60%
U2C5	1-56	1-5	1.63%	72103	1.65	2.69%

* Quoted in percent of peak assembly value.

5.3.8 EVALUATION OF INSTRUMENTED BOX POWER PEAKING FACTOR MEASUREMENT UNCERTAINTY WITH 50 DETECTOR STRINGS

Summary of Results

The estimates of uncertainty parameters for the F_q , F_r , and F_{xy} box instrumented power measurements with 50 detector strings are summarized in Table 5-29. Results include the mean, the standard deviation, the number of degrees of freedom, the 95/95 tolerance factor, and the upper 95/95 tolerance limit. The standard deviations are actually a little smaller for 50 detector strings, but the numbers of degrees of freedom are quite a bit less so that the upper 95/95 tolerance limits are a little larger.

Chi-Square Homogeneity Test Results

The results of the chi-square tests for k independent samples for the F_q , F_r , and F_{xy} instrumented box power measurements with 50 detector strings are given in Table 5-30, Table 5-31, and Table 5-32, respectively.

Normal Uncertainty Parameters

The normal uncertainty parameters for the F_q , F_r , and F_{xy} instrumented box power measurements with 50 detector strings are given in Table 5-33, Table 5-34, and Table 5-35, respectively. The normal uncertainty parameters are used if they are less favorable than the non-normal uncertainty parameters.

Non-Normal Uncertainty Parameters

The non-normal uncertainty parameters for the F_q , F_r , and F_{xy} instrumented box power measurements with 50 detector strings are given in Table 5-36, Table 5-37, and Table 5-38, respectively. The non-normal uncertainty parameters are used if they are less favorable than the normal uncertainty parameters.

Table 5-29 Summary of Uncertainties for the Measurement of Peak Assembly Power with 50 Detector Strings

Type	Mean	STD*	DOF	K	KSTD*
$F_{qM}(box)$	0.0%	1.51%	1865	1.71	2.57%
$F_{rM}(box)$	0.0%	1.32%	35	2.16	2.85%
$F_{xyM}(box)$	0.0%	1.48%	94	1.93	2.87%

* Quoted in percent of peak assembly value.

**Table 5-30 Chi-Square Test Results for Instrumented Box Fq Measurement with
50 Detector Strings**

Cycle	Timepoints	DOF	chi-square	CHI-95	PASSED?
U1C4	1-14	507	530.00	560.53	YES
U1C4	15-28	455	374.54	505.74	YES
U1C4	29-56	945	703.14	1017.68	YES
U1C5	1-73	2808	2548.25	2933.69	YES
U1C6	1-57	2016	1999.76	2121.73	YES
U2C4	1-65	2560	2261.11	2680.75	YES
U2C5	1-56	2255	2135.54	2368.04	YES
U2C6	1-37	1476	1541.47	1570.73	YES
U2C6	13-49	1404	1124.96	1496.34	YES
U3C4	1-58	1539	1319.17	1635.92	YES
U3C5	1-65	2432	2448.00	2549.73	YES
U3C6	1-23	770	768.85	835.67	YES
U3C6	24-53	899	747.10	969.88	YES

**Table 5-31 Chi-Square Test Results for Instrumented Box Fr Measurement with
50 Detector Strings**

Cycle	Timepoints	DOF	chi-square	CHI-95	PASSED?
U1C4	1-14	91	84.96	114.27	YES
U1C4	15-28	91	31.41	114.27	YES
U1C4	29-56	189	92.15	222.07	YES
U1C5	1-73	504	350.47	557.37	YES
U1C6	1-28	189	159.63	222.07	YES
U1C6	29-57	196	71.08	229.66	YES
U2C4	1-65	512	451.88	589.43	YES
U2C5	1-56	385	430.06	431.82	YES
U2C6	1-49	384	263.11	430.77	YES
U3C4	1-58	285	171.80	325.38	YES
U3C5	1-65	448	231.26	498.35	YES
U3C6	1-23	132	131.22	159.82	YES
U3C6	24-53	145	64.69	174.10	YES

Table 5-32 Chi-Square Test Results for Instrumented Box Fxy Measurement with 50 Detector Strings

Cycle	Time-points	Levels	DOF	chi-square	CHI-95	PASSED?
U1C4	1-56	1-3	1336	1406.80	1425.88	YES
U1C4	1-56	3-5	1169	1078.40	1251.96	YES
U1C5	1-73	1-5	2912	2453.77	3039.41	YES
U1C6	1-57	1-3	1190	1141.71	1273.90	YES
U1C6	1-57	4-5	1017	866.05	1092.59	YES
U2C4	1-65	1-3	1746	1782.63	1847.64	YES
U2C4	1-65	4-5	1032	1076.95	1108.36	YES
U2C5	1-56	1-5	2511	2413.50	2630.63	YES
U2C6	1-49	1	432	422.48	481.52	YES
U2C6	1-49	2-5	1365	1426.64	1455.95	YES
U3C4	1-58	1-5	1445	890.50	1538.73	YES
U3C5	1-65	1-5	2268	1731.65	2381.40	YES
U3C6	1-53	1	364	231.40	409.55	YES
U3C6	1-53	2	364	367.36	409.55	YES
U3C6	1-53	3-5	1106	1115.38	1186.03	YES

**Table 5-33 Normal Uncertainties for Instrumented Box Fq Measurement with
50 Detector Strings**

Cycle	Timepoints	STD*	DOF	K	KSTD*
U3C6	24-53	0.88%	6513	1.68	1.47%
U3C6	1-23	1.00%	4996	1.68	1.68%
U1C6	1-57	1.07%	13244	1.66	1.77%
U1C4	29-56	1.08%	6468	1.68	1.81%
U3C4	1-58	1.14%	8932	1.67	1.91%
U1C4	15-28	1.14%	3234	1.69	1.93%
U1C5	1-73	1.28%	16861	1.66	2.13%
U2C6	13-49	1.30%	8695	1.67	2.18%
U2C4	1-65	1.38%	15470	1.66	2.28%
U3C5	1-65	1.39%	14182	1.66	2.31%
U2C6	1-37	1.41%	8695	1.67	2.35%
U1C4	1-14	1.41%	3232	1.69	2.39%
U2C5	1-56	1.51%	13208	1.66	2.51%

* Quoted in percent of peak assembly value.

**Table 5-34 Normal Uncertainties for Instrumented Box Fr Measurement with
50 Detector Strings**

Cycle	Timepoints	STD*	DOF	K	KSTD*
U3C6	24-53	0.63%	1233	1.72	1.08%
U1C6	29-57	0.63%	1192	1.72	1.09%
U1C4	29-56	0.75%	1204	1.72	1.29%
U1C5	1-73	0.86%	3137	1.69	1.45%
U3C6	1-23	0.89%	948	1.73	1.53%
U1C4	15-28	0.89%	602	1.75	1.56%
U3C4	1-58	0.93%	1740	1.71	1.59%
U1C6	1-28	0.98%	1148	1.72	1.70%
U3C5	1-65	1.05%	2631	1.70	1.79%
U2C4	1-65	1.26%	3055	1.69	2.14%
U1C4	1-14	1.28%	602	1.75	2.24%
U2C6	1-49	1.32%	2303	1.70	2.25%
U2C5	1-56	1.47%	2456	1.70	2.50%

* Quoted in percent of peak assembly value.

**Table 5-35 Normal Uncertainties for Instrumented Box Fxy Measurement with
50 Detector Strings**

Cycle	Time- points	Levels	STD*	DOF	K	KSTD*
U3C6	1-53	1	0.94%	2234	1.70	1.61%
U3C6	1-53	2	0.95%	2332	1.70	1.62%
U1C6	1-57	1-3	0.98%	7912	1.67	1.64%
U3C6	1-53	3-5	1.04%	6943	1.68	1.74%
U1C4	1-56	1-3	1.15%	7784	1.67	1.92%
U3C4	1-58	1-5	1.24%	8932	1.67	2.07%
U1C6	1-57	3-5	1.33%	5332	1.68	2.24%
U2C4	1-65	1-3	1.37%	9295	1.67	2.30%
U1C5	1-73	1-5	1.39%	16861	1.66	2.30%
U2C6	1-49	1	1.37%	2303	1.70	2.33%
U1C4	1-56	3-5	1.41%	7670	1.68	2.36%
U3C5	1-65	1-5	1.48%	14182	1.66	2.47%
U2C6	1-49	2-5	1.48%	9212	1.67	2.48%
U2C4	1-65	4-5	1.59%	6175	1.68	2.67%
U2C5	1-56	1-5	1.64%	13208	1.66	2.74%

* Quoted in percent of peak assembly value.

**Table 5-36 Non-Normal Uncertainties for Instrumented Box Fq Measurement
with 50 Detector Strings**

Cycle	Timepoints	STD*	DOF	K	KSTD*
U3C6	24-53	0.88%	infinite	1.57	1.37%
U3C6	1-23	1.00%	infinite	1.45	1.45%
U3C4	1-58	1.14%	infinite	1.46	1.67%
U1C6	1-57	1.07%	infinite	1.57	1.68%
U1C4	15-28	1.14%	infinite	1.51	1.73%
U1C4	29-56	1.08%	infinite	1.62	1.74%
U3C5	1-65	1.39%	infinite	1.45	2.01%
U1C5	1-73	1.28%	infinite	1.62	2.08%
U1C4	1-14	1.41%	infinite	1.53	2.15%
U2C4	1-65	1.38%	1016	1.73	2.37%
U2C6	13-49	1.30%	87	1.95	2.53%
U2C6	1-37	1.41%	224	1.82	2.57%
U2C5	1-56	1.51%	1865	1.71	2.57%

* Quoted in percent of peak assembly value.

**Table 5-37 Non-Normal Uncertainties for Instrumented Box Fr Measurement
with 50 Detector Strings**

Cycle	Timepoints	STD*	DOF	K	KSTD*
U3C6	24-53	0.63%	infinite	1.52	0.95%
U1C6	29-57	0.63%	infinite	1.56	0.98%
U3C4	1-58	0.93%	infinite	1.34	1.25%
U3C6	1-23	0.89%	infinite	1.44	1.28%
U1C4	15-28	0.89%	22634	1.66	1.48%
U1C6	1-28	0.98%	infinite	1.58	1.55%
U1C5	1-73	0.86%	228	1.82	1.56%
U1C4	29-56	0.75%	41	2.11	1.58%
U3C5	1-65	1.05%	3352	1.69	1.78%
U1C4	1-14	1.28%	infinite	1.43	1.83%
U2C4	1-65	1.26%	757	1.74	2.20%
U2C5	1-56	1.47%	1360	1.72	2.52%
U2C6	1-49	1.32%	35	2.16	2.85%

* Quoted in percent of peak assembly value.

**Table 5-38 Non-Normal Uncertainties for Instrumented Box Fxy Measurement
with 50 Detector Strings**

Cycle	Time- points	Levels	STD*	DOF	K	KSTD*
U3C6	1-53	2	0.95%	infinity	1.43	1.36%
U3C6	1-53	1	0.94%	infinity	1.59	1.50%
U3C6	1-53	3-5	1.04%	infinity	1.49	1.54%
U1C6	1-57	1-3	0.98%	infinity	1.61	1.58%
U1C4	1-56	1-3	1.15%	infinity	1.56	1.78%
U3C4	1-58	1-5	1.24%	infinity	1.51	1.87%
U1C6	1-57	4-5	1.33%	infinity	1.51	2.01%
U3C5	1-65	1-5	1.48%	infinity	1.44	2.13%
U1C4	1-56	3-5	1.41%	infinity	1.55	2.19%
U1C5	1-73	1-5	1.39%	infinity	1.58	2.20%
U2C4	1-65	4-5	1.59%	infinity	1.52	2.42%
U2C4	1-65	1-3	1.37%	95	1.93	2.65%
U2C5	1-56	1-5	1.64%	15437	1.66	2.73%
U2C6	1-49	1	1.37%	56	2.03	2.78%
U2C6	1-49	2-5	1.48%	94	1.93	2.87%

* Quoted in percent of peak assembly value.

5.4 POWER PEAKING FACTOR SYNTHESIS UNCERTAINTY

5.4.1 ABB POWER PEAKING FACTOR SYNTHESIS UNCERTAINTY

The box power peaking factor and pin-to-box power peaking factor synthesis uncertainty parameters were estimated in Section 3.2 of Reference 25. The results, from Table 3.I, of Reference 25 are given in Table 5-39.

5.4.2 APS POWER PEAKING FACTOR SYNTHESIS UNCERTAINTY

The ABB synthesis uncertainties are a measure of the ability of the ROCS driven CECOR calculations to reproduce ROCS results rather than a measure of the ability of the ROCS calculations to predict instrument responses. It follows that the SIMULATE-3 driven CECOR calculations will be equally successful in reproducing SIMULATE-3 results. Therefore, the ABB synthesis uncertainties are used here for the SIMULATE-3 driven CECOR calculations.

The numerical values of the CECOR power-to-signal ratios, coupling coefficients, axial power distributions, and pin-to-box power peaking factors will be impacted by modeling differences such as variable axial mesh in ROCS versus uniform axial mesh in SIMULATE-3, axial and radial boundary conditions in ROCS versus explicit axial and radial reflectors in SIMULATE-3, microscopic cross section model in ROCS versus macroscopic cross section model in SIMULATE-3, DIT cross sections in ROCS versus CASMO-4 cross sections in SIMULATE-3, and MC pin power reconstruction in ROCS versus SIMULATE-3 pin power reconstruction in SIMULATE-3. However, the impact of these modeling differences on the ability of the CECOR code to reproduce the resulting values will be minimal.

The ABB synthesis uncertainties were derived from a single plane of power-to-signal ratios, coupling coefficients, and pin-to-box power peaking factors whereas the SIMULATE-3 driven CECOR calculations use five planes of power-to-signal ratios, coupling coefficients, and pin-to-box power peaking factors. This should cause the ABB synthesis uncertainties to be conservative for the SIMULATE-3 driven CECOR calculations.

Finally, ABB synthesis uncertainties were derived from plants with four instrument levels whereas Palo Verde has five instrument levels. This should cause the ABB synthesis uncertainties to be conservative for Palo Verde CECOR calculations.

Table 5-39 ABB and APS Uncertainties of the Synthesis Components of the Peak Pin Power Measurements

	\bar{D}	S	f	K	$\bar{D} + KS$
Box Power Synthesis *					
$F_{qS}(box)$	[]	[]	216	[]	[]
$F_{rS}(box)$	[]	[]	216	[]	[]
$F_{xyS}(box)$	[]	[]	260	[]	[]
Pin-to-Box Synthesis #					
$F_{pS}\left(\frac{pin}{box}\right)$	[]	[]	244	[]	[]

* Quoted in percent of peak assembly value

Quoted in percent of average pin value.

5.5 PIN POWER PEAKING FACTOR UNCERTAINTY

5.5.1 EVALUATION OF PIN POWER CALCULATION UNCERTAINTY

Introduction

This section follows the method documented in Chapter 5.0 of Reference 29.

The individual contributors to the overall calculation uncertainty are:

- (1) the pin-to-box power peaking factor calculation uncertainty given in Section 5.2.
- (2) the box power peaking factor calculation uncertainty given in Section 5.3.6.

Method

The total pin power calculation uncertainties can be computed by combining the box power and pin peaking components in accordance with the method outlined in Chapter 5.0 of Reference 29. The mean of the combined distribution is approximately given by

$$\mu \approx \bar{D} = \overline{D_{BC}} + \overline{D_{pC}} \text{ where}$$

μ = the mean of the distribution of the differences between the “TRUE” and SIMULATE-3 pin powers.

\bar{D} = the sample mean of the distribution of the differences between the “TRUE” and SIMULATE-3 pin powers.

$\overline{D_{BC}}$ = the sample mean of the distribution of the differences between the “TRUE” and SIMULATE-3 box powers.

$\overline{D_{pC}}$ = the sample mean of the distribution of the differences between the measured and SIMULATE-3 pin-to-box peaking factors.

The variance of the combined distribution is given approximately by

$$\sigma^2 \leq S^2 = S_{BC}^2 + S_{pC}^2 \text{ where}$$

σ = the standard deviation of the differences between the “TRUE” and SIMULATE-3 pin powers.

S = the sample standard deviation of the differences between the “TRUE” and SIMULATE-3 pin powers.

S_{BC} = the sample standard deviation of the differences between the “TRUE” and SIMULATE-3 box powers.

S_{pC} = the sample standard deviation of the differences between the “TRUE” and SIMULATE-3 pin-to-box peaking factors.

The number of degrees of freedom of the combined distribution is given by

$$\frac{S^4}{f} = \frac{S_{BC}^4}{f_{BC}} + \frac{S_{pC}^4}{f_{pC}} \text{ where}$$

f = number of degrees of freedom of the sample of the distribution of the differences between the “TRUE” and SIMULATE-3 pin powers.

f_{BC} = number of degrees of freedom of the sample of the distribution of the differences between the “TRUE” and SIMULATE-3 box powers.

f_{pC} = number of degrees of freedom of the sample of the distribution of the differences between the measured and SIMULATE-3 pin-to-box peaking factors.

Input Data

The uncertainty parameters for the components of the pin power calculations are given in Table 5-40.

Results

The uncertainty parameters for the pin power calculations are given in Table 5-41.

Table 5-40 Uncertainties of the Components of the Peak Pin Power Calculations

	\bar{D}	S	f	K	$\bar{D} + KS$
Calculated *					
$F_{qC}(box)$	0.00%	2.69%	72	1.98	5.34%
$F_{rC}(box)$	0.00%	1.57%	47	2.08	3.25%
$F_{xyC}(box)$	0.00%	1.83%	58	2.03	3.69%
Calculated #					
$F_{PC}\left(\frac{pin}{box}\right)$	[]	[]	[]	[]	[]

* Quoted in percent of peak assembly value

Quoted in percent of average pin value.

Table 5-41 Summary of Uncertainties of the Peak Pin Power Calculations

	\bar{D}^*	S^*	f	K	$\bar{D} + KS^*$
$F_q(pin)$	[]	[]	[]	[]	[]
$F_r(pin)$	[]	[]	[]	[]	[]
$F_{xy}(pin)$	[]	[]	[]	[]	[]

* Quoted in percent of peak pin value.

5.5.2 EVALUATION OF PIN POWER MEASUREMENT UNCERTAINTY WITH 61 DETECTOR STRINGS

Introduction

This section follows the method documented in Part III of Reference 25.

The individual contributors to the overall measurement uncertainty with 61 detector strings are:

- (1) the pin-to-box calculation uncertainty given in Section 5.2.
- (2) the 61 detector box power measurement uncertainty given in Section 5.3.7.
- (3) the box power synthesis uncertainty given in Section 5.4.1.
- (4) the pin-to-box synthesis uncertainty given in Section 5.4.1.

Method

The total pin power calculation uncertainties can be computed by combining the box power and pin-to-box components in accordance with the method outlined in section III.1 of Reference 25. The mean of the combined distribution is approximately given by

$$\mu \approx \bar{D} = \bar{D}_{BM} + \bar{D}_{PC} + \bar{D}_{BS} + \bar{D}_{pS} \text{ where}$$

μ = the mean of the distribution of the differences between the "TRUE" and CECOR pin powers.

\bar{D} = the sample mean of the distribution of the differences between the "TRUE" and CECOR pin powers.

\bar{D}_{BM} = the sample mean of the distribution of the differences between the "TRUE" and CECOR box powers.

\bar{D}_{PC} = the sample mean of the distribution of the differences between the measured and SIMULATE-3 pin-to-box peaking factors.

\bar{D}_{BS} = the sample mean of the distribution of the differences between the TEST ROCS and TEST CECOR box powers.

\bar{D}_{pS} = the sample mean of the distribution of the differences between the TEST ROCS and TEST CECOR pin-to-box power peaking factors.

The variance of the combined distribution is given approximately by

$$\sigma^2 \leq S^2 = S_{BM}^2 + S_{pC}^2 + S_{BS}^2 + S_{pS}^2 \text{ where}$$

σ = the standard deviation of the differences between the “TRUE” and CECOR pin powers.

S = the sample standard deviation of the differences between the “TRUE” and CECOR pin powers.

S_{BM} = the sample standard deviation of the differences between the “TRUE” and CECOR box powers.

S_{pC} = the sample standard deviation of the differences between the “TRUE” and SIMULATE-3 pin-to-box power peaking factors.

S_{BS} = the sample standard deviation of the differences between the TEST ROCS and TEST CECOR box powers.

S_{pS} = the sample standard deviation of the differences between the TEST ROCS and TEST CECOR pin-to-box power peaking factors.

The number of degrees of freedom of the combined distribution is given by

$$\frac{S^4}{f} = \frac{S_{BM}^4}{f_{BM}} + \frac{S_{pC}^4}{f_{pC}} + \frac{S_{BS}^4}{f_{BS}} + \frac{S_{pS}^4}{f_{pS}} \text{ where}$$

f = number of degrees of freedom of the sample of the distribution of the differences between the “TRUE” and CECOR pin powers.

f_{BM} = number of degrees of freedom of the sample of the distribution of the differences between the “TRUE” and CECOR box powers.

f_{pC} = number of degrees of freedom of the sample of the distribution of the differences between the measured and SIMULATE-3 pin-to-box peaking factors.

f_{BS} = number of degrees of freedom of the sample of the distribution of the differences between the TEST ROCS and TEST CECOR box powers.

f_{pS} = number of degrees of freedom of the sample of the distribution of the differences between the TEST ROCS and TEST CECOR pin-to-box power peaking factors.

Input Data

The uncertainty parameters for the components of the pin power measurements with 61 detector strings are given in Table 5-42.

Results

The pin power measurement uncertainties with 61 detector strings are given in Table 5-43.

Table 5-42 Uncertainties of the Components of the Peak Pin Power Measurements with 61 Detector Strings

	\bar{D}	S	f	K	$\bar{D} + KS$
Measured *					
$F_{qM}(box)$	0.0%	1.50%	16113	1.66	2.49%
$F_{rM}(box)$	0.0%	1.44%	857	1.73	2.49%
$F_{xyM}(box)$	0.0%	1.63%	16113	1.66	2.71%
Synthesized *					
$F_{qS}(box)$	[]	[]	216	[]	[]
$F_{rS}(box)$	[]	[]	216	[]	[]
$F_{xyS}(box)$	[]	[]	260	[]	[]
Calculated #					
$F_{pC}\left(\frac{pin}{box}\right)$	[]	[]	[]	[]	[]
Synthesized #					
$F_{pS}\left(\frac{pin}{box}\right)$	[]	[]	244	[]	[]

* Quoted in percent of peak assembly value

Quoted in percent of average pin value.

Table 5-43 Summary of Uncertainties of the Peak Pin Power Measurements with 61 Detector Strings

	\bar{D}^*	S^*	f	K	$\bar{D} + KS^*$
$F_q(pin)$	[]	[]	[]	[]	[]
$F_r(pin)$	[]	[]	[]	[]	[]
$F_{xy}(pin)$	[]	[]	[]	[]	[]

* Quoted in percent of peak pin value.

5.5.3 EVALUATION OF PIN POWER MEASUREMENT UNCERTAINTY WITH 50 DETECTOR STRINGS

Introduction

The individual contributors to the overall measurement uncertainty with 50 detector strings are:

- (1) the pin-to-box calculation uncertainty given in section Section 5.2.
- (2) the 50 detector box power measurement uncertainty given in Section 5.3.8.
- (3) the box power synthesis uncertainty given in Section 5.4.1.
- (4) the pin-to-box synthesis uncertainty given in Section 5.4.1.

Method

The method for combining uncertainties is the same as for 61 detector strings.

Input Data

The uncertainty parameters for the components of the pin power measurements with 50 detector strings are given in Table 5-44.

Results

The uncertainty parameters for the pin power measurements with 50 detector strings are given in Table 5-45.

Table 5-44 Uncertainties of the Components of the Peak Pin Power Measurements with 50 Detector Strings

	\bar{D}	S	f	K	$\bar{D} + KS$
Instrumented Box *					
$F_{qM}(box)$	0.0%	1.51%	1865	1.71	2.57%
$F_{rM}(box)$	0.0%	1.32%	35	2.16	2.85%
$F_{xyM}(box)$	0.0%	1.48%	94	1.93	2.87%
Synthesized Box *					
$F_{qS}(box)$	[]	[]	216	[]	[]
$F_{rS}(box)$	[]	[]	216	[]	[]
$F_{xyS}(box)$	[]	[]	260	[]	[]
Calculated #					
$F_{pC}\left(\frac{pin}{box}\right)$	[]	[]	[]	[]	[]
Synthesized #					
$F_{pS}\left(\frac{pin}{box}\right)$	[]	[]	244	[]	[]

* Quoted in percent of peak assembly value.

Quoted in percent of average pin value.

Table 5-45 Summary of Uncertainties of the Peak Pin Power Measurements with 50 Detector Strings

	\bar{D}^*	S^*	f	K	$\bar{D} + KS^*$
$F_q(pin)$	[]	[]	[]	[]	[]
$F_r(pin)$	[]	[]	[]	[]	[]
$F_{xy}(pin)$	[]	[]	[]	[]	[]

* Quoted in percent of peak pin value.

6.0 COLD MODEL AND NET (N - 1) ROD WORTH

Introduction

This section provides a benchmark comparison of the "cold model" developed using the CASMO-4/TABLES-3/SIMULATE-3 program package. The cold model represents a combination of cross section data produced by CASMO-4 at specific xenon free, isothermal, cold core conditions (i.e., temperatures between hot operating conditions and cold shutdown, with moderator temperature equal to fuel temperature) and a TABLES-3/CMS-LINK functionalization which is designed specifically for cold conditions. Thus, the cold model is based on a separate cross section set from the "hot" model benchmarked in Section 4.0 (the "hot" model cross sections are calculated at non-isothermal conditions, with xenon, and functionalized over critical operating temperatures only).

Measurement Technique

The benchmark of the cold model is based on typical startup calculations for Unit 1 Cycle 1 (U1C1), Unit 2 Cycle 8 (U2C8), and Unit 3 Cycle 7 (U3C7). The measured startup data in this section was obtained from low power physics tests (LPPT) consisting of reactivity coefficient, control rod worth, and boron concentration measurements. Unit 1 Cycle 1 was the only cycle that included startup test measurements performed at a very low (much lower than nominal) temperature. There was a set of measurements performed at 320°F in addition to measurements performed at the nominal HZP temperature of 565°F. The Unit 1 Cycle 1 startup tests at 320°F included a measurement of net (N - 1) rod worth. The net (N - 1) rod worth is defined as the reactivity worth of the insertion of all of the control rods except the most reactive rod, which remains stuck out.

The reactivity coefficients and boron concentration measurements presented in this section were performed as described in Section 4.0. The control rod bank worths were measured by the dilution method for Unit 1 Cycle 1 and by the rod swap method for Unit 2 Cycle 8 and Unit 3 Cycle 7. The Group A rod bank worth for Unit 1 Cycle 1 at 320°F was measured with the most reactive rod out (A - 1). The net (N - 1) rod worth measurement was then inferred by summing the individual bank worths, including the Group A worth minus the most reactive rod (A - 1).

Comparison Of Results

In order to assess the acceptability of the cold model method, the CASMO-4/TABLES-3/SIMULATE-3 cold model calculational results are compared to:

- (1) measured startup data,
- (2) applicable acceptance criteria (from ANSI/ANS standards, Reference 36), and
- (3) startup physics calculations based on CASMO-4/TABLES-3/SIMULATE-3 hot model.

The CASMO-4//TABLES-3/SIMULATE-3 cold model calculations are compared to Unit 1 Cycle 1 low power physics test (LPPT) measurements at 320°F and 565°F in Table 6-1 and Table 6-2, respectively. Table 6-1 includes the net (N - 1) rod worth measurement.

Table 6-3 presents a comparison of the cold model calculations with measurements from Unit 2 Cycle 8 LPPT and with hot model calculations at the same conditions. Table 6-4 presents a comparison of the cold model calculations with measurements from Unit 3 Cycle 7 LPPT measurements and with hot model calculations at the same conditions.

With the exception of the Unit 2 Cycle 8 IBW, all of the CASMO-4/TABLES-3/SIMULATE-3 cold model calculations compare very well with the measured data and are well within the ANSI/ANS acceptance criteria for startup measurements defined in Reference 36. The measured Unit 2 Cycle 8 IBW at 565°F is questionably low and appears to be an outlier. However, the observed difference was within the acceptance criteria. Most of the cold model observed differences were less than 5% (for observed differences given in relative units) in magnitude, the largest being -8.5% for Unit 1 Cycle 1 Group A - 1 rod worth. The net (N - 1) rod worth observed difference was -2.0% compared to an acceptance criteria of 10%. The maximum difference between the cold model CBCs and measurements is 27 ppm. The observed differences between the cold model calculations and measurements are in close agreement with the observed differences between the hot model calculations and measurements.

Statistical Analysis

Cold Model CBC, ITC, IBW, and Rod Bank Worth Statistics

All of the observed differences between CASMO-4/TABLES-3/SIMULATE-3 calculations using the cold model and measurements for reactivity (CBC), ITC, IBW, and rod worths are in excellent agreement with the observed differences between the CASMO-4/TABLES-3/SIMULATE-3 calculations using the hot model and measurements. The cold model observed differences are also well within the tolerance limits for the hot model presented in Section 4.0 (Benchmark Comparisons) for reactivity, ITC, IBW, and rod worths. Therefore, the tolerance limits for reactivity (CBC), ITC, IBW, bank rod worths, and total rod worth calculated by the cold model will be set equal to the tolerance limits for (CBC), ITC, IBW, bank rod worths, total rod worth from Section 4.0.

Net (N - 1) Rod Worth

Only one set of data is available to define the net worth bias and uncertainty. It was obtained during the U1C1 startup. With one data point, a meaningful bias and uncertainty cannot be obtained. Either the bank worth or the total worth bias and uncertainty can be used.

Using the uncertainty for an individual bank for the net worth is overly conservative. The bank worth uncertainty is dominated by banks of small worth, for which the percentage error is large even though the absolute error is well within the experimental uncertainty. The total worth bias and uncertainty is more appropriate since the total worth is more representative of the rod density of a net worth (N - 1) configuration. The net worth is less sensitive to modeling errors than the total worth, because in a stuck rod configuration, the core reactivity is driven by the unrodded portion of the core. The larger the stuck worth the smaller the error in net worth.

Based on the reasoning given above the net worth bias and uncertainty is set equal to total worth bias and uncertainty (from Section 4.4). Note that the net (N - 1) rod worth observed difference was -2.0%, well within the tolerance limits of total rod worth from Section 4.4.

Statistical Results

The tolerance limits for net (N - 1) rod worth are:

$$1.0 \pm 7.1\%$$

Summary And Conclusions

The excellent agreement between the CASMO-4/TABLES-3/SIMULATE-3 cold model results and the data obtained from both the hot model and startup measurements demonstrates the validity of the cold model to accurately estimate ITC, CBC, boron worths, and CEA worths under both rodded and unrodded configurations over a range of cold temperatures and burnups. The close agreement between the cold model data and the measurements at 320°F confirms that the SIMULATE-3 interpolation of the TABLES-3/CMS-LINK data provides valid results at conditions which do not correspond to a state point explicitly calculated by CASMO-4.

Table 6-1 U1C1 Cold Model Comparisons at 320°F

Parameter	Rod Position	Meas	SIMULATE-3 Calculation (Cold Model)	Difference (M - C)	Difference^a (%)	Acceptance Criteria^b
CBC (ppm)	All rods out (ARO)	1057	1046	11	N/A	± 50 ppm
ITC (pcm/°F)	ARO	-1.28	-1.75	0.47	N/A	± 5 pcm/°F ^c
IBW (ppm/%rho)	ARO to Grps 5 - 1 Inserted	-72.7	-75.6	2.9	-4.0	± 15%
CBC (ppm)	Grps 5 - 1 inserted	822	806	16	N/A	N/A
ITC (pcm/°F)	Grps 5 - 1 inserted	-3.70	-4.18	0.48	N/A	± 5 pcm/°F ^c
CEA Worths by Dilution (pcm)	Group 1	-1418	-1379	-39	2.8	± 100 pcm or ± 15%
	Group 2	-750	-742	-8	1.1	± 100 pcm or ± 15%
	Group 3	-722	-719	-3	0.4	± 100 pcm or ± 15%
	Group 4	-241	-230	-11	4.6	± 100 pcm or ± 15%
	Group 5	-101	-103	2	-2.0	± 100 pcm or ± 15%
	Group B	-3615	-3776	161	-4.5	± 100 pcm or ± 15%
	Group A - 1 (1 most reactive rod out)	-547	-598	51	-9.3	± 100 pcm or ± 15%
	Net (N - 1)	-7397	-7547	150	-2.0	± 10%

a. $(100*(M-C)/M)$

b. Reference ANSI/ANS-19.6.1-1997 (note: individual CEA worth limits based on the greater of 15% or 100 pcm and ± 10% for the sum of groups)

c. The ITC acceptance criterion is defined separately for U1C1 in Reference 39 as ± 5 pcm/°F. For all other cycles, the acceptance criterion is ± 2 pcm/°F.

Table 6-2 U1C1 Cold Model Comparisons at 565°F

Parameter	Rod Position	Meas	SIMULATE-3 Calculation (Cold Model)	Difference (M - C)	Difference ^a (%)	Acceptance Criteria ^b
CBC (ppm)	All rods out (ARO)	1025	1008	17	N/A	± 50 ppm
ITC (pcm/°F)	ARO	-4.40	-3.53	-0.87	N/A	± 5 pcm/°F ^c
IBW (ppm/%rho)	ARO to Grps 5 - 3 Inserted	-87.3	-88.6	1.3	-1.5	± 15%
CBC (ppm)	Grps 5 - 3 inserted	893	877	16	N/A	N/A
ITC (pcm/°F)	Grps 5 - 3 inserted	-9.70	-8.80	-0.9	N/A	± 5 pcm/°F ^c
CEA Worths by Dilution (pcm)	Group 1	-1231	-1168	-63	5.1	± 100 pcm or ± 15%
	Group 2	-1037	-974	-63	6.1	± 100 pcm or ± 15%
	Group 3	-790	-772	-18	2.2	± 100 pcm or ± 15%
	Group 4	-445	-429	-16	3.6	± 100 pcm or ± 15%
	Group 5	-277	-278	1	-0.4	± 100 pcm or ± 15%

a. $(100*(M-C)/M)$

b. Reference ANSI/ANS-19.6.1-1997 (note: individual CEA worth limits based on the greater of 15% or 100 pcm and ± 10% for the sum of groups)

c. The ITC acceptance criterion is defined separately for U1C1 in Reference 39 as ± 5 pcm/°F. For all other cycles, the acceptance criterion is ± 2 pcm/°F

Table 6-3 U2C8 Cold Model Comparisons at 565°F

Parameter	Rod Position	Meas	SIMULATE-3 Calculation (Cold Model)	SIMULATE-3 Calculation (Hot Model)	Difference^a (Meas vs. Cold Model)	Difference^a (Meas vs. Hot Model)
CBC (ppm)	ARO	2176	2132	2125	44	51
CBC (biased^b) (ppm)	ARO	2176	N/A	2158	N/A	18
ITC (pcm/°F)	ARO	0.50	0.36	0.84	0.14	-0.48
ITC (biased^c) (pcm/°F)	ARO	0.50	N/A	0.56	N/A	-0.06
IBW (ppm/%rho)	ARO	-126.4	-140.2	-139.6	13.8 (-10.9%)	13.2 (-10.4%)
CBC (ppm)	Reference bank in	2021	1961	1955	60	66
CBC (biased^b) (ppm)	Reference bank in	2021	N/A	1988	N/A	33
ITC (pcm/°F)	Reference bank in	N/A	-3.79	-3.26	N/A	NA/
Ref. Bank Worth (pcm)	Grp 2 & 3	-1226	-1220	-1218	-6 (0.5%)	-8 (0.7%)
Test Bank Worths by Rod Swap (pcm)	Grp 1 & 5	-1067	-1026	-1027	-41 (3.8%)	-40 (3.7%)
	Grp 4 & B6	-945	-990	-989	45 (-4.8%)	44 (-4.7%)
	Grp B7 & B16	-1071	-1093	-1093	22 (-2.1%)	22 (2.1%)
	Grp B9 & B10	-1258	-1188	-1189	-70 (-5.6%)	-69 (-5.5%)
	Grp A2 & A20	-899	-954	-953	55 (6.1%)	54 (-6.0%)
	Grp A3 & A19	-902	-957	-956	55 (-6.1%)	54 (-6.0%)

- a. Absolute differences = Meas - Calc, Relative (%) differences = 100*(Meas - Calc)/Meas.
- b. A 33 ppm bias was applied to the hot model startup test predictions.
- c. A -0.28 pcm/°F bias was applied to the hot model ITC in the startup test predictions.

Table 6-4 U3C7 Cold Model Comparisons at 565°F

Parameter	Rod Position	Meas	SIMULATE-3 Calculation (Cold Model)	SIMULATE-3 Calculation (Hot Model)	Difference^a (Meas vs. Cold Model)	Difference^a (Meas vs. Hot Model)
CBC (ppm)	All rods out (ARO)	2149	2096	2087	53	62
CBC (biased^b) (ppm)	All rods out (ARO)	2149	N/A	2123	N/A	26
ITC (pcm/°F)	ARO	0.08	0.10	0.56	-0.02	-0.48
ITC (biased^c) (pcm/°F)	ARO	0.08	N/A	0.31	N/A	-0.23
IBW (ppm/%rho)	ARO	-140.1	-139.3	-138.5	-0.8 (0.6%)	-1.6 (1.1%)
CBC (ppm)	Reference bank in	1982	1927	1918	55	64
CBC (biased^b) (ppm)	Reference bank in	1982	N/A	1954	N/A	28
ITC (pcm/°F)	Reference bank in	N/A	-4.73	-4.25	N/A	N/A
Ref. Bank Worth (pcm)	Grp 3 & 4	-1192	-1213	-1220	21 (-1.8%)	28 (-2.3%)
Test Bank Worths by Rod Swap (pcm)	Grp 1 & 2	-778	-784	-781	6 (-0.8%)	3 (-0.4%)
	Grp 5 & B6	-938	-934	-933	-4 (0.4%)	-5 (0.5%)
	Grp B7	-706	-725	-725	19 (-2.7%)	19 (-2.7%)
	Grp B9	-667	-681	-679	14 (-2.1%)	12 (-1.8%)
	Grp B10 & B16	-802	-817	-813	15 (-1.9%)	11 (-1.4%)
	Grp A2 & A20	-982	-1030	-1030	48 (-4.9%)	48 (-4.9%)
	Grp A3 & A19	-974	-1028	-1027	54 (-5.5%)	53 (-5.4%)

- a. Absolute differences = Meas - Calc, Relative (%) differences = 100*(Meas - Calc)/Calc
- b. A 36 ppm bias was applied to the hot model startup test predictions.
- c. A -0.25 pcm/°F bias was applied to the hot model ITC in the startup test predictions.

7.0 CONCLUSIONS

This report justifies Arizona Public Service's (APS) use of and ability to use the CASMO-4/SIMULATE-3 and CECORLIB reactor physics method. The APS CASMO-4/SIMULATE-3 method has been validated by an extensive benchmark consisting of comparisons of calculated physics parameters to measurements from both Pressurized Water Reactors (PWR) and Critical Experiments. The results were used to determine a set of biases and uncertainties and a method for maintaining and updating these biases and uncertainties for application in the calculation of key PWR physics parameters.

Based on the results from this benchmarking effort, APS concludes that the CASMO-4/SIMULATE-3 method applies to all steady-state PWR reactor physics calculations. The accuracy of this method is sufficient for use in:

- reload design
- physics input to safety analysis
- physics input to fuel and clad performance
- physics input to mechanical design
- physics input to thermal-hydraulic analysis
- input to LOCA/Non-LOCA transient analysis
- CECOR coefficients
- startup test predictions
- core physics data books
- Shutdown Margin
- Inputs to reactor protection system and monitoring system (COLSS/CPC) functions and set-point and uncertainty updates
- other safety related physics parameters in support of refueling, safety analysis, and operation

See Table 1-2 in Section 1.3 for a summary of the biases and uncertainties calculated for the CASMO-4/SIMULATE-3 method presented in this Topical Report.

Arizona Public Service intends to replace the DIT/ROCS/MC method with CASMO-4/SIMULATE-3 while retaining the ability to use the DIT/ROCS/MC method.

Arizona Public Service maintains a continuing core follow program, comparing core physics models with plant operation and surveillance tests. When appropriate, Arizona Public Service will update biases and uncertainties to reflect current core designs using the methods of this Topical Report.

8.0 REFERENCES

1. Malte Edenius, Kim Ekberg, Bengt H. Forssen, Dave Knott, *CASMO-4, A Fuel Assembly Burnup Program, User's Manual*, STUDEVIK/SOA-95/1, STUDEVIK of America, Inc., USA, STUDEVIK Core Analysis AB, Sweden, 1995.
2. Dave Knott, Bengt H. Forssen, Malte Edenius, *CASMO-4, A Fuel Assembly Burnup Program, Methodology*, STUDEVIK/SOA-95/2, STUDEVIK of America, Inc., USA, STUDEVIK Core Analysis AB, Sweden, 1995.
3. Clas Gragg, Malte Edenius, *CASLIB User's Manual*, STUDEVIK/SOA-95/24, STUDEVIK of America, Inc., USA, STUDEVIK Core Analysis AB, Sweden, 1995.
4. David M. Ver Planck, Jerry A. Umbarger, *Tables-3 Library Preparation Code for SIMULATE-3, Users Manual*, STUDEVIK/SOA-95/16, STUDEVIK of America, Inc., USA, 1995.
5. Arthur S. DiGiovine, Joel D. Rhodes, III, Jerry A. Umbarger, *SIMULATE-3, Advanced Three-Dimensional Two-Group Reactor Analysis Code, User's Manual*, STUDEVIK/SOA-95/15, STUDEVIK of America, Inc., USA, 1995.
6. *CASMO-3G Validation*, YAEC-1363A, Yankee Atomic Electric Company, 1988.
7. *SIMULATE-3 Validation and Verification*, YAEC-1659A, Yankee Atomic Electric Company, 1988.
8. Letter, USNRC to G. Papanic, Jr. (YAEC), *Acceptance for Referencing of Topical Report YAEC-1363, CASMO-3G Validation*, March 21, 1990.
9. Letter, USNRC to G. Papanic, Jr. (YAEC), *Acceptance for Referencing of Topical Report YAEC-1659, SIMULATE-3, Validation and Verification*, February 20, 1990.
10. Palo Verde Nuclear Generating Station UFSAR, Revision 9, December 1997.
11. *Statistics -- The Exploration and Analysis of Data*, 2nd Edition, J. L. Devore and R. Peck, Duxbury Press, 1993.
12. ANSI N15.15-1974, *American National Standard Assessment of the Assumption of Normality (Employing Individual Observed Values)*, October 3, 1973.
13. *CRC Handbook of Tables for Probability and Statistics, 2nd Edition*, W. H. Beyer, CRC Press, 1968, Page 138.
14. *Statistical Methods in Nuclear Material Control*, J. L. Jaech, DOE Technical Information Center, 1973, Pages 71, 72, and 393.
15. *DOT 4.3 Users Manual*, ABB Combustion Engineering Nuclear Fuel, Windsor, Connecticut, CE-CES-97, Rev. 1, 1992.
16. CENPD-382-P, Rev. 0, *Methodology for Core Designs containing Erbium Burnable Absorbers*, October 1990.
17. CENPD-382-P SUP 1-P, Rev. 0, *Methodology for Core Designs containing Erbium Burnable Absorbers*, February 1992, Section 8.5.
18. *CMS-LINK User's Manual*, SOA-9704 Rev, May 30, 1997.

19. Certificate of Conformance (Letter - SSR:98-120), CMS-Link Version 1.07.10 981109, December 2, 1998
20. David G. Knott, Malte Edenius, *CASMO-4 Benchmark Against Critical Experiments*, Proprietary, SOA-94/13, Studsvik of America, Inc., USA, 1994.
21. David G. Knott, Malte Edenius, *CASMO-4 Benchmark Against MNCP*, Proprietary, SOA-94/12, Studsvik of America, Inc., USA, 1994.
22. *Southern California Edison Company PWR Reactor Physics Methodology Using CASMO-3/SIMULATE-3*, September 1990.
23. *Duke Power Company Nuclear Design Methodology Using CASMO-3/SIMULATE-3P*, DPC-NE-1004, January 1990.
24. Root Cause Investigation Report -- 2-6-0109, *Unit 2 Cycle 7 Initial Startup*, C. F. Karlson, June, 1996.
25. A. Jonsson, W. B. Terney, and M. W. Crump, *Evaluation of Uncertainty in the Nuclear Power Peaking Measured by the Self-Powered, Fixed In-Core Detector System*, ABB Combustion Engineering Nuclear Fuel, Windsor, Connecticut, CENPD-153-P-A, Rev. 1-P-A, May, 1980.
26. Sidney Siegel, *Nonparametric Statistics for the Behavioral Sciences*, pp. 175-179, McGraw Hill Book Company, 1956.
27. *Factors for One-Sided Tolerance Limits and for Variables Sampling Plans*, D. B. Owen, U.S. Dept. of Energy, March 1963, Pages 46-54 (Table 2.4).
28. W. J. Conover, *Practical Non-Parametric Statistics*, pp. 118-122, J. Wiley and Sons, Inc.
29. *The ROCS and DIT Computer Codes for Nuclear Design*, ABB Combustion Engineering Nuclear Fuel, Windsor, Connecticut, CENPD-266-P-A, April, 1983.
30. A. Jonsson (ABB-CE), D. R. Harris (RPI), R. Y. Chang, O. J. Thomsen (SCE, Irvine), *Analysis of Critical Experiments with Erbium-Uranium Fuel*, Transactions, American Nuclear Society, Annual Meeting, 1992.
31. L. W. Newman, "Uranium-Gadolinium: Nuclear Model Development and Critical Experiment Benchmark", DOE/ET/34212-41, BAW-1810 (1984).
32. A. Jonsson, "The DIT Nuclear Fuel Assembly Physics Design Code", *Nucl. Sci. Eng.*, 100, 363 (1988).
33. W. A. Rhoades, R. L. Childs, *An Updated Version of the DOT 4 One- and Two-Dimensional Neutron/Photon Transport Code*, ORNL-5851, Oak Ridge National Lab. (1982).
34. M. Edenius et al., CASMO-3G, *A Fuel Assembly Burnup Program, User's Manual*, STUDSVIK/NFA-86/7 (1986).
35. *DORT - Two Dimensional Discrete Ordinate Transport Code*, ORNL-5851, RSIC CCC-484, Radiation Shielding Information Center, Oak Ridge National Lab. (1989).
36. ANSI/ANS-19.6.1-1997, *Reload Startup Physics Tests for Pressurized Light Water Reactors*.

37. C. F. Karlson, *Continuing Advances in In-Core Power Distribution Measurement Methods Using SIMULATE-3 and CECOR 3.4*, Nuclear Science and Engineering, **121**, 57, 1995.
38. CE-CES-129, Rev 4-P, *Methodology Manual for Physics Biases and Uncertainties*, June 1997.
39. Letter ANPP-35288-EEVB/LJM/98.05, *PVNGS - Unit 1 - Docket No. STN 50-528 (License NPF-41) - Startup Report*, 2/25/86.